Towards A Synthetic Cell Model That Displays Receptor Mediated Endocytosis

Artur Kubilis

A Thesis Presented for the Degree of Doctor of Philosophy

Department of Chemistry

University of Durham

2015

Declaration

The work reported herein was carried out in the Department of Chemistry, University of Durham, England between October 2011 and October 2014. Unless otherwise stated all work is my own and has not been submitted for a qualification at this or any other university.

Statement of Copyright

“I would like to dedicate this thesis to my parents Elena and Juozas Kubiliai”

Acknowledgements

I would like to start by acknowledging my supervisor, Professor Neil Cameron, for giving me opportunity to study in his research group. I would like to say words of gratitude for spent time during the research meetings, all the priceless ideas, inspiration and advices.

I would like thank to Dr. Ahmed Eissa for synthesis of the glycopolymers used in the electroformation studies, for functionalisation of the PS beads and for helping hand in polymer synthesis, and report writing process.

I would like to extend my thanks to all past and present members of the NRC and SAP group for friendly and motivating atmosphere. It was a pleasure working alongside with each of you. I would especially like thank to amazing post - docs: David Johnson, Paul Thornton and Sarah Hehir for all the advices, discussions, patience and many, many more. Special mentions go to Daniel Tams, Matt Didsbury, Mike Smith, Ross Carnachan, Lauren Cowie, Zong Jingyi and Nicole Shields for their friendship.

Furthermore, I must thank Fanny Joubert, who has been the best “colleague” over three years from the first day in the NRC group. I would like to thank all the people who I have met during those amazing three years with a special mention to William Hannon, Tom Ciotkowski, Ryan Poland, Julia Aleszczyk and Stewart Yarlett. The past three years would not have been as enjoyable and unforgettable without you all.

Last but not least I would like thank to my family and Monika Kosa for their endless love, support and encouragement. I am so grateful to you for everything you have done for me.

Funding

I would like to acknowledge The Leverhulme Trust for both the funding for this thesis and an opportunity to learn and develop thorough those three years.

Abstract

This project is an iterative exploration towards a minimal synthetic cell model based on an amphiphilic glycopolymer that assembles into GUVs that display receptor mediated endocytosis.

Chapter one is a general introduction chapter on the literature related to the present work including topics such as synthetic vesicles, natural cell membrane and its synthetic models, and the importance of transmembrane transport in the living cells.

Chapter two includes electroformation method applications on model molecules: lipid 1, 2 - dioleoyl - sn - glycerol - 3 - phosphocholine and the block copolymer poly (butadiene - b - ethylene oxide). Electroformation studies performed with a custom - made electroformation kit were accomplished successfully. Conditions suitable for the production of giant liposomes and polymersomes were obtained and the created structures were characterised, and analysed. A Full Factorial Design of Experiment Approach applied to the electroformation experiments on block copolymer poly (butadiene - b - ethylene oxide) revealed that the most influential factor on the final self - assembly outcome is the volume of deposited amphiphilic molecule on the glass slide.

Chapter three deals with giant unilamellar vesicle electroformation from the novel glycopolymer polyethylene - block - poly(ethylene glycol) β - D - glucoside and a variety of poly [N - 2 - (β - D - glucosyloxy) ethyl acrylamide] - b - (n-butylacrylate) glycopolymers with different block ratios and molar mass. Self - assembly experiments with novel amphiphilic materials were accomplished with desirable results - conditions

required for giant unilamellar vesicle formation were obtained; moreover, the collected data indicated that glycosylated block copolymer poly [N - 2 - (β - D - glucosyloxy) ethyl acrylamide] - b - (n-butylacrylate) with a block ratio 1 : 10 (hydrophilic block to hydrophobic block ratio) is a suitable amphiphilic material for the synthetic cell model creation.

Chapter four describes thorough studies performed on giant glycopolymersomes electroformed from polymer poly [N - 2 - (β - D - glucosyloxy) ethyl acrylamide] - b - (n-butylacrylate) with a block ratio 1 : 10. Polymersomes were reported to be stable and resistant to minor changes of osmolality and pH in their surrounding environment. Interaction studies confirmed that, despite the reported selective interactions between GUVs and PS - Con A beads, an evident uptake of nanoparticles in the glycopolymersome were not observed; however, findings presented in this chapter are promising and convincing that RME could be performed in a purely synthetic system in the near future upon applying desirable membrane modifications allowing the regulation of toughness and permeability.

Chapter five presents a recap of conclusions and general suggestions for continuation and further development of the project.

Chapter six describes general experimental procedures, materials and instrumentation utilised in this project.

Table of Contents

Abbreviations

6 - FAM	Carboxyfluorescein
A_{450nm}	Absorbance of 450 nm light
AC	Alternating Current
ASGPR	Asialoglycoprotein Receptor
BP	Band Pass
Con A	Concanavalin A
CuAAC	Copper - catalyzed azide - alkyne cycloaddition
DC - SIGN	Dendritic Cell - Specific Intercellular adhesion molecule - 3 - Grabbing Non - integrin
DC	Direct Current
DIC	Differential Interference Contrast
$Đ_M$	Polydispersity
DOE	Design of Experiment
DOPA	1, 2 - dioeoyl - sn - glycerol - 3 - phosphate
DOPC	1, 2 - dioleoyl - sn - glycerol - 3 - phosphocholine
DOPEAN6 - FAM	1,2 - dioleoyl - sn - glycerol - 3 - phosphoethanolamine - N - (carboxyfluorescein)
DSC	Differential Scanning Calorimetry
DV	Deposited Volume
EDAC	*N* - (3 - dimethylaminopropyl) – *N* '- ethylcarbodiimide hydrochloride
egg PC	L - α - phosphatidylcholine
f	Frequency

FF	Full Factorial
FFDOE	Full Factorial Design of Experiment
GUV	Giant Unilamellar Vesicle
H^+	Hydrogen ion
HCl	Hydrochloric acid
He - Ne	Helium - Neon
HEPES	4 - (2 - hydroxyethyl) - 1 - piperazineethanesulfonic acid
ITO	Indium Tin Oxide
LP	Long Pass
M_n	Number average molecular weight
M_w	Weight average molecular weigh
MWCO	Molecular Weight Cut Off
n - BA	n - butyl acrylate
NA	Numerical Aperture
NaCl	Sodium Chloride
NHS	*N* - hydroxysuccinimide
P(NGEA) - b - (BA)	Poly [N - 2 - (β - D - glucosyloxy) ethyl acrylamide] - b - (n-butylacrylate)
PBd - b - PEO	Polybutadiene - b - poly (ethylene oxide)
PBS	Phosphate Buffered Saline
PDMS	Poly (dimethylsiloxane)
PE - b - (Glu) PEG	Polyethylene - block - poly (ethylene glycol) β - D - glucoside
PE - b - PEG	Polyethylene - block - poly (ethylene glycol)

pH	Negative logarithmic value of the hydrogen ion concentration
PL	Plain
PMT	Photon Multiplying Tube
PS - Con A	Polystyrene beads functionalised with Concanavalin A
PS - RCA_{120}	Polystyrene beads functionalised with *Ricinus Communis* Agglutinin
PS	Polystyrene
RAFT	Reversible Addition - Fragmentation chain Transfer polymerisation
RCA_{120}	*Ricinus Communis* Agglutinin
RME	Receptor Mediated Endocytosis
SP	Short Pass
t	Time
T_g	Glass transition temperature
THF	Tetrahydrofuran
T_m	Melting temperature
U	Voltage
wt %	Weight percent

List of Figures

List of Tables

Aims

The overall aim of this project is to develop a synthetic cell model that displays receptor mediated endocytosis. There is ever - increasing interest in preparing cell - sized vesicles in order to mimic the cell membrane properties and functions. Using established and new techniques the generation of giant unilamellar vesicles (GUVs) from novel amphiphilic glycopolymers, their subsequent characterisation, and properties adjustments in order to create a purely synthetic cell model with the ability to interact with external species functionalised with lectins are hoped to be achieved.

1. Introduction

1.1. Synthetic vesicles

The "synthetic vesicle" is a specific closed compartment created from an amphiphilic material during a self - assembly process in aqueous media (see Figure 1-1.). A single - or multi - layered membrane boundary composed of amphiphilic molecules separates an inside - enclosed aqueous media from the surroundings. Amphiphiles are composed of a hydrophilic (from Greek: *philia* - meaning friendship) "head" and single or multiple hydrophobic (from Greek: *phobos* - meaning fear) "tails" as presented in Figure 1-1.[1]

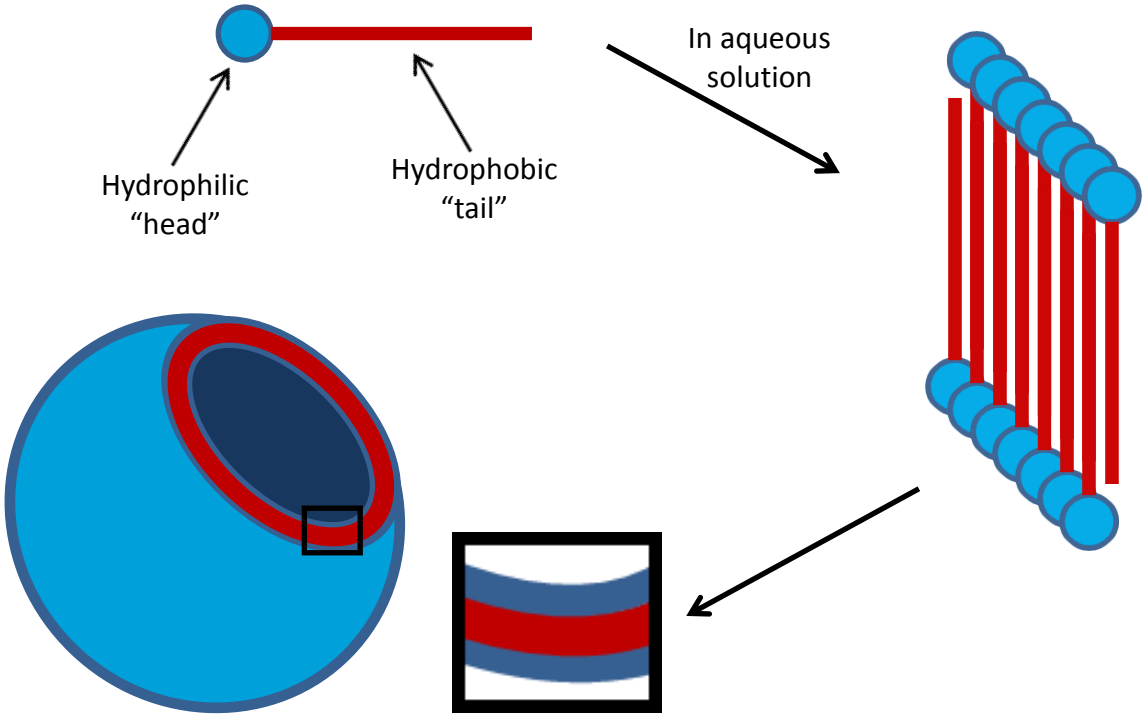

Figure 1-1. Self - assembly: from amphiphilic molecule to membrane and vesicle.

The amphiphiles in the membranes are arranged in a way that the hydrophilic parts are in contact with the surrounding aqueous media and the hydrophobic parts are "hidden" in the membrane interior to prevent unfavourable contact with water molecules.

Synthetic vesicles vary in size: small vesicles have a diameter from between 0.02 µm to 0.2µm, large from 0.2 µm to 1 µm and giant larger than 1 µm, as presented in Figure 1-2.[2] Giant vesicles are also divided into categories by their structure: unilamellar, oligolamellar, multilamellar and multivesicular (Figure 1-2.).[2] This thesis is concentrated on giant unilamellar vesicles (GUVs) created from lipid or/and polymer membrane monolayers.

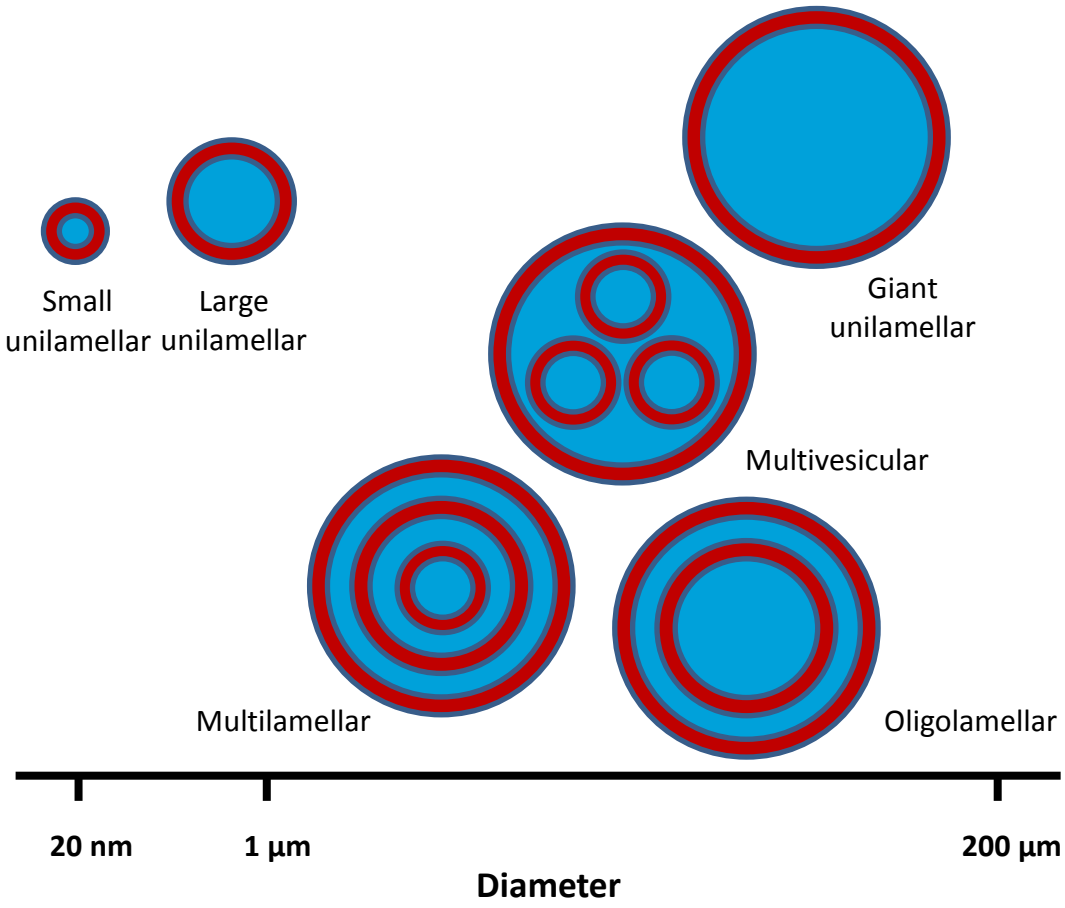

Figure 1-2. Types of synthetic vesicles based on their size and structure.

There are four major types of synthetic vesicles based on their composition:

- liposomes - created from lipids
- polymersomes - created from polymers
- peptosomes - created from polypeptides
- mixed - created from a mix two of different types of amphiphilic materials.

1.2. Principle of self - assembly: from amphiphilic molecule to vesicle

Both lipids and amphiphilic block copolymers are able to aggregate to give a variety of self - assembled structures when introduced into aqueous surrounding media, if their concentration is above the critical micelle concentration (CMC).[3] The CMC is a parameter indicating a minimal amphiphilic material concentration in media above which micelles are formed by self - assembly. The aggregation of amphiphilic molecules in an aqueous environment is a process driven by van der Waals, hydrophobic and electrostatic interactions, and hydrogen bonding.[1, 4] In general, the presence of an individual hydrophobic molecule in an aqueous environment is entropically highly unfavourable. To decrease entropy, water molecules aggregate into high order clathrate - like structures around the hydrophobic molecules, joining together using hydrogen bonds.[5] However, these structures can still significantly increase entropy thorough disturbance of the native water molecule hydrogen bonding. To decrease the total entropy of the solution and reduce the amount of

clathrate - like structures, hydrophobic molecules tend to aggregate into multi - molecular structures with a variety of morphologies such as micelles, cylindrical micelles, lamellae and vesicles. The morphology of self - assembled structures depends on a number of factors both related directly to the structure of the amphiphile (geometry of the amphiphilic molecule and chemical composition) and the properties of the solution in which self - assembly occurs (concentration, pH, temperature, additives and used solvents).[1, 4, 6-7]

The shape of the self - assembled structure can be predicted initially from the molecular packing parameter of the amphiphilic molecule which is defined as:[1-3, 7-10]

$$\boldsymbol{P = \frac{v}{a \times l}} \qquad \textbf{(1-1)}$$

where $\boldsymbol{P}$ is the packing parameter, $\boldsymbol{v}$ is the hydrophobic volume of the amphiphile, $\boldsymbol{a}$ is the interfacial area and $\boldsymbol{l}$ is the chain length normal to the interface. Furthermore, the packing parameter is related to the curvature by:[6]

$$\boldsymbol{P = 1 + H \times l + \frac{K \times l^2}{3}} \qquad \textbf{(1-2)}$$

where $\boldsymbol{P}$ is the packing parameter, $\boldsymbol{l}$ is the chain length normal to the interface, $\boldsymbol{H}$ is the mean curvature and $\boldsymbol{K}$ is its Gaussian curvature, both given by the two radii of curvature $\boldsymbol{R_1}$ and $\boldsymbol{R_2}$:[6]

$$\boldsymbol{H = \frac{1}{2}\left(\frac{1}{R_1} + \frac{1}{R_2}\right)} \qquad \textbf{(1-3)}$$

$$\boldsymbol{K = \frac{1}{R_1 \times R_2}} \qquad \textbf{(1-4)}$$

For a spherical micelle the packing parameter has to be ≤⅓. The micelle - forming amphiphilic material must have a large headgroup a_0, and a packed hydrocarbon chain with a small volume ***v***. Micelle - forming amphiphilic materials are called cone - shaped. As the value of the packing parameter increases, the morphology of the aggregates may change accordingly. If the packing parameter value is from ⅓ to ½, cylindrical micelles are formed from truncated cone - shaped molecules. With a further increase in packing parameter value from ½ to 1, vesicle formation is expected. The amphiphilic molecules with packing parameter around 1 are called cylinders and form planar bilayers. Molecules with packing parameter >1 are wedge - shaped and usually self - assemble into inverted structures.[1, 4]

1.3. Liposomes

Liposomes are spherical, self - closed vesicles created from natural lipids present in biological membranes. The research field of liposomes has expanded enormously since initial experiments in 1965 reported by Bangham et al.;[11] they have been utilised in numerous applications across several areas. The unique properties and versatility of liposomes with respect to well - established preparation methods, adjustable composition, size variety and internal capacity has led to widespread of these unique structures to its industrial scale applications such as pharmaceutics, cosmetics, food technology and proteomics.[2, 7, 12]

The main building blocks of liposomes are phospholipids which are derived from either glycerol or sphingosine as presented in Figure 1-3. Phosphoglycerides contain two fatty acids esterified at two of the oxygen atoms of the glycerol and a phosphate ester at

the third oxygen atom. The only exception is sphingomyelin, derived from sphingosine which already contains a long hydrocarbon chain; the second carbon atom is esterified to fatty acid and the sphingosine head group is esterified to a phosphoric acid, which is in turn ester - linked to a choline. The most common fatty acids utilised in liposomes formation contain 16 or 18 carbon atom chains. They are normally unbranched and saturated; however, sometimes they contain one or more non - conjugated double bonds in *cis* - configuration.[7]

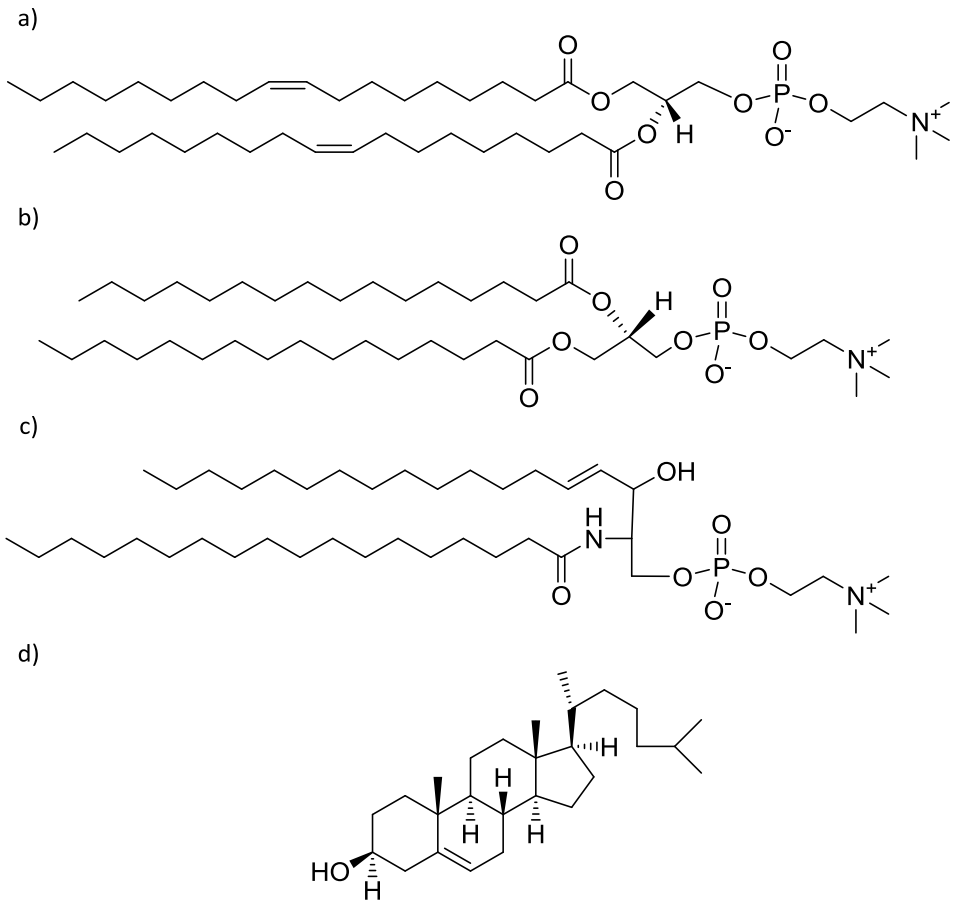

Figure 1-3. Lipids essential for the membranes and vesicles formation: a) 1, 2 - dioleoyl - sn - glycerol - 3 - phosphocholine, b) 1, 2 - dipalmitoyl - sn - glycero - 3 - phosphocholine, c) N - stearoyl - D - erythro - sphingosylphosphorylcholine, d) cholesterol.

1.4. Polymersomes

Polymersomes are spherical, self - closed vesicles created from synthetic polymers. The polymersome formation process is based on the same principles as liposome formation. Block copolymers with the ability to form vesicles are mainly composed of covalently connected hydrophilic and hydrophobic blocks.

1.4.1. Architecture of vesicle - forming block copolymers

The most conventional and standard block copolymers widely used for vesicular structure formation during the self - assembly process are AB linear type polymer systems[13]; however, it has also been reported that more complex structures such as ABA,[14] ABC,[15] ABCA,[16] and ABABA[17] copolymers are able to form vesicles in an aqueous media. Moreover dendritic,[18] macrocyclic,[19] and graft[20] copolymers might also self - assemble into vesicular type structures under strictly controlled conditions. Together with a polymer's chemical composition and architecture complexity, its solubility and vesicle - formation ability in different solvents might change significantly.[21] It is necessary to take into account the choice of solvent or solvent mixtures for specific polymers when planning a self - assembly experiment.

1.4.2. Vesicle morphology

Thermodynamic and kinetic aspects play a crucial role in vesicle morphology. It has been shown that the self - assembly tendencies of block copolymers depends on

many factors such as: the chain stretching in the core; the repulsion among corona chains; and the interfacial energy.[1, 3-4] In addition, the size and shape of the created structures can be controlled during the experiments by adjusting copolymer composition and concentration,[22] the nature of solvent or solvent mixture,[23] the temperature at which self - assembly is performed,[24-25] the dispersity of the amphiphilic polymer[26-27], and the presence of various additives such as surfactants,[28] homopolymers [27] or ions.[29-30]

The molecular mass of the amphiphilic block copolymer is a factor strongly influencing vesicle morphology and vesicular membrane thickness, rigidity, and permeability. An investigation conducted with polybutadiene - b - poly (ethylene oxide) by Bermudez et al.[31] shown an increase of vesicle wall thickness upon increasing the polymer molecular mass. With an increase of bilayer thickness, the rigidity and stability of the membrane increases accordingly.[32]

The chemical composition and architecture of amphiphilic polymers are other important factors influencing the type of structures created in the self- assembly process. The strong tendency towards vesicle formation is strongly related to linear block copolymers; however, it has been reported that amphiphilic macrocyclic systems based on cyclodextrins,[19] cryptands[33] and calixarenes[34] might also form vesicles.

Dispersity is another parameter determining the type of self - assembled structures. The dispersity is defined using the dispersity index $Đ_M$, which is described as a ratio of the weight average molecular weight M_w to the number average molecular weight M_n:

$$Đ = \frac{M_w}{M_n} \qquad \textbf{(1-5)}$$

It is generally suggested that, under the same conditions, individual monodisperse block copolymers and their polydisperse mixtures produce different self - assembly structures. A detailed self - assembly experiment performed on the block copolymer poly (styrene - b - acrylic acid) (PS - b - PAA) revealed that with an increase of the dispersity index of the poly (acrylic acid) block the average size of the formed vesicles decreases.[35]

The ability of block copolymer molecules to self - assemble into a variety of microstructures with different morphologies and sizes is also affected by the solution conditions in which self - assembly occurs (i.e. water content in the solvent mixture, nature of the common solvent, pH, temperature, and polymer concentration). Studies on the system PS_{410} - b - PAA_{25} revealed that micelles and rods appear at lower polymer concentration in comparison to the concentration at which vesicle formation was observed.[22] It has been reported that addition of micro - and millimollar amounts of inorganic salts, acids or based to the self - assembly solution induces morphology changes of the created structures.[36]

1.5. GUV preparation methods

In the last few decades there has been a growing interest in vesicles - their preparation methods, properties and possible applications. For several years great effort has been devoted to the study of vesicle preparation methods with the ability to control the size and shape of the self - assembled structures. Particular interest has been devoted to giant unilamellar vesicles due to their size similarity to living cells.

In general, all methods reported for liposomes formation are also valid for the formation of polymersomes, peptosomes or mixed vesicles. Traditionally, preparation methods are divided in two groups: solvent - free and solvent displacement techniques. In the first group, the vesicle - forming material is placed in contact with an aqueous medium in its dry state and is gently hydrated to form vesicles. This technique offers the possibility to produce the self - assembled structures without the use of organic solvents (and possible system contamination), which can be advantageous for certain future applications. In the second group of preparation methods, the amphiphilic material is first dissolved in the required organic solvent or solvent mixture and then mixed with an aqueous solution under stirring. Upon removal of the organic phase, polymersomes are formed. These conditions are theoretically solvent - free; however, practically it is not possible to completely remove all solvent from the system and its residues may interfere with other objects in further studies and/or applications.

Depending on the individual system properties, each method can yield mixed self - assembled structures such as micelles, vesicles or tubes.[10] After fabrication of vesicles, their size distribution can be decreased by vortexing, extrusion, sonication and freeze - thaw cycles or by combination of these methods.[7, 37-38]

1.5.1. Solvent - free methods

Several solvent - free GUV preparation methods have been developed; however, there are two which are the most popular: film and solid rehydration, and electroformation.

1.5.1.1. Film and solid rehydration

One of the first methods of vesicle preparation was invented in 1969 by Reeves and Dowben; it is known as the rehydration method.[39] Initially, amphiphilic material is dissolved in an appropriate solvent (or solvent mixture) and a thin film of material is produced on a solid surface by evaporating the solvent using a rotary evaporator, high vacuum pump or under a nitrogen stream. Upon addition of an aqueous solution, water hydrates the polymer layers which start to detach from the solid surface and finally form vesicles.[40] This self - assembly method is most suitable for lipids or polymers that are charged; however, it has been shown that GUV formation can be achieved using this method with amphiphilic molecules that are in zwitterionic form if the dry film contains nonelectrolytic monosaccharides (fructose, mannose or glucose).[41] The presence of these molecules between the layers of amphiphilic material increases the osmotic pressure differences during the hydration step and enhances GUV formation. It has also been shown, that the amount of deposited polymer or lipid on the glass surface has a significant influence on the vesicle size and size distribution.[42] Furthermore, it is important to note that the spontaneous swelling methods must be carried out in the amorphous state above the glass transition temperature (T_g) of the amphiphilic material.[25]

The method of solid rehydration is analogous to the film rehydration method; the only difference is that the amphiphile is not deposited on the solid surface as a thin layer, but is hydrated directly in an aqueous solution as a bulk powder. To achieve vesicle formation a longer and more vigorous sample agitation is required in comparison to the film rehydration method.[27, 37]

Both film and solid rehydration methods were reported to be more suitable suitable for preparing rather small multilamellar vesicles than giant unilamellar vesicles.[7, 37]

1.5.1.2. Electroformation

The electroformation method was invented by Angelova and Dimitrov in 1986, in which the effects of lipid self - assembly in aqueous media and electroosmosis were combined to allow the formation of vesicles with a significantly shorter preparation time than by the standard rehydration method.[40] This technique is similar to the film rehydration method; however, the amphiphile is spread on a pair of electrodes instead of on a solid surface. The electrodes can be made from indium tin oxide (ITO) - coated glass slides[13, 38, 40] or platinum wires[43]. This method allows the creation of homogeneous GUVs using different electric current parameters and varying composition of hydration media. Upon addition of an aqueous solution, either alternating (AC) or direct electric current (DC) is applied to increase and facilitate hydration of the amphiphilic film. The electroformation method has been shown to be an effective method for producing giant unilamellar vesicles which are characterised by a long stability period.[44] This property is a significant advantage, because of the possibility to use GUVs in other experiments without concerns related to the microstructure stability. Another beneficial aspect is that vesicles created by this method often remain connected to the residual amphiphilic film on the electrode, which can be used as back pressure during the micromanipulation experiments. GUVs are often prepared in a sucrose solution and later transferred into a visualisation chamber filled with isotonic glucose solution. This leads to easier recognition and characterisation of the vesicles because of the contrast difference between their

interior and exterior. In addition the density difference between the internal sucrose solution and the external glucose solution makes the vesicles sink to the bottom of the visualisation chamber where they remain stable[45] and can be visualised.

1.5.2. Solvent displacements methods

1.5.2.1. Transformation of single emulsions

Lipid stabilised emulsion

There are two steps in the preparation of vesicles from lipid stabilised w/o emulsions. Initially, a bilayer - forming lipid is dissolved in an appropriate organic solvent and mixed with an aqueous solution under vigorous stirring to produce an emulsion. Then the emulsion is poured into a two - phase system consisting of an upper oil phase containing the lipid and a lower aqueous phase. Due to the density differences, water droplets migrate from the top of the emulsion to the bottom and disturb the two phase system. Vesicles are formed in the lower aqueous phase. This system was reported to be suitable for GUV preparation.[46]

Surfactant stabilised emulsions

This method is also called the lipid - coated ice droplet hydration method. Initially a surfactant - stabilised w/o emulsion is generated by a micro - channel emulsification system. In comparison to the previous method, the water droplets are effectively stabilised by a surfactant mixture and not with bilayer - forming lipids. The water droplets are frozen by transferring the emulsion into liquid nitrogen. GUVs are formed

after replacement of the surfactant mixture with the bilayer - forming amphiphile under conditions in which the water droplets remain frozen; and replacement of the oil with an aqueous suspension containing small vesicles made from the lipids of which the final GUVs are made.

1.5.2.2. Transformation of a double emulsions

Using a microfluidic technique it is possible to produce w/o/w lipid - stabilised double emulsions which can be used as a starting system for GUV preparation. In this specialised system each internal water droplet is coated with the lipid molecules in such a way that the lipid hydrophilic head points towards the water droplet and hydrophobic tail towards the external oil. Removal of the volatile oil (organic solvent) leads to the formation of giant unilamellar vesicles. The advantage of this method is that it allows encapsulating large amounts of water soluble molecules inside the produced GUVs, giving a large number of vesicles with a narrow size distribution in a short time. The main drawback of this technique is the possible difficulties with complete solvent removal from the vesicular solution.[2, 7, 21]

1.6. The cell membrane and membranes within the cell

Biological membranes are essential for all living organisms to stay alive. Together with the cytoskeleton they form a structure of the smallest structural, functional and biological unit of every living organism - a living cell. Moreover, all of

the intracellular structures are surrounded by membranes and represent closed membrane vesicles. Due to selective permeability of all cell membranes they are responsible for control and regulation of the composition of internal fluids inside every coated structure. Membranes are responsible for regulating and sending information signals between cells; they also participate in energy accumulation and release through processes such as oxidative phosphorylation and photosynthesis. Therefore, they are not just a semi - permeable barrier separating internal fluids of coated structures from the external media; they play an active part in the life of the cell.

1.6.1. Structure of the cell membrane

A cell membrane is a fundamental part of every living cell - it separates the cell interior and external environment. Moreover, it sustains selective permeability which allows regulation of the passage of molecules and ions into and out of the cell.[47]

The cell membrane is a complex system created from a continuous double layer of lipid molecules supported by membrane proteins, and additional biomolecules. The majority of the biological membranes are built mainly from three classes of lipids: phospholipids, glycolipids and cholesterol.[47-48] The membrane is asymmetrical - the lipid composition differs between the inner and outer monolayer accordingly to their functions. The fluid mosaic model introduced by S. J. Singer and G. l. Nicolson in 1972[49] accurately describes the structure of a cell membrane. According to the proposed description a cell membrane is described as a two - dimensional liquid crystalline state supported via non - covalent interactions of the hydrophobic lipid chains. Phospholipids are able to freely perform movements within the membrane

such as: lateral diffusion (diffuse within their lipid layer); rotation (rotate around their own long axis); or flexion (bending of hydrocarbon chains). It is also known that phospholipids are able to perform sporadically (less than once per month for an individual molecule) a “flip - flop” movement, where the phospholipid molecule exchanges between internal and external membrane layer.[47-49]

1.6.2. Synthetic biological cell models

In the last few years, tremendous progress has been made in the exploration of the living cell. Knowledge of cellular signalling, gene regulation and cellular structure has been expanded significantly; however, the phenomenon of the creation of cells from prebiotic origins is still unknown. The biological cell is a very compartmentalized system where every part is related to each other in a unique way and therefore it is difficult to study their properties and overall influence on the cell in such a complex structure. The way to overcome this hindrance is to study separately each of the cell components and to create minimal model systems with the ability to mimic compartments of a biological cell. Initially, studies on synthetic cell membranes were initiated and subsequently models simulating various functional aspects of a biological cell were developed.

1.6.2.1. Cell membrane models

Pure lipid monolayers and bilayers

Pure lipid monolayers and bilayers are sometimes called “black lipid bilayers” (BLB) because of their appearance under an optical microscope. The BLB model was first reported by Mueller et al. [50] in 1962. It was a pioneering work towards mimicking a biological cell membrane; due to their membrane thickness comparable to that of plasma membranes together with an adjustable lipid composition, BLB’s are currently considered as the simplest model of a biological membrane suitable to be employed in studies on the basic physical characteristics of the natural membrane. The lipid bilayers usually exist as membrane stacks (lyotropic liquid crystals) and lipid monolayers in free - standing membrane form. However, none of these model membranes are good candidates for most studies. One of the main limiting factors is the poor stability of lipid monolayers [51-52] which eliminates the possibility to utilise this model in many membrane studies. This property also limits characterisation of the membrane with powerful methods such as AFM, TEM, SEM or SPR. Another drawback of this model is the fixed plane shape which is not suitable for particle uptake and release studies.

Supported bilayers

In order to increase the stability and robustness of initially prepared BLB models, the technique of preparing supported bilayers was developed.[53] The stability problem was eliminated by using a solid support under the lipid bilayer [54], which extended the lifespan of the created lipid bilayers to weeks or even months [55]. Another advantage of solid supported bilayers over the standard BLB model is that water present between the lipids layer and the support maintains the membrane fluidity which is important for membrane studies. Moreover, because of the solid support this model can be

characterised using powerful membrane characterisation techniques such as AFM, SEM or SPS. The main drawbacks of this technique are lack of flexibility, and coupling between lipid membrane and support, which significantly influences lateral diffusion.

Polymer cushioned bilayers

To improve the stability and flexibility of lipid membranes, further modifications were introduced to the model system. The surface of the solid support was cushioned with a layer of hydrophilic polymer which increased the gap between the lipid bilayer and the solid support.[56-57] Moreover, in comparison to supported bilayers this alteration increased the amount of aqueous solution between the species and improved the membrane flexibility without decreasing its stability. The ordinary supported bilayer models do not prevent undesirable non - specific interactions between the protein and the surface of the solid support, triggering denaturation; however, a hydrated protein support makes this system a more suitable environment for the proteins, which could be used in interaction studies with membranes.[58]

Vesicles (liposomes and polymersomes)

A free lipid or amphiphilic polymer membrane is able to close up on itself to form a vesicle which encloses an aqueous solution in its interior. These structures produced with a size comparable to that of a cell can be considered as simple cell models because they capture a fundamental feature of cellular membranes - compartmentalisation.[6, 21, 43, 59-61] The GUV membrane is also characterised by extensional and bending elasticity which are typical for biological membranes and are not mimicked by other models.[6] GUVs can be produced either from naturally occurring lipids [2, 7, 40-41, 62] with a composition similar to biological membranes, or from synthetic block copolymers.[8, 10, 13, 37, 63-65] The mechanical and chemical

properties of vesicles are strongly related to the characteristics of their building blocks.[31-32, 63, 65-66] Liposome membrane characteristics are not easily tuneable due to the chemical properties of lipids - they possess unsaturated fatty acids which are sensitive to oxidation and ester bonds which hydrolyse easily. Thus, liposomes have a limited chemical stability and lifespan.[2, 67] In contrast to liposomes, polymersomes are easily tuneable with ability to adjust bending and stretching elasticity, thickness and permeability by changing the composition of their building blocks.[6, 21, 59, 68]

Micrometre - sized giant vesicles are considered as suitable objects for mimicking natural cells due to their size similarity. Therefore experiments on this specific type of self - assembled structure were continued with the aim of mimicking different aspects of the cell.

1.6.2.2. Mimicking the cell membrane using GUVs

Asymmetric membrane

Initially, GUVs were fabricated from a single type of lipid molecule; however, with improvements in preparation techniques, fabrication of vesicles from mixed materials became possible. The first step towards the preparation of naturally asymmetric membranes was GUVs fabricated from natural lipid extracts.[7, 69-70] This type of vesicular membrane is particularly interesting, due its natural composition and asymmetry as found in cell membranes. Also, it is difficult to produce asymmetric membranes stable for at least a couple of hours using a purely synthetic mix of lipids. The lipids in such structures tend to phase separate into domains which results in membrane destabilisation and finally liposome collapse.[59]

Studies on asymmetric vesicular membranes including experiments with giant polymersomes are more promising than research conducted on liposomes. Polymersomes are in general more stable and rigid; moreover, their building blocks can be tailored easily to adjust the properties of the fabricated structures.[8-9, 59, 68] One of the most common methods of achieving GUVs with asymmetric membranes is mixing the same block copolymers with a different block ratio or different molar masses.[27-28] Another technique of preparing mixed vesicles is based on adding lipid [71-73] or peptide [74-76] additives in a required concentration to the polymer mixture followed by a standard self - assembly procedure.

Functionalised membrane

Understanding the physical and chemical properties of natural membranes is an important step towards the creation of a synthetic cell. Surface modifications are another important aspect of the cell membrane which is crucial for maintaining its functions, activity and selectivity. Knowledge in this field was expanded enormously by experiments involving functionalised block copolymers. Synthetic techniques and methodologies are well developed nowadays, allowing complex functionalisation of block copolymers required to mimic naturally occurring ligands and receptors on the surface of cells. The most common biological ligands introduced on the surface are sugars, aptamers, peptides and proteins.[60, 68] There are three main routes to obtain vesicle surface modification: conjugation of a functional unit to a formed vesicle surface; self - assembly of a polymersome from mixed functionalised and non - functionalised block copolymers; and self - assembly of block copolymers having functionalised hydrophilic blocks.[68, 77-79] The main requirements for such surface modifications are their availability in an aqueous environment, prevention of

crosslinking between vesicles and ligands, and irreversibility of functionalisation. Moreover, functionalisation should minimally interfere in the hydrophobic - hydrophilic balance of the block copolymer otherwise the functionalised macromolecules can lose their ability to form GUVs. The literature on polymersome surface modification shows a variety of chemical methods allowing conjugating ligands and other functional entities to vesicular surfaces.

Protein incorporation

Incorporation of fully functional proteins into synthetic membranes is another important step towards understanding the phenomena of natural cells. The pioneering step was made by Rigaud et al. [80] in 1988 by successful incorporation of a protein bacteriorhodopsin, the light - driven proton pump from *Halobacterium halobium*, into a LUV membrane. Following this discovery, two main techniques of protein incorporation into the membrane of synthetic vesicles were established. The first is based on a fusion of LUVs containing incorporated protein with target GUVs.[81-82] Another method utilises large proteoliposomes: initially, structures are partly dried on the electrode surface and then the electroformation process is performed which results in the formation of GUVs containing incorporated membrane proteins.[83]

1.7. Transmembrane transport in cells

Biological cells are equipped with a variety of membranes which introduce compartmentalisation into their structure and separate them from the surrounding medium; however, the cells cannot survive without strictly controlled exchange of required substances with their environment. The collection of cellular mechanisms

that regulate the passage of solutes and molecules thorough the cell membrane is called membrane transport.[84] Due to a selective permeability of the biological membranes, the cells have the distinct ability to separate substances with different chemical and physical properties, maintain a gradient of various compounds between the interior and exterior and be permeable to certain types of substances, while not to others. In combination with transport proteins, membrane play a crucial role in the exchange system between the surroundings and the cell interior.[47] There are several types of membrane transport, depending mainly on the physical and chemical characteristics of the transported cargo, and on the thermodynamic aspects of the passage through the cell membrane.

Every process which occurs in living cells must comply with basic thermodynamic principles. Keeping in mind that the biological cell is a specialised compartment separated from the surroundings with a membrane selectively permeable to various substances, therefore thermodynamically the flow of substances from one compartment to another can occur in the direction of a concentration, or electrochemical, gradient, or against it. Exchange in the system which occurs in the direction of the gradient is thermodynamically favourable due to a decrease of potential and therefore is no need for input of external energy to the system (passive transport); however, if transport is performed against the gradient, it increases the potential of the system and therefore it requires an input of external energy to the system (active transport). A general principle of thermodynamics, which regulates the transport of substances thorough membranes, states that the exchange of free energy, $\Delta \boldsymbol{G}$, as a result of the transport of a mole of a substance with a concentration $\boldsymbol{C_1}$ from one compartment to another with concentration $\boldsymbol{C_2}$ is:[84]

$$\Delta \boldsymbol{G} = \boldsymbol{R}\mathbf{T}\,\mathbf{log}\frac{\boldsymbol{C_2}}{\boldsymbol{C_1}} \qquad \textbf{(1-6)}$$

Where $\boldsymbol{R}$ is the gas constant and $\boldsymbol{T}$ is temperature expressed in K. If $\boldsymbol{C_2} < \boldsymbol{C_1}$ then $\Delta \boldsymbol{G} < \mathbf{0}$ and the process is thermodynamically favourable; moreover it occurs without the external energy input to the system. Upon reaching equilibrium, where $\boldsymbol{C_2} = \boldsymbol{C_1}$ and $\Delta \boldsymbol{G} = \mathbf{0}$ the process automatically terminates.

1.7.1. Passive transport

Passive transport is a passage of atoms, molecules and other biochemically important compounds across the cell membrane without any input of external energy; the process is driven by an increase of the system entropy. The most common types of passive transport through biological cells are diffusion, facilitated diffusion and osmosis. The rate of passive transport is influenced by the nature of the bilayer (i.e. organisation and characteristics of the membrane lipids and proteins) and characteristics of the transported substance such as hydrophobicity, size, charge and concentration gradient.[84] The relative permeability of a phospholipid bilayer differs significantly for various substances that can be found in the surroundings of the cell, as presented in Table 1-1.[47]

Table 1-1. Relative permeability of various substances thorough a phospholipid membrane.

#	Type of substance	Example of substance	Relative permeability
1.	Gases	N_2, O_2, CO_2	Permeable
2.	Small uncharged polar molecules	Water, ethanol, urea	Fully or partially permeable
3.	Large unchanged polar molecules	Glucose, fructose, galactose	Not permeable
4.	Ions	K^+, Ca^{2+}, Cl^-	Not permeable
5.	Charged polar molecules	ATP, amino acids, glucose 6 - phosphate	Not permeable

1.7.1.1. Simple diffusion, osmosis and facilitated diffusion

Diffusion is a spontaneous movement of material through a membrane down a concentration gradient until the concentration is uniform throughout and reaches equilibrium. The velocity of diffusion through a pure phospholipid membrane depends on the concentration gradient, hydrophobicity, size and charge of the diffusing molecules.[47-48] Gases and small uncharged polar molecules (as presented in Table 1-1 1 and 2) are small enough to freely diffuse through a cell membrane between lipid molecules and do not require any assistance from embedded membrane proteins. Water molecules are also able to freely diffuse through a cell membrane induced by the water concentration difference between the internal and external compartments down a concentration gradient; diffusion of water molecules is called, exclusively, osmosis.[47]

Many large uncharged polar molecules and ions (as presented in Table 1-1 3 and 4) are insoluble in lipids and/or too large to fit through the membrane pores, and therefore

need assistance from special membrane proteins to cross the membrane. This type of transport is called facilitated diffusion and it is considered as passive diffusion since it does not require any input of external energy.[47] Unlike simple diffusion where the rate of the process is linear with the concentration gradient, facilitated diffusion is saturable with respect to the concentration difference between two compartments separated by the cell membrane.[48]

1.7.2. Active transport

Active transport is a specialised movement of molecules in which they penetrate through the cell membrane in a direction against their concentration or electrochemical gradient and therefore an external energy input to the system is crucial to achieve a high concentration of the required substances within the cell in comparison to its surroundings. Active transport is usually involved in accumulation of molecules vital for maintaining cell functions such as ions, glucose and amino acids. There are two main types of active transport: primary and secondary. In primary active transport, chemical energy in ATP (adenosine triphosphate) is utilised directly to transport a cargo, while in secondary active transport, initially chemical energy is used to generate electrochemical gradient which is subsequently employed in payload carriage.[47-48]

1.7.2.1. Primary active transport

Primary active transport is performed by membrane proteins - pumps called ATPases which use the cell's metabolic energy to transport their cargo across the plasma membrane. One of the best known examples of primary active transport in the animal world is the sodium - potassium pump which is responsible for maintaining the potential of the cell. ATPases obtain energy required to perform active transport by hydrolysis of ATP; however, there are other proteins performing primary active transport which use redox potential or photon energy to maintain their own activity.[48]

1.7.2.2. Secondary active transport

Secondary active transport is performed by transmembrane proteins which perform active transport of molecules and ions against their concentration gradient; however, in contrast to primary active transport, metabolic energy is not used directly to perform transportation. Secondary active transport is based on an electrochemical gradient created by pumping ions which are used as the driving force for the process; they are allowed to move down their electrochemical gradient, which is a favorable process, but at the same time against their concentration gradient which is unfavorable.[48] There are two mechanisms of secondary active transportation: antiport and symport; in antiport, two species of ions are carried across the membrane in opposite directions, while in symport, species are carried in the same direction. In both mechanisms one of the ion species is called the driving ion, because its

movement down its concentration gradient generates energy required for driving uphill another molecule (driving molecule).[47-48]

1.7.3. Bulk Transport

As described above, passive or active transport can be performed for water and other small molecules which can penetrate a cell membrane by diffusion, by being carried by special membrane proteins or by being pumped by membrane pumps against their gradient. These mechanisms are suitable for small objects; however, cannot be applied for transporting macromolecules or even particles. To overcome this hindrance, cells have developed a separate mechanism named endocytosis for large cargo such as proteins or polysaccharides. There are three main types of cellular endocytosis: pinocytosis, phagocytosis and receptor - mediated endocytosis (RME), which differ in the type of carried material (as presented in Figure 1-4).[47-48]

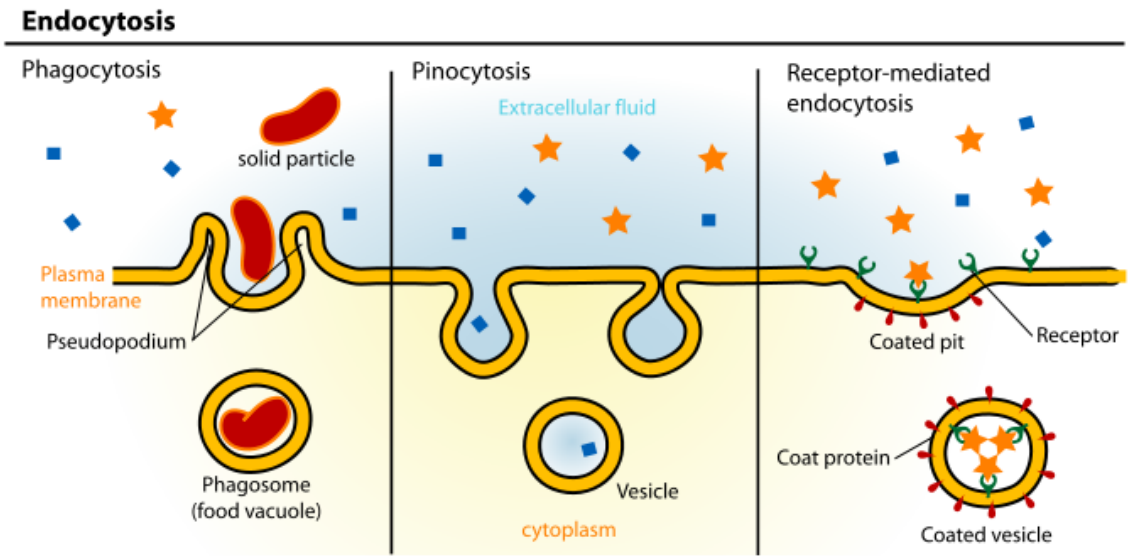

Figure 1-4. Three main types of cellular endocytosis.[85]

1.7.3.1. Pinocytosis

Pinocytosis is one of the endocytosis pathways used for absorption of extracellular fluids into the cell. This mechanism is non - selective and during the process all solutes present in the surrounding solution are transferred to the cell in small vesicles. Pinocytosis, unlike phagocytosis or RME, engulfs already dissolved and processed molecules which are suitable for direct absorbtion by the cell. Pinocytosis is mainly involved in obtaining nutrients from the extracellular surroundings required for a cell to maintain its biological functions.[47]

1.7.3.2. Phagocytosis

Phagocytosis is another endocytosis pathway utilised in absorbtion of extracellular solid particles into the cell, using vesicles called phagosomes. Unlike pinocytosis, phagocytosis is specific for absorbed particles; however, the cargo is transported in bulk and, upon fusion with a lysosome containing hydrolytic enzymes, broken down inside the cell.[47] Phagocytosis is developed in a variety of organisms; some single celled organisms use phagocytosis for obtaining nutrients, while multicellular animals utilise phagocytosis as an effective way to eliminate pathogens and cellular debris.

1.7.3.3. Receptor - Mediated Endocytosis

Receptor - mediated endocytosis (RME) is the most specialised type of endocytosis which involves special membrane proteins containing receptor sites specific for internalised molecules.[47-48] RME, unlike pinocytosis, is a selective mechanism uptake of macromolecules, which is initiated by binding of extracellular ligands to a specific receptor present on the membrane surface. This pathway is widely utilised by cells to obtain desired biologically - active substances such as hormones, antibodies or metabolites; however, in some cases, undesired macromolecules can also be transported through the plasma membrane to the cell interior, such as toxins or viruses.[47-48] A general scheme of RME is presented in Figure 4-1 (in Chapter 4). There are two main pathways by which RME can occur - the classic, clathrin - mediated and the non - classic lipid - raft dependent route.

Clathrin mediated endocytosis is a widely known and reported process by which all up - to date known eukaryotic cells absorbs nutrients, antigens, growth factors, recycling receptors and in some cases even pathogens.[86] This type of uptake of material inside the cell was first recorded by Roth and Porter in 1964.[87] They obtained electron microscopy images of vesicles with specific coats; however, not until 1976 Pearse discovered that the protein clathrin forms supports around vesicles and described this phenomenon as “vesicles in a basket”.[88] The formation of clathrin - coated vesicle includes five stages: initiation, cargo selection, coat assembly, scission and finally uncoating. The initial two stages are performed by cargo receptors, adaptor and accessory proteins, which triggers a soluble form of clathrin present in the cytosol called triskelia, to polymerise into hexagons and pentagons which forms a “basket” and supports formation of vesicle.[89] Clathrin is unable to bind directly to the plasma

membrane or to cargo receptors; moreover, clathrin is fully dependent on adaptor proteins and their complexes, which provide the link with plasma membranes and coordinates assembly of coatings around the endocytic vesicle.[86, 89-91] Upon internalisation, clathrin uncoats and the vesicle fuses with endosome.

One important non - classical lipid - raft mediated endocytic pathway involves protein called caveolin, which is present in cell membrane lipid rafts and therefore is called the caveolin - mediated pathway.[91] A caveolin is responsible for stabilisation of a specialised, flask - shaped vesicle, rich in sphingolipids and cholesterol plasma membrane microdomains called caveolae.[92] Caveolae were first observed by electron microscopy by Palade[93] and Yamada[94], and were described as 60 - 80 nm pits in plasma membrane; however, their functions at that time were unknown. The first hypothesis about endocytic functions of caveolae was formed by Bruns et al. in 1968.[95]

Caveolae remain stable at the cell surface for long periods; however, their internalisation can be induced by various agents. These include single molecules of sterols and glycosphingolipids,[96] as well as large molecular complexes such as cholera toxin,[97] simian virus 40[98-99] and bacteria.[100] Upon invagination, caveolae can fuse with an endosome (analogous to classic pathway) or with caveosomes.

Data published by Rejman et al. revealed that RME pathway by which cells internalise certain cargo is strongly dependent on particle size.[101] Collected data concluded that microspheres with a diameter lower than 200 nm are endocytosed thorough the classic clathrin - mediated pathway. Upon increase in particle size, a shift to non - classic lipid - raft - mediated internalisation is observed; moreover, this uptake mechanism became dominant for microspheres with a diameter of 500 nm.

2. Vesicle Formation Using Model Molecules

2.1. Introduction

Vesicle electroformation is the initial step in this project. Electroformed polymersomes are to be used in designing a synthetic cell model; however further research requires a stable, reliable and reproducible way of generating giant unilamellar vesicles (GUVs). The optimisation of the electroformation process can only be achieved using experimental systems with many trials; however it is a material and time consuming process. Synthetic cell models are to be created from novel amphiphilic glycopolymers synthesised within our group; however synthetic strategies are usually time consuming and complex procedures which result in small amounts of the desirable product. With this in mind, the electroformation process was investigated in depth using model vesicle - forming species to determine the patterns of change in experiments produced by changing variable parameters, and also to reduce the amount of used resources, and time.

The study on the model lipid 1, 2 - dioleoyl - sn - glycerol - 3 - phosphocholine (DOPC) was initiated in order to become familiar with the electroformation technique, methodology of sample preparation and characterisation of formed structures. The lipid DOPC was chosen as the starting material for the electroformation study due its known self – assembly properties; it easily forms liposomes of differing sizes, due to its low transition temperature and optimal hydrophobic - hydrophilic block ratio.[102-104] Therefore it is a suitable material for improving the electroformation technique as it should determine the correlation between typical vesicle properties (morphology, size,

distribution in solution) and electroformation parameters as its derivatives L - α - phosphatidylcholine (egg PC) and 1, 2 - dioeoyl - sn - glycerol - 3 - phosphate (DOPA).[105]

Following electroformation experiments on the lipid, it was decided to begin electroformation studies on the model block copolymer poly (butadiene - b - ethylene oxide) (PBd - b - PEO). It was anticipated that the polymersomes electroformation tendencies would be more closely related to the glycopolymersomes than liposomes due to block structure, high molecular mass and macromolecule size. The block copolymer PBd - b - PEO was chosen as the model polymersome forming material for the study due its known self – assembly properties; it is suitable for the formation of stable vesicles with a variety of sizes depending on the block ratio and self – assembly method.[8, 38, 65]

It has been reported that during the electroformation process there are a number of variables which have a significant influence on liposome formation: quantity of compound deposited on the glass surface and quality of the prepared film, electroformation time, detachment time, electric field current, electric field voltage, electric signal frequency and electrical signal waveform.[2, 105-106] Variation in one of the parameters might also be significant in polymersome electroformation and therefore it was decided to investigate the relationship between electroformation factors and polymersome formation. Unfortunately, due to resources limitation it is impossible to review every set of parameters experimentally, thus a design of experiment (DOE) approach was used to determine the most important factors during electroformation with PBd - b - PEO. All of this is hoped to provide a greater understanding of the electroformation process, which will allow us to optimise the experimental conditions

to achieve an appropriate average diameter of polymersomes, and glycopolymersomes in future research.

2.2. Liposomes electroformation from DOPC

During GUV electroformation studies with DOPC, two main stages in the process can be distinguished. Initially it was important to determine the conditions under which the lipid generates vesicles. Following this, optimisation of the vesicle forming process was performed.

The electroformation process has a number of variable parameters which have significant influence on the formation of vesicles:

- Quantity of lipid or polymer deposited on the glass surface
- Solvent for film preparation
- Electroformation time
- Detachment time
- Electric field current
- Electric field voltage
- Electric signal frequency
- Electrical signal waveform.

The electroformation experiment is initiated by preparation of lipid film covering ITO glass slide. A fixed volume of the lipid DOPC solution in chloroform is applied to the conductive side of the glass slide and left in a desiccator for 2 hours for the solvent evaporation and lipid film formation. Following evaporation the electroformation process is performed using AC with sinusoidal waveform, fixed voltage and frequency for a required time. Finally a detachment stage is commenced using AC with square waveform, fixed voltage and frequency.

Data presented in Table 2-1 provides a summary of the variable conditions examined during the research on liposome electroformation. All the experiments were replicated three times in order to enhance the reliability of collected data.

Following a thorough literature review it was decided to use a voltage of 1.2 V, and a frequency of 10 Hz to 5 Hz, sin to square waveform; these parameters were listed to be suitable for GUV formation from lipids.[103, 106-107] The main research goal was to achieve stable vesicle formation, and to determine the values of other variables facilitating the self - assembly process.

Initial Experiments

Experiments were initiated with conditions #1 listed in Table 2-1. These initial conditions however were deemed to be unsuccessful, due to the sample failing to form any structures similar to lipid self-assembly structures. The resulting structure formed only asymmetrical lipid aggregates without any regular structure.

Lipid self-assembly structures are affected by several variables; these include time allocated for solvent evaporation, regular film formation on the glass slide and electroformation time. Experiments with conditions #2 were performed to examine

the impact of longer evaporation and electroformation times; however there were no changes observed in the electroformation solution. The structures formed had the same range of size, lack of symmetry and regular structure, and suggested that the concentration or volume used for the film preparation were insufficient to form the required structures.

Influence of Deposited Lipid Mass

Further analysis, following experiments with conditions #2, concluded that the lipid concentration used for the film preparation is insufficient; due to excess of solvent, the lipid solution spreads on the glass surface and forms a very thin layer inadequate for liposome formation. Conditions #3 and #4 were designed in order to investigate the influence of deposited lipid mass on experimental results; and are analogues of conditions #1 and #2, differing in the quantity of deposited lipid on the glass surface. Experiments using conditions #3 resulted in asymmetric aggregate formation; however experiments with conditions #4 resulted in the formation of small, micelle – like structures.

Table 2-1. Conditions used for the electroformation of GUVs from DOPC.

#	Concentration (mg/ml)	Volume used for film preparation (µl)	Film evaporation time (h)	Total time (electroformation + detachment) (h)	Observation
1	1	5	2	2+0.5	asymmetrical aggregates
2	1	5	16	4+1	asymmetrical aggregates
3	1	20	2	2+0.5	asymmetrical aggregates
4	1	20	16	4+1	micelle - like
5	10	5	16	4+1	vesicles aggregates
6	10	5	16	3+0.5	vesicles aggregates
7	5	5	16	3+0.5	asymmetrical aggregates
8	5	5	2	3+0.5	asymmetrical aggregates
9	10	5	2	3+0.5	many vesicles
10	10	5	2	1.5+0.5	many vesicles
11	10	3	2	3+0.5	many vesicles
12	10	3	2	4+0.5	larger
13	10	3	2	4+1	very large

All experiments were performed using waveform from sin to square and frequency from 10 Hz to 5 Hz; voltage was 1.2 V and temperature was kept stable at 18 ^{o}C, and these parameters were not changed during the experiment.

Increase in Mass of Deposited Lipids

Due to changes in experimental procedures, in particular the results acquired through increasing the mass of deposited lipid, it was decided to continue investigation with increased (2.5 times more than in initial preceding experiments) mass of deposited lipid as presented in #5, and reduced electroformation time as presented #6. Both sets of conditions resulted in reproducible liposome aggregate formation with the variety of sizes as presented in Figure 2-1. The initial intention to establish the conditions required to form liposomes was successful - vesicles were formed; however further

research was continued in order to optimize liposome electroformation conditions and achieve single GUV formation.

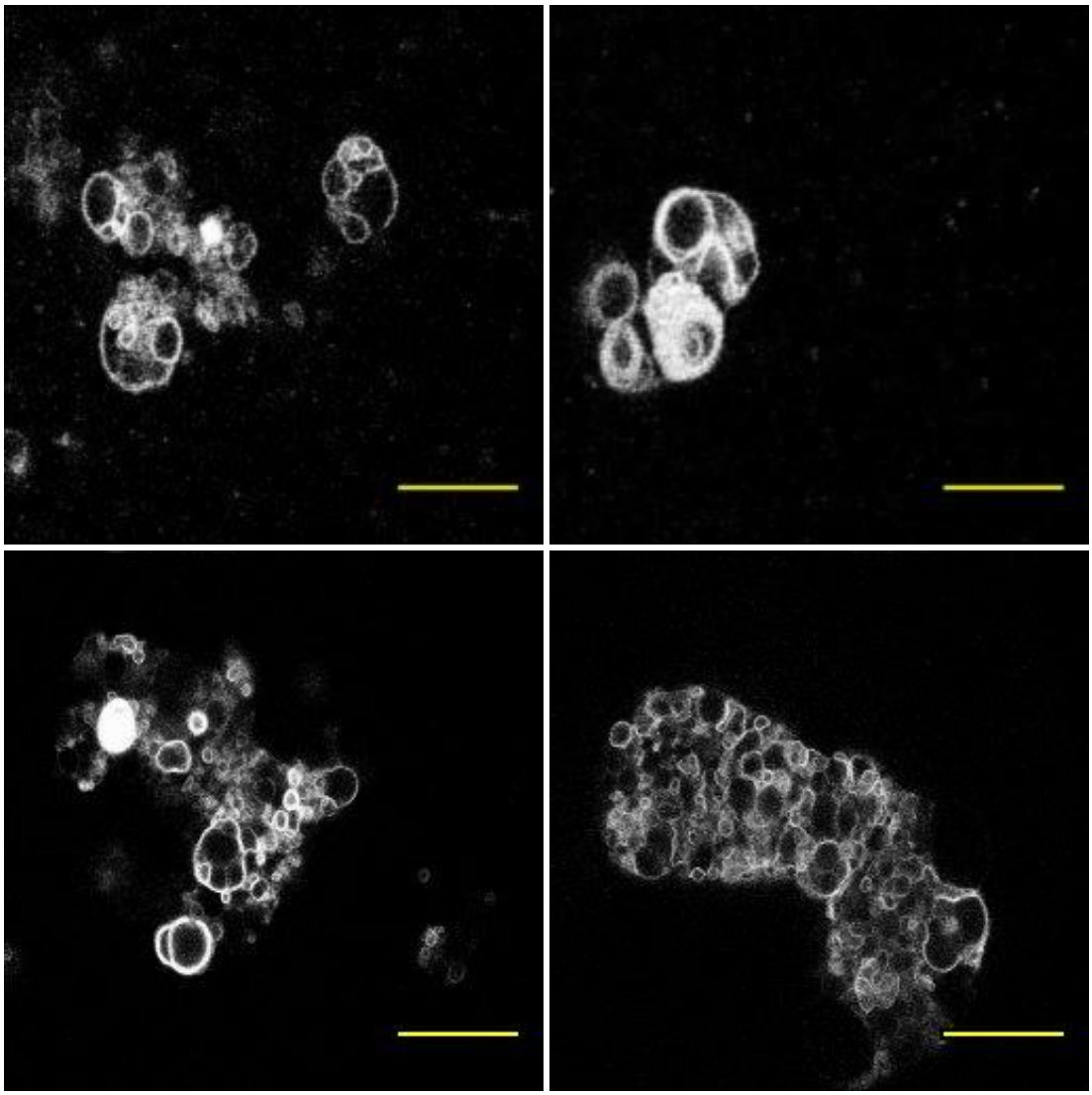

Figure 2-1. Confocal microscopy images of giant liposome aggregates. Images were captured after electroformation under conditions #6 (as presented in Table 2-1.). Hydrophobic fluorescent dye Nile Red was used for sample visualisation. Scale bar size is 50 µm.

Optimisation of GUV Formation

The optimisation process was initiated using parameters analogous to #6 but with 0.5 times lower concentration of lipid solution as listed in #7, and decreased solvent evaporation time as listed in #8. Both sets of these conditions did not result in vesicle formation, moreover only asymmetrical aggregates were formed. The results produced, informed the decision not to change the concentration of the starting lipid solution, but to reduce the volume of deposited lipid on the glass surface. Conditions employed for the optimisation processes are presented in #7 - #13. The optimisation process was performed varying two parameters: volume of deposited lipid and electroformation/detachment times. The largest single GUVs were achieved using the electroformation conditions #13 and images of the formed structures are presented in Figure 2-2. Large amounts of vesicle aggregates and single unilamellar vesicles were detected in the electroformation solution.

2.2.1. DOPC vesicles formed under optimal conditions

Experiments using condition #13 presented in Table 2-1 resulted in reproducible GUV formation. Significant amounts of giant liposome aggregates were detected in the sample; however high number of single units was present in the specimen as presented in Figure 2-2.

Giant liposomes were formed with an average density of 143 ± 14 vesicles per square mm with an average diameter of 26.0 ± 2.0 μm calculated over the population of 430 vesicles. DOPC lipid has a strong tendency to form liposomes with a size from

20 µm to 30 µm as presented in the Figure 2-3; 50 % of the whole population is in this size range.

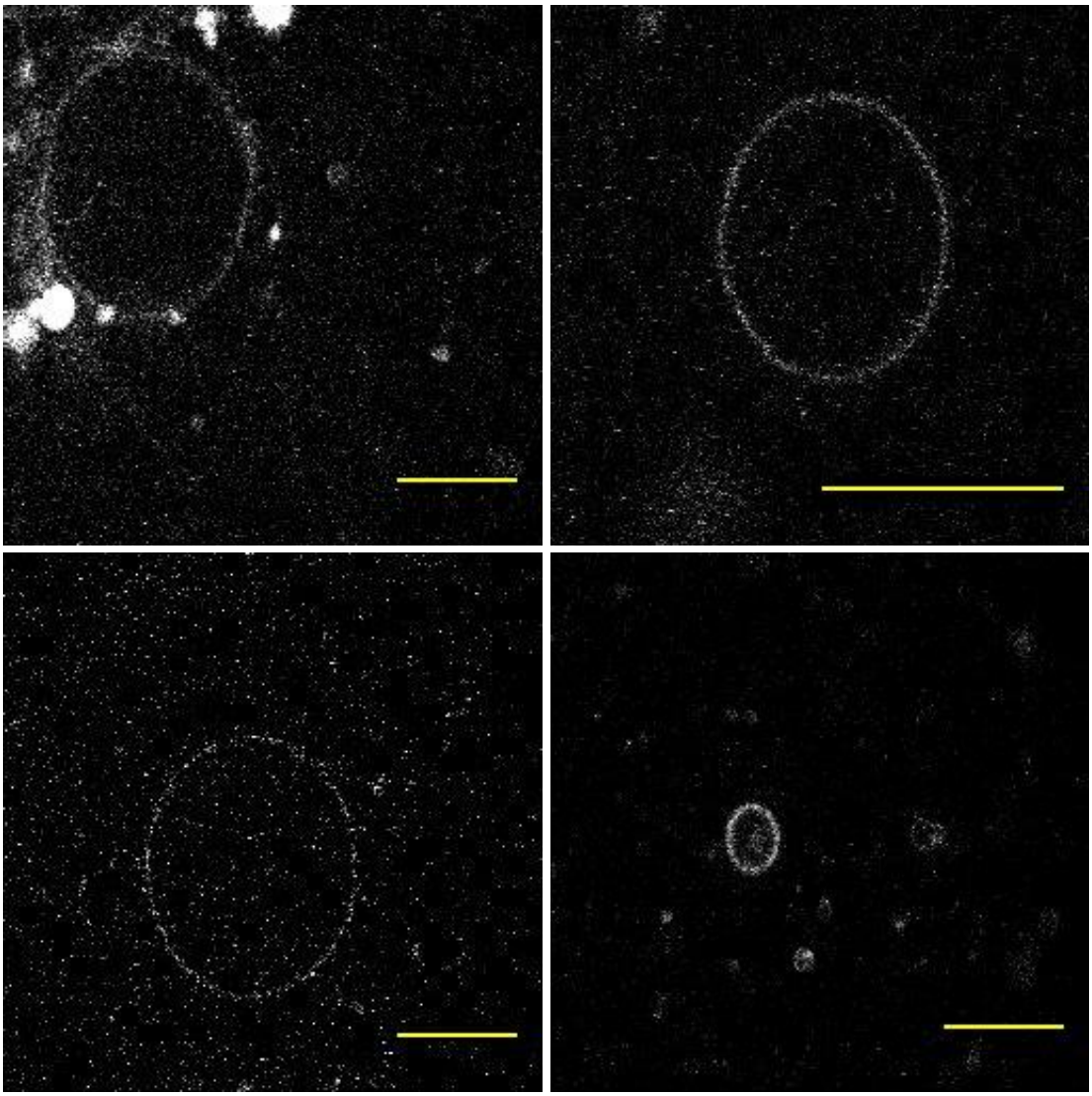

Figure 2-2. Confocal microscopy images of single lipid GUVs after the electroformation process optimisation (under conditions #13, as presented in Table 2-1.). Hydrophobic fluorescent dye Nile Red was used for sample visualisation. Scale bar size is 50 µm.

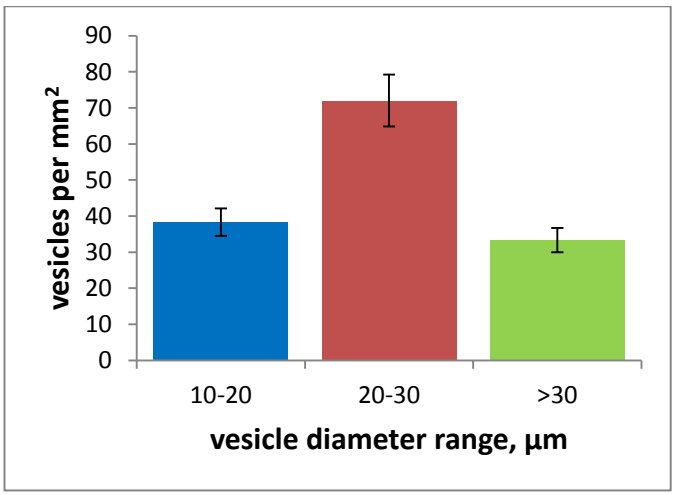

Figure 2-3. Distributions of DOPC vesicle diameters (formed under conditions #13 in Table 2-1). Only vesicles with diameter larger than 10 µm were included in the statistics.

2.3. Polymersome electroformation from polymer PBd - b - PEO

Studies on giant vesicle formation from polymer PBd - b - PEO were initiated utilising a design of experiment approach in order to investigate the influence of electroformation parameters on the self - assembly process. The optimal electroformation conditions discovered during the full factorial design of experiment (FFDOE) (procedure “A”) were used for the giant polymersomes formation; vesicles were observed, characterised and compared to the structures obtained using a different protocol adapted from Monroy et al. (procedure “B”).[38]

2.3.1. Full factorial design of experiment

A full factorial design of experiments is not the cheapest and the fastest model of experiment design; however, it has been chosen as a model to perform research on the electroformation system due to its reliability and conservatism. The full factorial design of experiments contains all possible combinations of a set of factors. There is little scope for ambiguity when all combinations of the factor settings are used. The appropriate statistical analysis for a factorial design allows the determination if there is an overall difference in vesicle average diameter using “high” values of chosen electroformation parameters instead of “low” ones. In addition, it provides information about the interactions between the main parameters and their influence on the final electroformation result.

An assessment of electroformation samples was based on the average vesicle diameter and was calculated as described in 6.3.2.4. Experiments were performed with systematically varied chosen electroformation conditions from low (-) to high (+) value (Table 2-2) in a pattern suggested by the FFDOE software. Forty eight electroformation experiments were performed during the statistical study; the collected data are presented in Table 2-3.

Table 2-2. Chosen continuous electroformation parameters with two factor levels included in the DOE.

Factor level	Time (h)	AC Waveform	Voltage (V_{pp})	Frequency (Hz)	Deposited Volume (µl)
Min (-)	0.5	sinusoidal	0.2	10	5
Max (+)	5	sinusoidal	15	1000000	30

Table 2-3. Collected electroformation data for the full factorial design of experiments.

#	Pattern of Parameters				Average Diameter [µm]		
	Time	Voltage	Frequency	Deposited Volume	Run 1	Run 2	Run 3
1	-	-	-	-	0	1.0	0
2	-	-	-	+	18.4	18.0	18.5
3	-	-	+	-	0	0	0
4	-	-	+	+	0	0	0
5	-	+	-	-	0	0	1.0
6	-	+	-	+	1.0	0	1.0
7	-	+	+	-	13.7	0	13.7
8	-	+	+	+	20.9	22.0	21.0
9	+	-	-	-	0	1.0	0
10	+	-	-	+	18.4	19.0	18.6
11	+	-	+	-	0	0	1.0
12	+	-	+	+	18.2	18.0	18.3
13	+	+	-	-	16.2	16.0	16.3
14	+	+	-	+	13.9	14.0	14.0
15	+	+	+	-	0	11.9	12.0
16	+	+	+	+	0	0	0

Initial analysis of the collected data, based on the contrast and individual p-values revealed that thirteen out of fifteen parameters and their interactions have a statistically significant influence on the electroformation outcome (Figure 2-4, marked with asterisk).

Term	Contrast	Individual p-Value
Deposited Volume	3.52896	<.0001*
Time	1.59688	0.0022*
Voltage	0.83646	0.0579
Frequency	-0.74396	0.0892
Deposited Volume*Time	-0.27854	0.5214
Deposited Volume*Voltage	-3.23729	<.0001*
Time*Voltage	-0.76271	0.0803
Deposited Volume*Frequency	-0.77271	0.0762
Time*Frequency	-2.09313	0.0003*
Voltage*Frequency	1.64729	0.0021*
Deposited Volume*Time*Voltage	-2.55479	<.0001*
Deposited Volume*Time*Frequency	-0.00688	0.9891
Deposited Volume*Voltage*Frequency	1.53521	0.0027*
Time*Voltage*Frequency	-4.35854	<.0001*
Deposited Volume*Time*Voltage*Frequency	-2.18896	0.0003*

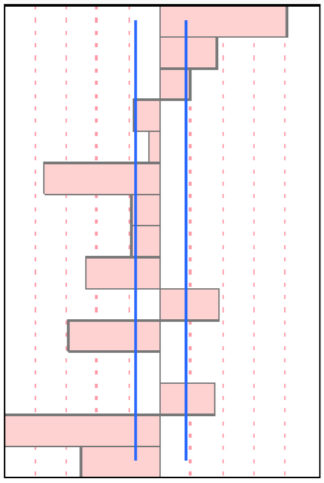

Figure 2-4. Terms, contrast values, graphical contrast and absolute contrast boundary visualisation (blue line), and individual p - values for electroformation parameters and their interactions. Only parameters and interactions, which exceed absolute contrast boundary (cross blue line) and have a p - value lower than 0.05 can be included in the statistical model (marked with asterisk).

An effect of the significant terms was analysed using effect leverage plots. The leverage plot for a chosen term shows the unique effect of adding this term to the model, assuming all the other effects are already included in the model. A sample mean is displayed as dashed blue line, regression line is presented as solid red and the confidence bands are shown as dashed red curves. The effect of a term is considered significant if confidence curves cross the horizontal mean line; however, if confidence curves are asymptotic to the mean line or do not cross it then the term effect is considered as not significant. The importance of the analysed term could be concluded from the slope of the leverage plot.

A detailed study revealed that only the terms shown in Figure 2-5 and Figure 2-6 can be included in the statistical prediction model. Rejected interactions were deemed to

be necessary due to the increasing value of the total model error and decreasing the prediction accuracy.

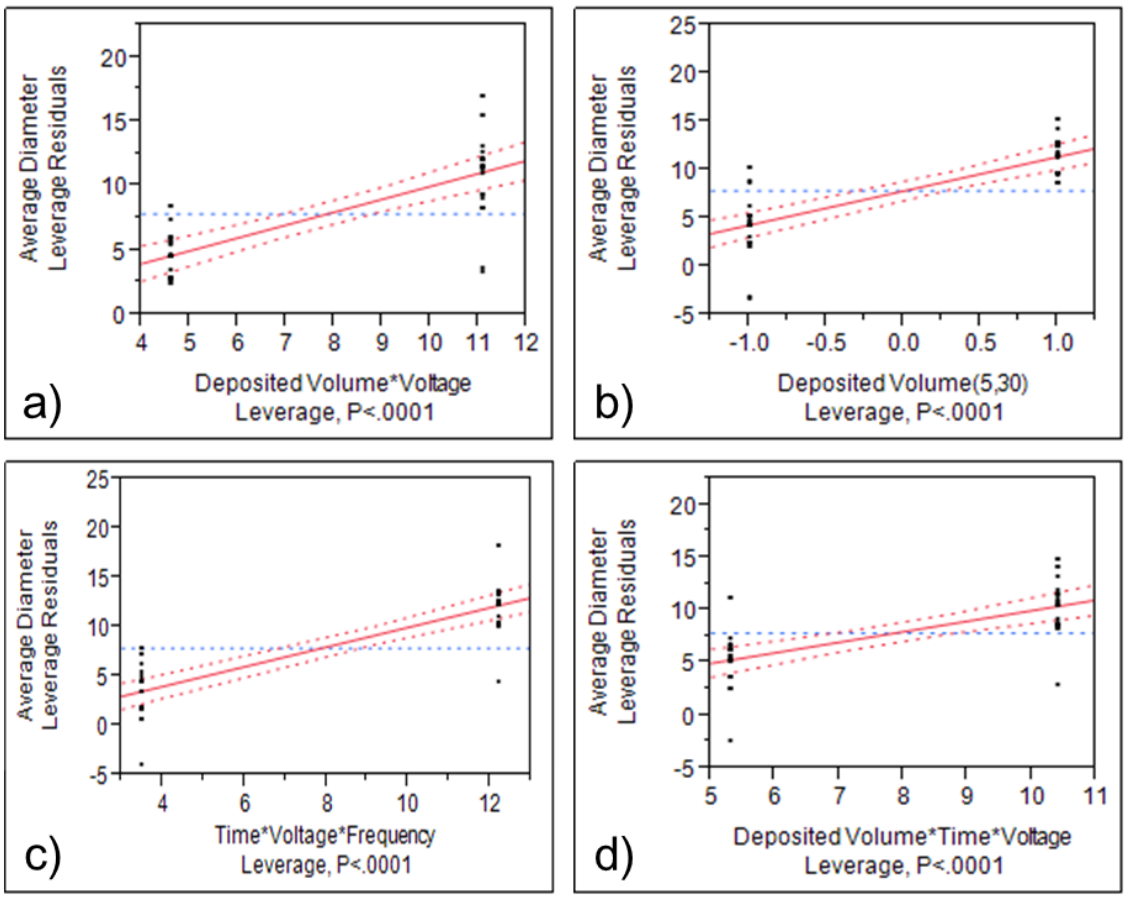

Figure 2-5. Effect leverage plots of the most influential terms included in the model: a) deposited volume and voltage interaction, b) deposited volume, c) time, voltage and frequency interactions, d) deposited volume, time and voltage interactions. Lines in the graphs represent: regression line (continous red), 95 % confidence curves (dashed red lines), a sample mean (the horizontal blue line).

Based on the leverage plots slope for deposited volume and voltage interactions, and time, voltage and frequency interactions it can be concluded that these terms are the most influential in the whole model (Figure 2-5 a) and Figure 2-5 c)). The confidence

curves for the parameter interactions (dashed red) cross the horizontal mean line (dashed blue); this shows that these factors significantly affect vesicles yield. Variations in the parameters change the average vesicle size by more than 9 µm which is 50 % of the highest average vesicle diameter registered during the study.

The deposited volume is the second most important parameter in the model (Figure 2-5 b)). Confidence curves confirm that this factor significantly affects the electroformation outcome. An adjustment in the deposited volume increases the average vesicle diameter by 8 µm which is the 45 % of the highest value registered during the DOE.

The leverage plot presented in Figure 2-5 d) shows that deposited volume, time and voltage interactions significantly affect vesicle size; however their influence on the final experiment output is lower than the previously mentioned terms (5 µm, 28 %).

The terms presented in Figure 2-6 were also included in the model; however, their influence on the electroformation result is much lower (<5 µm) than the parameters described previously and presented in the Figure 2-5.

The complete model plot in Figure 2-7 shows the experimental average diameter values versus the average diameter values predicted using the prediction formula. A regression line (continuous red) and 95 % confidence curves (dashed red lines) cross the sample mean (the horizontal blue line), which shows that the whole factorial model (all effects included in the model) explains a significant proportion of the variation in average vesicle diameter. The analysis of variance quantities (presented in Figure 2-7) confirm that the statistical model is significant. The low p-value (< 0.0001) of the created model implies that the difference found in the average diameter values

produced by this experiment is expected only 1 time in 10000 similar trials if the model factors do not affect average diameter. The R square value of 0.90 below the graph shows that a two factor model explains 90 % of the variation in data, which is fully satisfactory for the purposes of predicting the electroformation results.

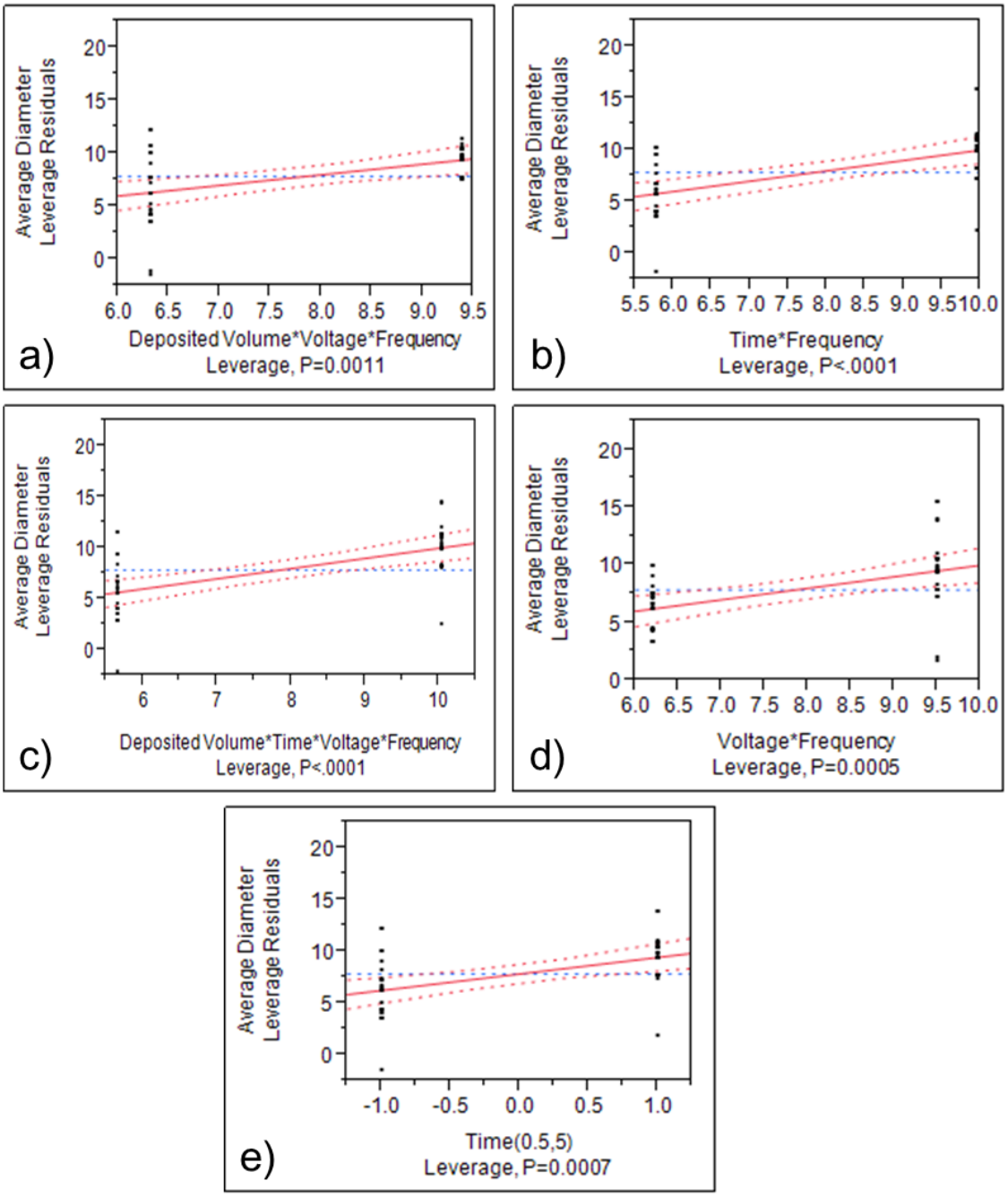

Figure 2-6. Effect leverage plots of the other significant terms included in the model: a) deposited volume, voltage and frequency interactions, b) time and frequency interactions, c) deposited volume, time, voltage and frequency interactions, d) voltage and frequency interactions, d) time. Lines in the graphs represent: regression line (continous red), 95 % confidence curves (dashed red lines), a sample mean (the horizontal blue line).

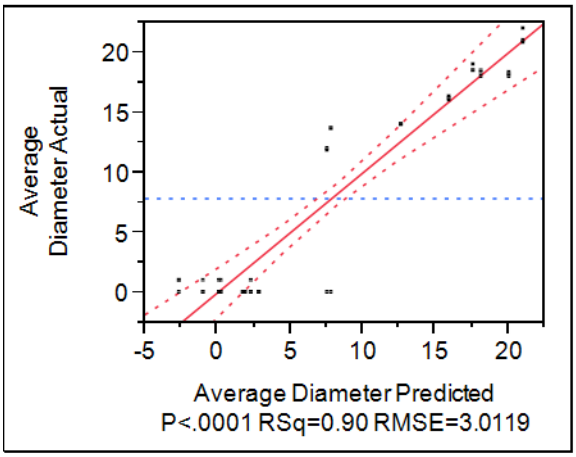

Figure 2-7. Leverage plots of actual by predicted values with analysis of variance. Lines in the graphs represent: regression line (continous red), 95 % confidence curves (dashed red lines), a sample mean (the horizontal blue line).

The collected data prove that a prediction model based on a full factorial design of experiments allows us to accurately predict the electroformation result. A prediction formula was determined and will be used in further electroformation studies based on procedure A. The original prediction formula derived from FFDOE results for determining average diameter of vesicles is as follows:

$$\boldsymbol{Average\ Diameter} = \mathbf{7.85} + \sum_{i=1}^{9} \boldsymbol{M_i} \qquad \textbf{(2-1)}$$

Where:

$$\boldsymbol{M1} = 3.59 \times \frac{(DV - 17.5)}{12.5} \qquad \textbf{(2-2)}$$

$$\boldsymbol{M2} = 1.60 \times \frac{(t - 2.75)}{2.25} \qquad \textbf{(2-3)}$$

$$\boldsymbol{M3} = \frac{(DV - 17.5)}{12.5} \times \frac{(U - 7.60)}{7.40} \times (-3.24) \qquad \textbf{(2-4)}$$

$$\boldsymbol{M4} = \frac{(t - 2.75)}{2.25} \times \frac{(f - 5.00 \times 10^5)}{5.00 \times 10^5} \times (-2.10) \qquad \textbf{(2-5)}$$

$$\boldsymbol{M5} = \frac{(U - 7.60)}{7.40} \times \frac{(f - 5.00 \times 10^5)}{5.00 \times 10^5} \times 1.65 \quad \textbf{(2-6)}$$

$$\boldsymbol{M6} = \frac{(DV - 17.5)}{12.5} \times \frac{(t - 2.75)}{2.25} \times \frac{(U - 7.60)}{7.40} \times (-2.56) \quad \textbf{(2-7)}$$

$$\boldsymbol{M7} = \frac{(DV - 17.5)}{12.5} \times \frac{(U - 7.60)}{7.40} \times \frac{(f - 5.00 \times 10^5)}{5.00 \times 10^5} \times 1.54 \quad \textbf{(2-8)}$$

$$\boldsymbol{M8} = \frac{(t - 2.75)}{2.25} \times \frac{(U - 7.60)}{7.40} \times \frac{(f - 5.00 \times 10^5)}{5.00 \times 10^5} \times (-4.36) \quad \textbf{(2-9)}$$

$$\boldsymbol{M9} = \frac{(DV - 17.5)}{12.5} \times \frac{(t - 2.75)}{2.25} \times \frac{(U - 7.60)}{7.40} \times \frac{(f - 5.00 \times 10^5)}{5.00 \times 10^5} \times (-2.19) \quad \textbf{(2-10)}$$

Where: $\boldsymbol{DV}$ - deposited volume, $\boldsymbol{f}$ - frequency, $\boldsymbol{U}$ - voltage, $\boldsymbol{t}$ - time.

The actual average diameters were compared to the predicted ones as presented in Figure 2-8. The percent deviation of the predicted values varies from 1.1 % to up to 633.3 % as presented in the Table 2-4. The highest deviations are observed for the average diameters lower than 10 µm, exclusively in the range below 3 µm (from 33.3 % to 633.3 %) The origin of the high error is the model prediction inaccuracy in this data region; however, for research purposes this deviation is acceptable.

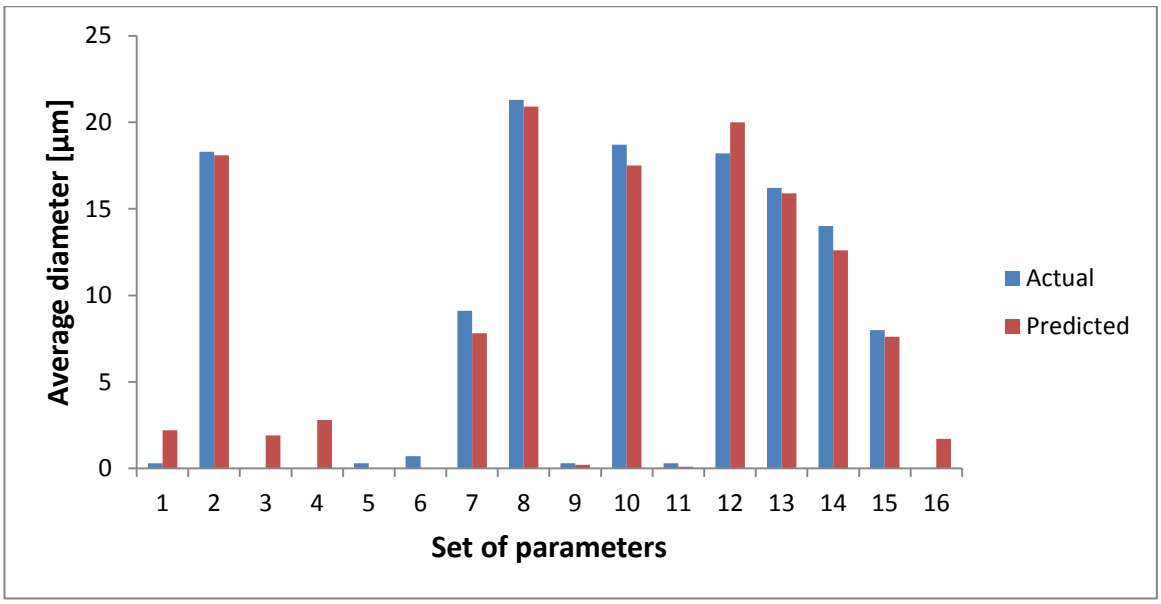

Figure 2-8. Actual versus predicted average diameter values.

Further studies are planned to be performed on the giant vesicles with size higher than 10 µm (highlighted values in the Table 2-4). The created model allows us to predict the average diameter values in the region of interest with a deviation lower than 10 % which is fully satisfactory.

Table 2-4. Comparison of the actual versus predicted average diameters. Highlighted values represent experiments which resulted in GUV formation with average size larger than 10 µm.

#	Average Value [µm]	Predicted Value [µm]	Percent Deviation [%]
1	0.3	2.2	633.3
2	18.3	18.1	1.1
3	0	1.9	NA
4	0	2.8	NA
5	0.3	0	100
6	0.7	0	100
7	9.1	7.8	14.3
8	21.3	20.9	1.9
9	0.3	0.2	33.3
10	18.7	17.5	6.4
11	0.3	0.1	66.7
12	18.2	20	9.9
13	16.2	15.9	1.9
14	14	12.6	10.0
15	8	7.6	5.0
16	0	1.7	NA

2.3.2. Electroformation using procedure “A”

Conditions required for reproducible electroformation of giant vesicles were determined during the DOE (conditions #8 in Table 2-2). Experiments using condition #8 resulted in stable and reproducible polymersome formation. Some detached polymer film pieces and asymmetrical polymer aggregates were detected in the sample and they were linked to the vesicles as presented in Figure 2-9. The observed phenomena might be caused by too severe electroformation conditions; upon applying an electric field, some parts of the deposited polymer film could crack and partly detach. During the electroformation process, these could detach fully from the glass slide and remain in the solution; however, some of them could still remain attached to the vesicle surface and that might influence polymersome membrane behavior in further experiments.

The self – assembly structures were formed with an average density of 37 ± 4 vesicles per square mm. In comparison to liposome electroformation (see 2.2.1), the yield was considerably lower; however, it was sufficient to perform further studies with the created structures. An average diameter of 20.9 ± 2.0 µm was calculated over a population of 37 polymersomes. The distribution of diameters demonstrates that polymer PBd - b - PEO, under the investigated electroformation conditions, has a tendency to form polymersomes with a size from 10 µm to 20 µm (see Figure 2-10). The number of vesicles observed in the sample decreases gradually with increase in size. Polymersomes with diameter larger than 30 µm represented only 16 % of the total population. The largest observed GUV size was more than 50 µm.

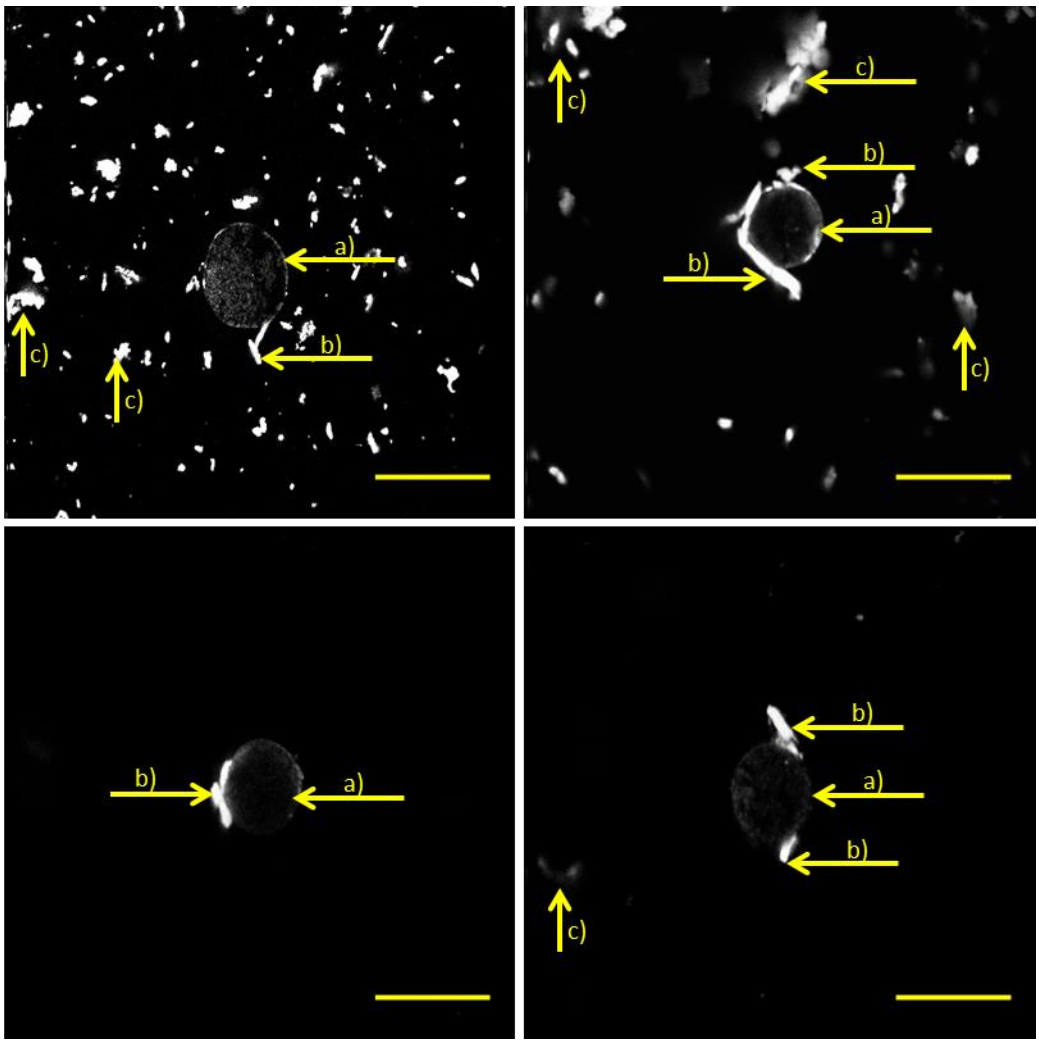

Figure 2-9. Confocal microscopy images of polymer GUVs formed using procedure "A" (under conditions #8, as presented in Table 2-3): GUV a), polymer film pieces attached to the GUV b), examples of asymmetrical aggregates present in the sample c). Hydrophobic fluorescent dye Nile Red was used for sample visualisation. Scale bar size is 50 µm.

As described previously, GUVs have been electroformed successfully using a procedure based on liposome electroformation protocols and conditions discovered using a DOE approach. These results are very promising for future research; however the procedure and conditions used to achieve vesicle formation were deemed to be non -

optimal. Based on the collected data, it was decided to continue research on vesicle electroformation from the polymer PBd - b - PEO in order to optimise the process.

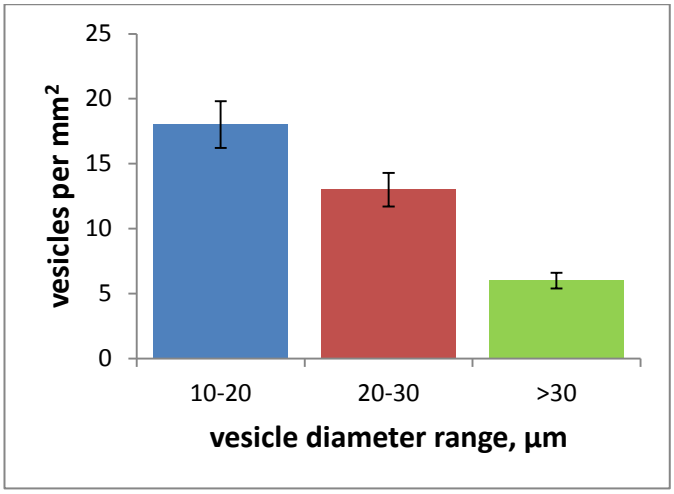

Figure 2-10. Distributions of PBd - b - PEO vesicle diameters (formed using procedure "A"). Only vesicles with diameter larger than 10 µm were included in the statistics.

2.3.3. Electroformation using procedure "B"

Conditions suitable for a vesicle formation from polymer PBd – b – PEO have been discovered utilising a DOE approach; however, they were deemed to be non - optimal due to the requirement for a high amount of polymer for the slide preparations (as described in 6.3.2.2) and harsh experiment conditions which resulted in the electroformation of asymmetrical aggregates. Following a detailed literature survey it was decided to adapt a protocol developed by Monroy et al. [38] in order to optimise electroformation parameters. The concentration of polymer PBd - b - PEO solution in chloroform used for the electroformation slides preparation was reduced from 5 mg/ml to 2 mg/ml. The electroformation voltage was decreased from 15 V to 9

V, frequency from 1 MHz to 10 Hz and the total electroformation time was reduced to 0.5 h (the detachment step was excluded).

The changes in the experimental procedure and conditions resulted in the reproducible formation of stable, giant unilamellar polymersomes as presented in Figure 2-11. Initial observations revealed a significant decrease in the amount of asymmetrical structures and detached polymer film pieces in the electroformation sample.

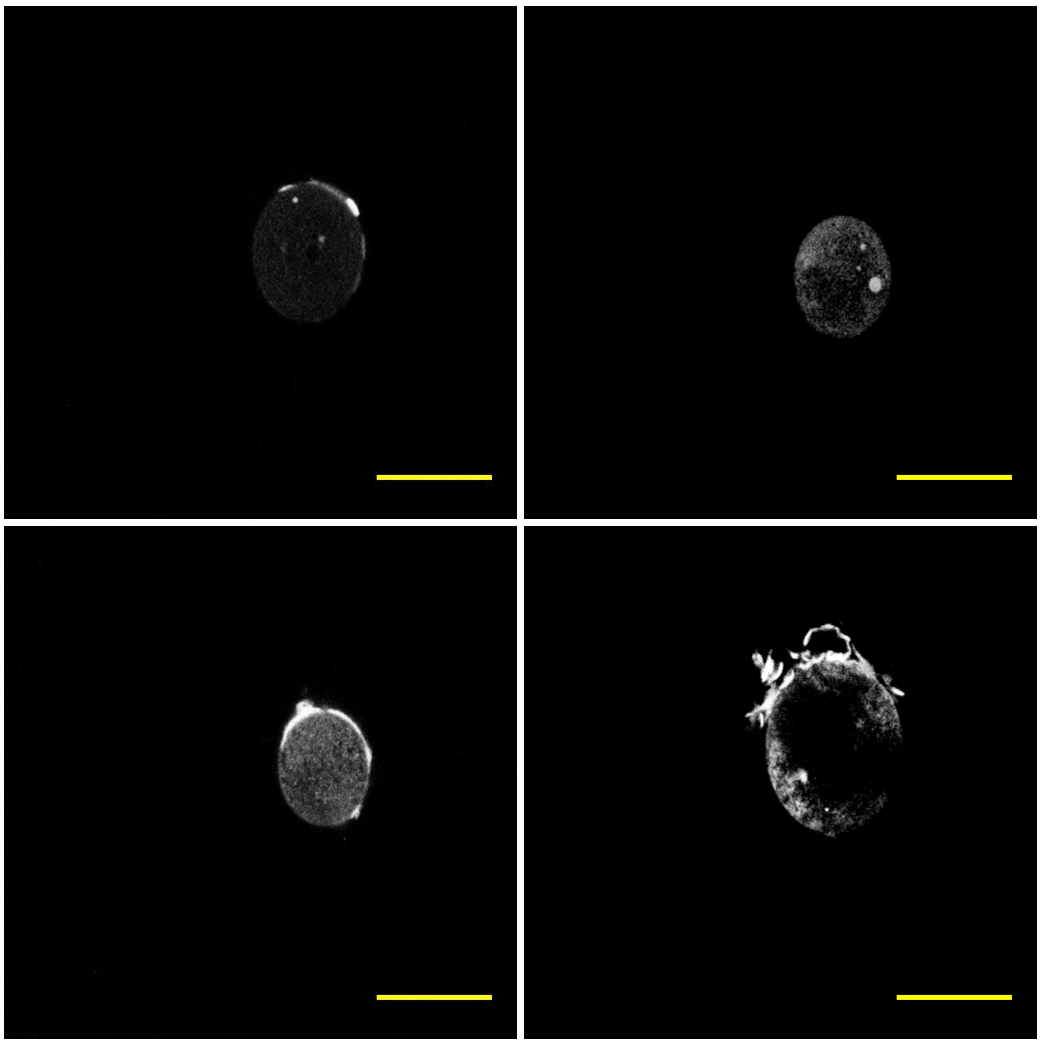

Figure 2-11. Confocal microscopy images of GUVs formed from polymer PBd - b - PEO using procedure "B". Hydrophobic fluorescent dye Nile Red was used for sample visualisation. Scale bar size is 50 µm.

Self - assembled structures were formed with an average density of 40 ± 4 vesicles per square mm, which is slightly higher than that using electroformation procedure A and conditions #8 (see Table 2-2). In comparison to previous experiments, a significant increase in average diameter from 20.9 ± 2.0 µm to 29.8 ± 3.0 µm was observed over a population of 40 vesicles. Polymersome diameters were distributed more equally than previously, with a tendency to form polymersomes with diameters from 20 µm to

30 µm as presented in Figure 2-11. Those structures form 43 % of the population. The largest observed GUVs size was more than 60 µm.

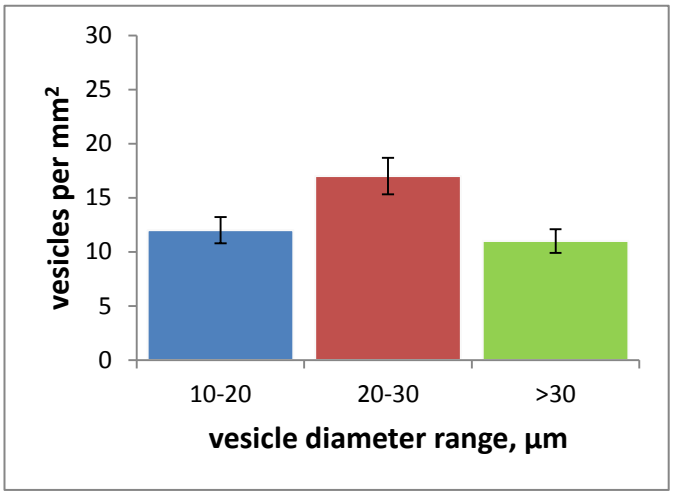

Figure 2-12. Distributions of PBd – b - PEO vesicles diameters (formed using procedure "B"). Only vesicles with diameters larger than 10 µm were included in the statistics.

2.4. Conclusions

The initial electroformation studies on the model lipid DOPC and polymer PBd - b - PEO were accomplished successfully. Conditions suitable for the production of stable giant liposomes were obtained. Lipid vesicles were electroformed with an average density of 143 ± 14 units per square mm and an average diameter of 26.0 ± 2.0 μm.

The FFDOE approach was completed successfully. The prediction model explains 90 % of the variations in average vesicle diameter. The created model allows us to accurately predict the electroformation result for the block copolymer PBd - b - PEO. The prediction formula was obtained and can be used in further electroformation studies based on procedure "A". The influence of electroformation factors and their interactions on the average vesicle diameter was determined. The most influential factor is the deposited volume. The most important factor interactions are: time, voltage and frequency, deposited volume and time, and deposited volume, time and voltage.

Electroformation using procedure "A" resulted in polymersomes with an average density of 37 ± 4 vesicles per square mm and average diameter of 20.9 ± 2.1 μm. The change in electroformation protocol and conditions described as procedure "B" resulted in the formation of vesicles with an average density of 40 ± 4 vesicles per square mm and average diameter of 28.8 ± 2.9 μm.

Research on polymersome electroformation from the polymer PBd - b - PEO was accomplished. The main goals were achieved: two sets of conditions for the formation

of GUVs in a yield required for further studies on polymersomes were discovered, the process was reported as stable and reproducible.

3. Polymersome Formation from Glycopolymers

3.1. Introduction

The commercially available polymer PBd - b - PEO was used as a model to investigate tendencies in polymersome electroformation. The studies on PBd - b - PEO were successful, resulting in the discovery of two sets of conditions that led to reproducible, single GUV formation. Therefore, it was decided to proceed to electroformation studies with the novel amphiphilic glycopolymers polyethylene - block - poly(ethylene glycol) β - D - glucoside (PE - b - (Glu) PEG) and poly [N - 2 - (β - D - glucosyloxy) ethyl acrylamide] - b - (n-butylacrylate) (PNGEA - b - BA) in order to test their capability for polymersome formation.

3.2. Polymersome electroformation from glycopolymer PE - b - (Glu) PEG

Part of this chapter is adapted with permission from:

A. M. Eissa, M. J. P. Smith, A. Kubilis, J. A. Mosely and N. R. Cameron, *Journal of Polymer Science Part A-Polymer Chemistry* **2013**, *51*, 5184-5193

3.2.1. Block copolymer PE - b - (Glu) PEG solubility check

It is essential before each electroformation process to correctly prepare films from the vesicle - forming material. The material is initially dissolved in a pure solvent or solvent mixture that gives the highest polymer solubility, and then deposited on an ITO - covered glass slide surface in order to create a homogenous polymeric film. The choice of solvent is a crucial step in the formation of high quality polymeric layers suitable for electroformation. Amphiphilic polymers are a very specific group of compounds, with a strong tendency to form cloudy solutions, and often do not fully dissolve in single solvents. This characteristic arises from the structure of the polymer material: amphiphilic block copolymers possess hydrophilic and hydrophobic blocks which differ in their physical and chemical properties i.e. solubility in organic solvents. For this reason, it was decided to assess the polymer solubility in solvent mixtures created from two solvents before starting electroformation experiments. One of them should be a good solvent for the hydrophobic block, another for the hydrophilic block of the macromolecule; moreover, they should be miscible. According to these criteria, common solvents were divided into pairs, which could possibly be suitable for the polymer mixture preparation (Table 3-1).

Table 3-1. Solvents mixtures used to determine the solubility of polymer PE - b - (Glu) PEG.

#	Solvent 1	Solvent 2	Observation
1	tetrahydrofuran	water	white suspension - insoluble
2	diethyl ether	acetone	white suspension - insoluble
3	acetonitrile	water	white suspension - insoluble
4	acetone	water	white suspension - insoluble
5	tetrahydrofuran	methanol	white suspension - insoluble
6	isopropanol	water	white suspension - insoluble
7	chloroform	methanol	soluble at ratio 4 : 3

Solubility of polymer PE - b - (Glu) PEG was investigated using every pair of solvents present in the table mixed in different ratios analogous as present in Table 3-2.

Each pair of solvents presented in Table 3-1 was mixed in different ratios (analogous as presented in Table 3-2) and solubility of glycopolymer was investigated. Analysis of the collected data suggests that block copolymer PE - b - (Glu) PEG has very limited solubility in most of the tested solvent mixtures. The most suitable pair of solvents has been found to be chloroform and methanol in a volume ratio of 4 : 3 (as presented in #7 Table 3-2) ; however, polymer solubility was strictly limited to a final concentration of 1.5 mg/ml. Upon increasing above this concentration, the solution became hazy and white solid polymer particles remained undissolved in the solution.

Table 3-2. Chloroform and methanol solvent ratios used to determine the solubility of polymer PE - b - (Glu) PEG.

#	Solvent 1	Solvent 2	Solvent Ratio	Observation
1	chloroform	----------	Pure Solvent 1	white suspension
2	chloroform	methanol	8 : 1	white suspension
3	chloroform	methanol	8 : 2	white suspension
4	chloroform	methanol	8 : 3	white suspension
5	chloroform	methanol	8 : 4	white suspension
6	chloroform	methanol	8 : 5	cloudy
7	chloroform	methanol	8 : 6	clear
8	chloroform	methanol	8 : 7	cloudy
9	chloroform	methanol	8 : 8	white suspension
10	----------	methanol	pure solvent 2	white suspension
11	chloroform	methanol	1: 8	white suspension
12	chloroform	methanol	2 : 8	white suspension
13	chloroform	methanol	3 : 8	white suspension
14	chloroform	methanol	4 : 8	white suspension
15	chloroform	methanol	5 : 8	white suspension
16	chloroform	methanol	6 : 8	white suspension
17	chloroform	methanol	7 : 8	white suspension

3.2.2. Polymersome electroformation from the block copolymer PE - b - (Glu) PEG

Research on GUV electroformation was performed using the sets of conditions listed in Table 3-3. Initial polymer concentration for the film preparation was kept at the low level of 0.5 mg/ml in order to eliminate the possibility of undissolved polymer particles being deposited on the glass slides. Experiments were performed using different electrical signal waveform and frequency, switching from sinusoidal to square and from 10 Hz to 5 Hz respectively. Literature suggests that the electroformation process must be performed at a temperature higher than the polymer's glass

transition temperature.[103] For the glycopolymer used the melting transition was found to be 109 ^{o}C from differential scanning calorimetry analysis; however, due to the temperature level restriction in the electroformation kit by the aqueous solution evaporation process and electroformation chamber decontamination, electroformation was carried out at a static temperature of 80 ^{o}C.

Initially experiments were performed using conditions #1 and #2 (presented in Table 3-3) in order to investigate the polymer response to changeable electroformation and detachment times. First trials revealed that changes in listed factors do not have a significant influence on the electroformation output.

Previous experiments with DOPC reported in subchapter 2.2 suggested that the amount of deposited material on the ITO surface is essential for the self – assembly structures formation. For that reason, after the initial experiments analysis, it was decided to increase the amount of deposited polymer by spreading multiple layers of polymer on the glass surface. Conditions #3 were analogous to #2, differing by multi – layered polymer film preparation; however, conditions #3 did not produce any changes and asymmetrical aggregates appeared (identical) as observed after utilising the first two sets of conditions.

Table 3-3. Conditions used for the GUVs electroformation from PE - b - (Glu) PEG.

#	Volume used for film preparation (µL)	Time (h)	Voltage (V)	Observation
1	20	2.5 + 0.5	1.2	asymmetrical aggregates
2	20	3 + 1	1.2	asymmetrical aggregates
3	5 x 20	3 + 1	1.2	asymmetrical aggregates
4	5 x 20	3 + 1	5	micelle - like
5	5 x 20	3 + 1	10	big and medium single GUVs
6	5 x 20	3 + 1	15	small vesicles and aggregates
7	3 x 20	3 + 1	10	GUVs and aggregates
8	3 x 20	4 + 1	10	GUVs and aggregates
9	5 x 20	4 + 1	10	larger GUVs
10	5 x 20	5 + 1	10	medium GUVs
11	8 x 20	4 + 1	10	smaller GUVs
12	8 x 20	5 + 1	10	distribution of vesicle sizes

All experiments were performed using waveform from sin to square and frequency from 10 Hz to 5 Hz; temperature was kept stable at 80 ^{o}C and films were evaporated for 16 h. These parameters were not changed during the experiment.

Theoretically, all the amphiphilic materials form at least one of the self – assembly structures under favorable conditions. Consequently it was decided to continue experiments with multi – layered polymer films until the formation of any self – assembled structure was observed. Upon increasing voltage to 5 V, as represented in #4, micelle – like symmetrical structures appeared in the electroformation sample. Initial changes in the voltage resulted in the electroformation experiment output, and collected data suggested that it is necessary to increase the voltage further in order to facilitate hydration of the polymer film by inducing stronger periodic motions and enhancing interlayer repulsion through electrostatic/ electroviscous effects of the rigid

polymer layers. Increasing the voltage to 10 V (#5) resulted in GUVs formation as presented in Figure 3-1. The largest observed polymersomes were approximately 50 µm in diameter. Vesicles were found individually or in mixed clusters of GUVs with MUVs and SUVs, mostly stacked at the bottom of the visualization chamber. The created polymersomes were oval in shape; however not perfectly symmetrical, which suggested that structures are in a semi – solid entrapped state due to the low temperature in the visualization chamber in comparison to the polymer melting transition temperature. Initial research on glycopolymersomes formation from polymer PE - b - (Glu) PEG was accomplished and conditions required for the polymersomes electroformation were discovered; however, further studies were performed in order to optimise self - assembly conditions.

An additional increase in voltage to 15 V (#6) resulted in the vesicle size decreasing; only small polymersomes and asymmetrical aggregates appeared in the sample. Decreasing the amount of polymer layers on the glass surface (from 5 layers to 3) as represented by #7 and #8, or increasing (from 5 layers to 8 layers) as represented by #11 or #12 result in a decrease in vesicle size and quantity, as presented in the Figure 3-2. Vesicles appeared, but with a much lower diameter than in the first successful GUV formation experiments (the largest observed structures were around 10 µm).

Increasing electroformation time from 3 h + 1 h to 4 h + 1 h (#9 in comparison to #5) and to 5 h + 1 h (#10) also resulted in the GUV size and number decreasing.

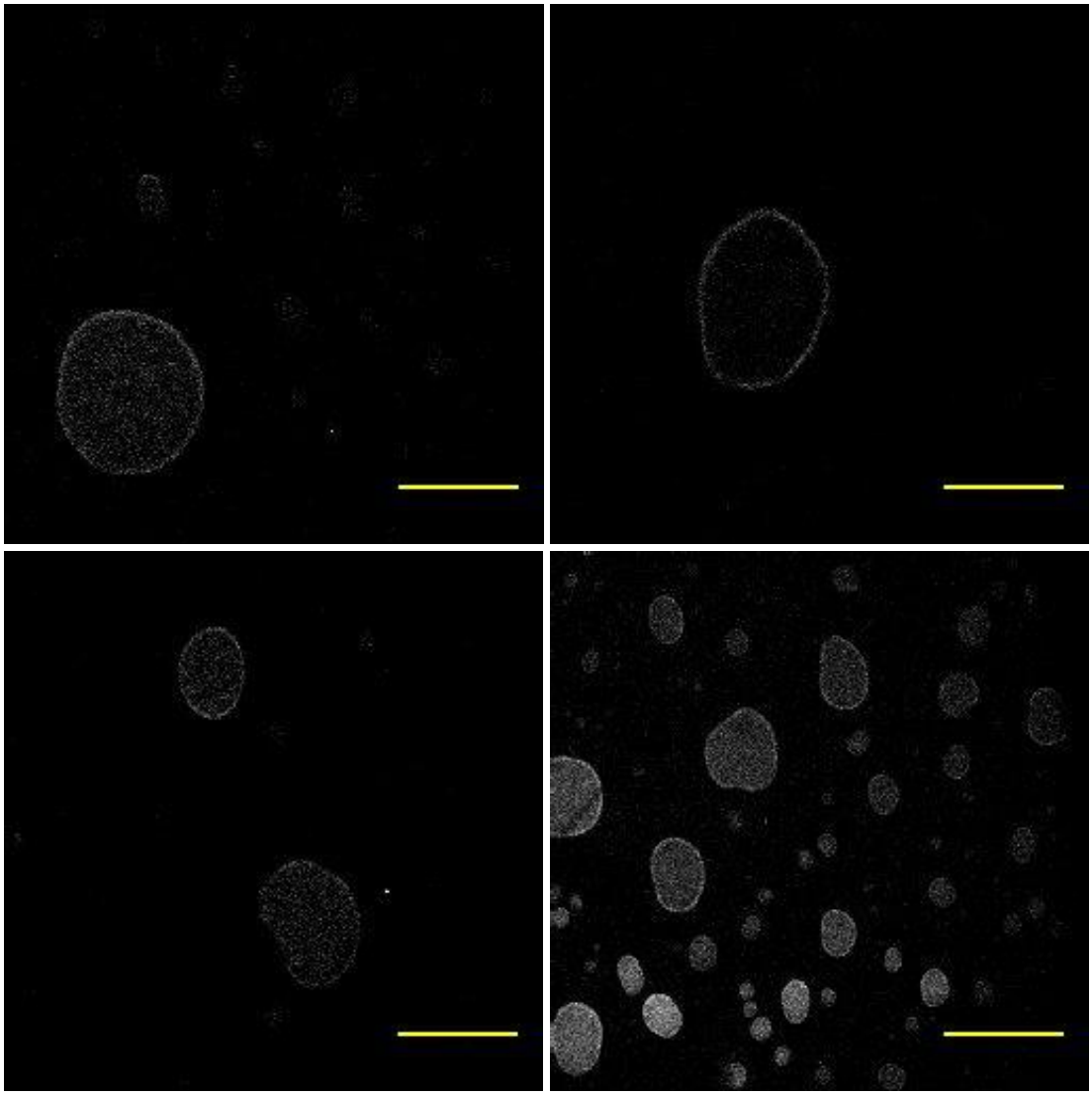

Figure 3-1. Confocal images of polymersomes formed under conditions #9 (as presented in Table 3-3). Hydrophobic fluorescent dye Nile Red was used for sample visualisation. Scale bar size is 50 µm.

Preliminary evidence presented implies that polymer PE - b - (Glu) PEG forms glycosylated GUVs; however, the glycopolymer membrane rigidity is likely to be very high and that makes the polymersomes inappropriate to utilise as a model cell membrane system to study biological processes mediated by carbohydrates. For that reason we decided to use a glycopolymer with a more liquid - like poly (butyl acrylate) hydrophobic block.

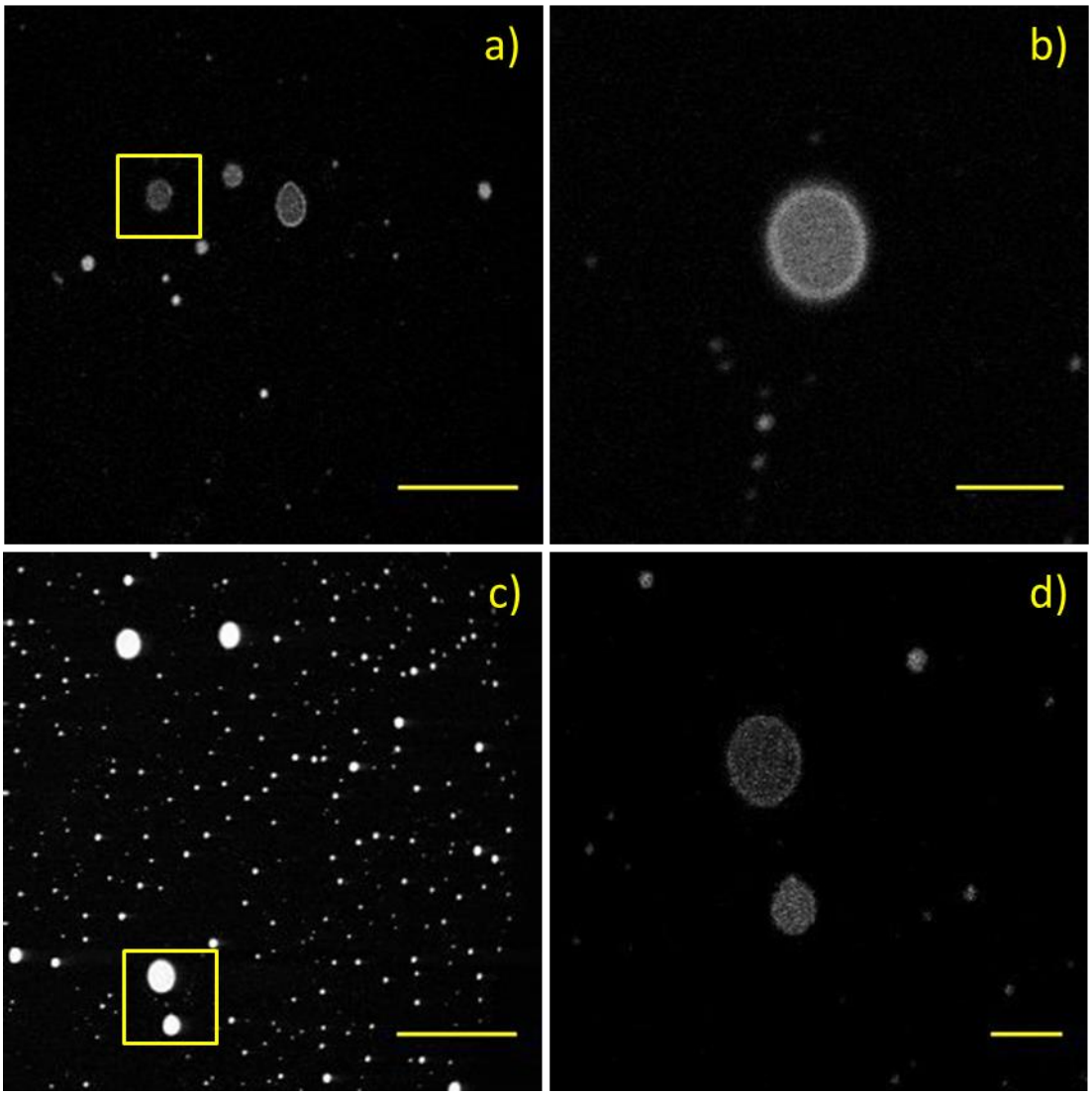

Figure 3-2. Confocal images of polymersomes after unsuccessful optimisation trial (using condition #12 as presented in Table 3-3). Hydrophobic fluorescent dye Nile Red was used for sample visualisation. Images b) and d) are digitally zoomed images of the vesicles presented in the images a) and c) marked with yellow box. Scale bar size in the images a) and c) is 50 µm; in the images b) and d) is 10 µm.

3.3. Polymersomes electroformation from glycopolymer PNGEA - b - BA

3.3.1. Electroformation studies on glycopolymers PNGEA - b - BA using procedure "A"

Electroformation studies on the novel amphiphilic copolymer PNGEA - b - BA were performed using electroformation procedure "A" and conditions #8 (see Table 3-3); the set of parameters discovered during the design of experiments. Electroformation experiments were performed on glycosylated block copolymers with different molar mass and block ratio (see Table 3-4). Vesicles were formed with different yields as presented in Figure 3-3.

Table 3-4. Compositions of P(NGEA)n - b - (BA)m block copolymers used in the electroformation study.

#	Glycopolymer	$(NGEA)_n$ (n)	$(BA)_m$ (m)	Block ratio (n : m)	Estimated packing parameter values
1	A1	16	38	1 : 2	below ⅓
2	E1	14	40	1 : 3	below ⅓
3	H1	13	77	1 : 6	from ⅓ to ½
4	H2	13	200	1 : 15	from ½ to 1
5	J1	8	10	1 : 1	below ⅓
6	K1	8	38	1 : 5	from ⅓ to ½
7	M1	6	62	1 : 10	from ½ to 1

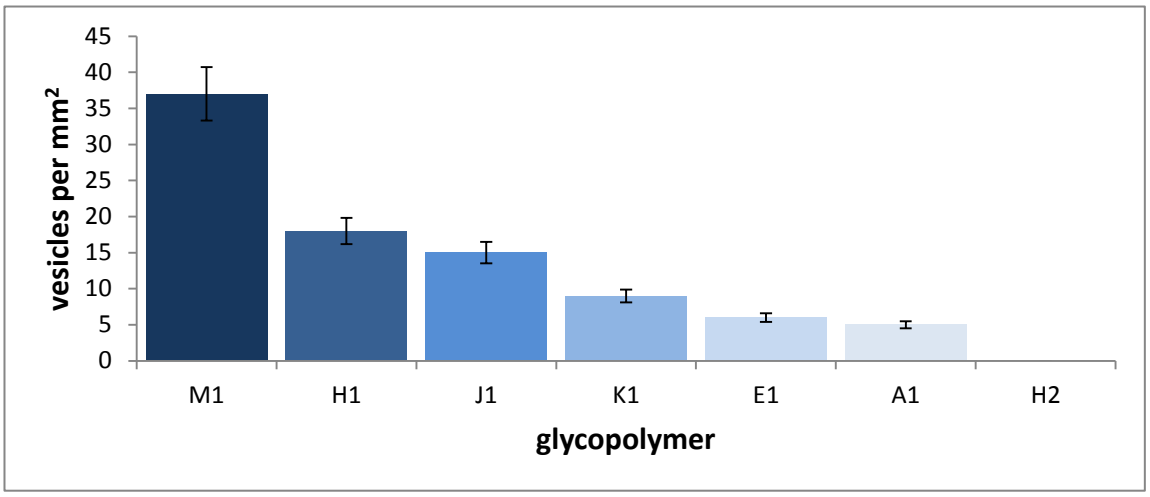

Figure 3-3. Density of vesicles in glycopolymer samples after initial electroformation experiments on glycopolymers PNGEA - b - BA using procedure "A".

Initial research revealed that glycopolymers PNGEA - b - BA are able to form GUVs; however all samples contained large amounts of deposited polymer film pieces and asymmetrical aggregates as presented in Figure 3-4 and Figure 3-5. Polymersomes were not formed from glycopolymer H2.

The highest yield of polymersomes was achieved after electroformation using glycopolymer M1. GUVs were formed with a broad size distribution as typical for electroformation. The largest observed vesicles were around 50 µm. Experiments with other glycopolymers resulted in a significantly lower yield of polymersomes, with a tendency to form asymmetrical polymer aggregates.

Following a thorough analysis of the collected data it was decided to perform further electroformation experiments with glycopolymer M1, due to its strong tendency to form GUVs.

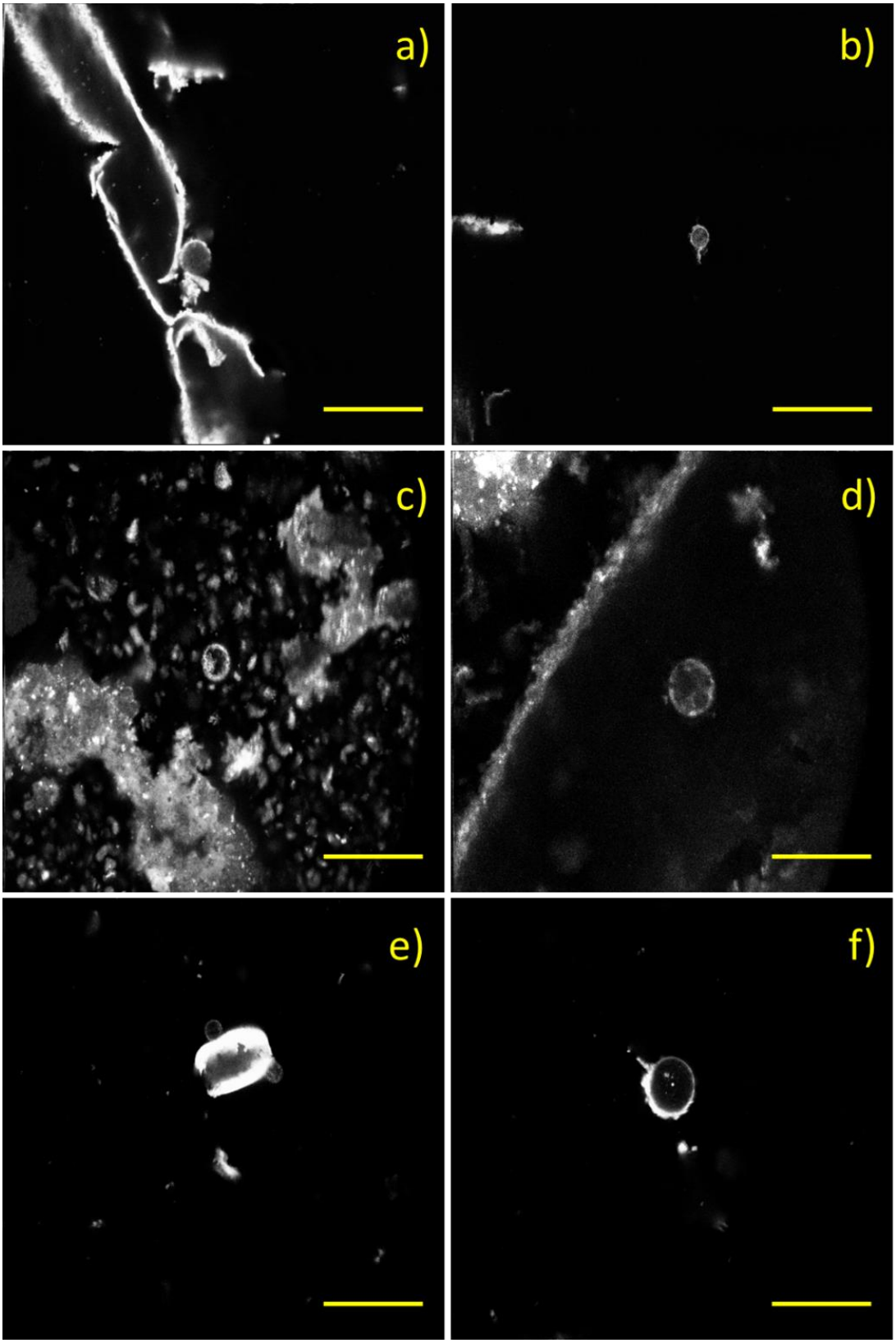

Figure 3-4. Confocal microscopy images of electroformation samples from PNGEA - b - BA block copolymers using procedure "A". Images are presented in

order: A1 (a, b), E1 (c, d), H1 (e, f). Fluorescent dye Rhodamine B octadecyl ester perchlorate was used for sample visualisation. Scale bar size is 50 µm.

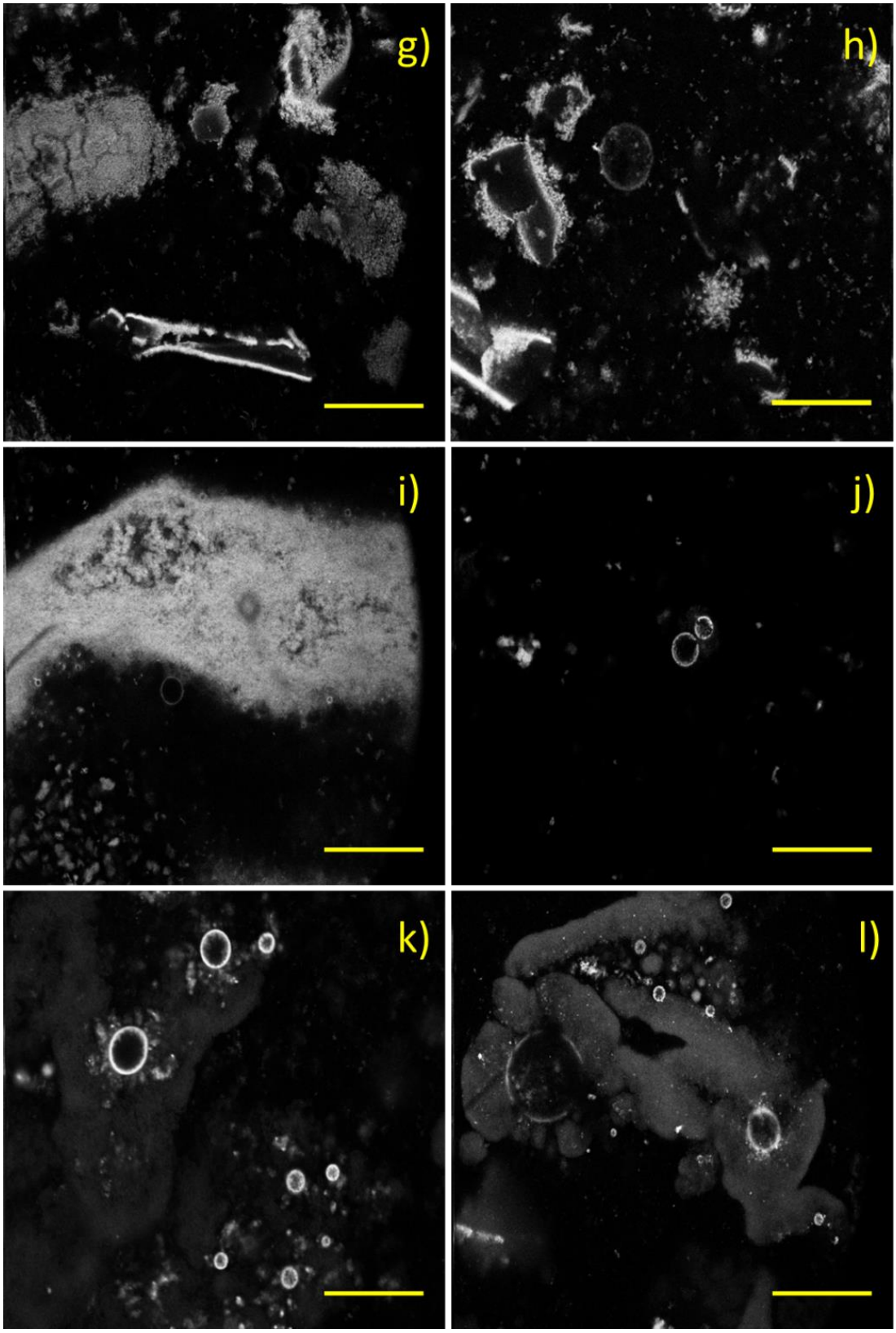

Figure 3-5. Confocal microscopy images of electroformation samples from PNGEA - b - BA block copolymers using procedure "A". Images are presented in

order: J1 (g, h), K1 (i, j), M1 (k, l). Fluorescent dye Rhodamine B octadecyl ester perchlorate was used for sample visualisation. Scale bar size is 50 µm.

3.3.2. Glycopolymersome electroformation from glycopolymer M1

Electroformation experiments performed under procedure "A" resulted in the formation of stable, giant unilamellar polymersomes as presented in Figure 3-5 k) and Figure 3-5 l). GUVs were produced with an average density of 37 ± 4 vesicles per square mm. An average diameter of 19.7 ± 2.0 µm was determined over a population of 37 vesicles. The distribution of vesicle diameters shows a strong tendency to form polymersomes with size from 10 µm to 20 µm as presented in Figure 3-6. Vesicles with diameter smaller than 20 µm form 73 % of the whole population. The largest observed GUV size was 53.9 µm.

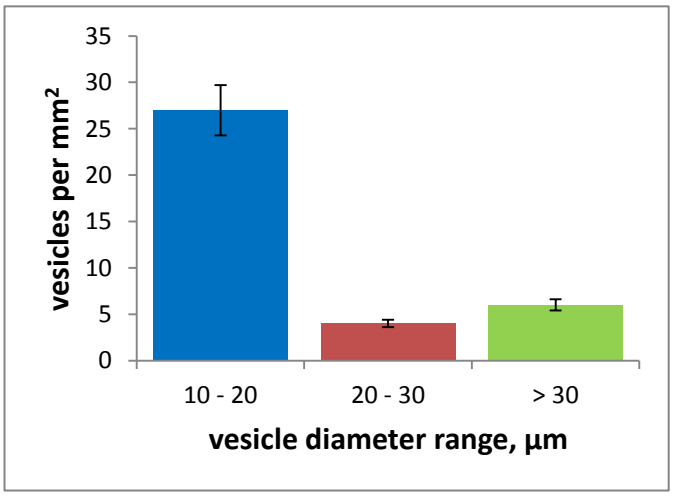

Figure 3-6. Distributions of M1 vesicle diameters (formed using procedure A). Only vesicles with diameter larger than 10 µm were included in the statistics.

3.3.3. Electroformation studies on glycopolymers PNGEA - b - BA using procedure “B”

Initial electroformation experiments based on procedure “B” were deemed to be successful due to the formation of stable vesicles with a variety of sizes (see Figure 3-7 and Figure 3-8); however all samples contained large amounts of deposited polymer film pieces and asymmetrical aggregates analogous to those observed in electroformation samples based on procedure “A”.

Due to differences in block copolymer composition, giant vesicles were formed with different yields as presented in Figure 3-9. The highest yield of polymersomes was observed after electroformation of glycopolymers H2 (Figure 3-7 a) and Figure 3-7 b)). The majority of the polymersomes were formed with a narrow size distribution from 3 µm to 6 µm; only one structure larger than 10 µm was observed. Electroformation from the glycopolymer M1 resulted in significantly lower yield of vesicles in comparison to H2 (Figure 3-9), however the majority of self-assembled structures were larger than 10 µm (see Figure 3-8 g) and Figure 3-8 h)).

In comparison to previous experiments based on procedure “A” (see 3.3.1.), the general trend for the vesicle electroformation was similar for the glycopolymers M1, K1, J1, E1 and A1; however, tendency was different for the glycopolymers H1 and H2. Electroformation experiments based on procedure “B” resulted in vesicle formation from glycopolymer H2, while self – assembled structures were not obtained from glycopolymer H1 (which is opposite as concluded from experiments based on the procedure “A”).

Following a thorough analysis of collected data it was decided to perform more detailed electroformation studies with glycopolymers M1 and H2, due to their strong tendency to generate GUVs.

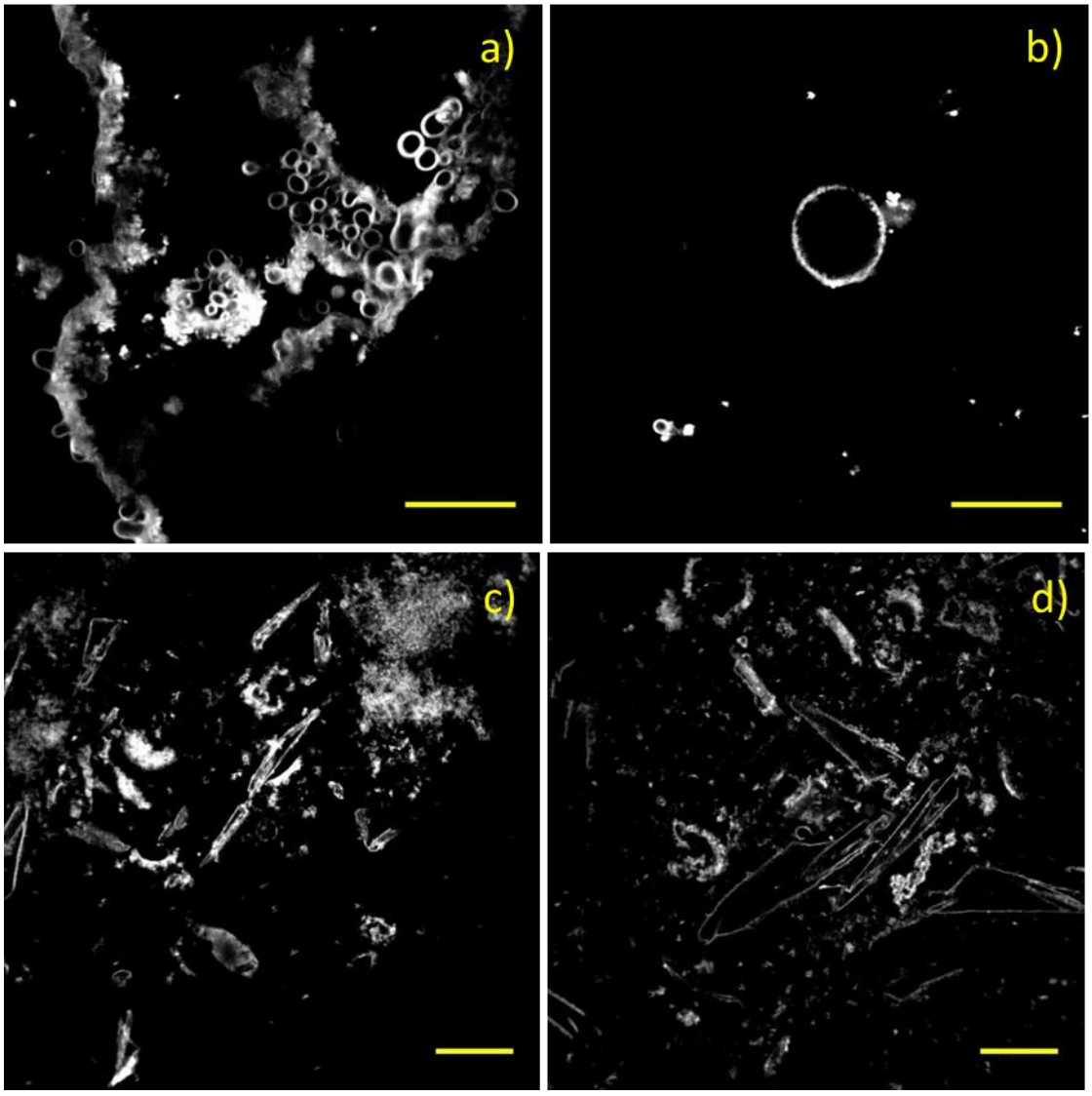

Figure 3-7. Confocal microscopy images of electroformation samples from PNGEA - b - BA block copolymers using procedure "B". Images are presented in order: H2 (a, b), J1 (c, d). Hydrophobic fluorescent dye Rhodamine B octadecyl ester perchlorate was used for sample visualisation. Scale bar size is 30 µm.

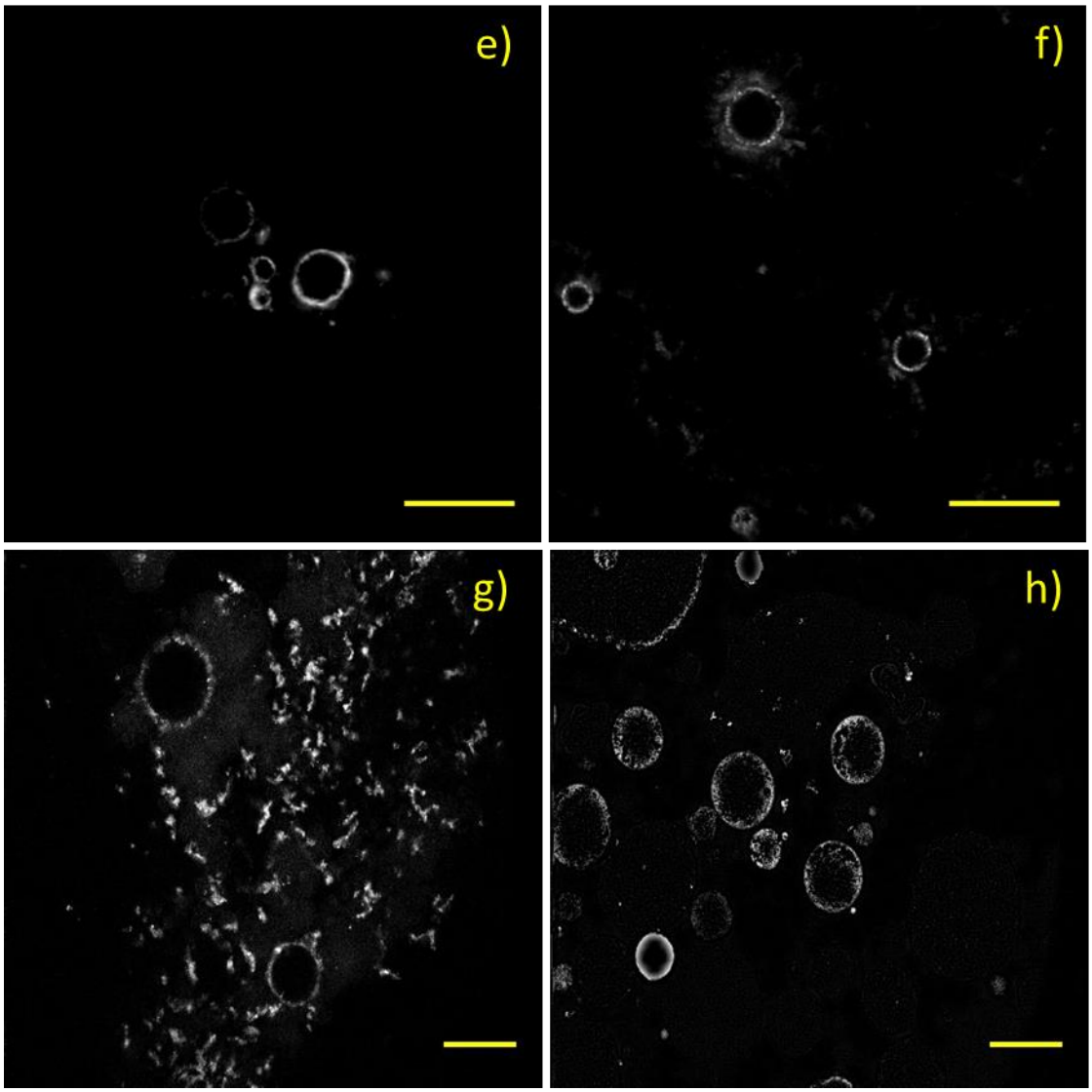

Figure 3-8. Confocal microscopy images of electroformation samples from PNGEA - b - BA block copolymers using procedure "B". Images are presented in order: K1 (e, f), M1 (g, h). Hydrophobic fluorescent dye Rhodamine B octadecyl ester perchlorate was used for sample visualisation. Scale bar size is 30 µm.

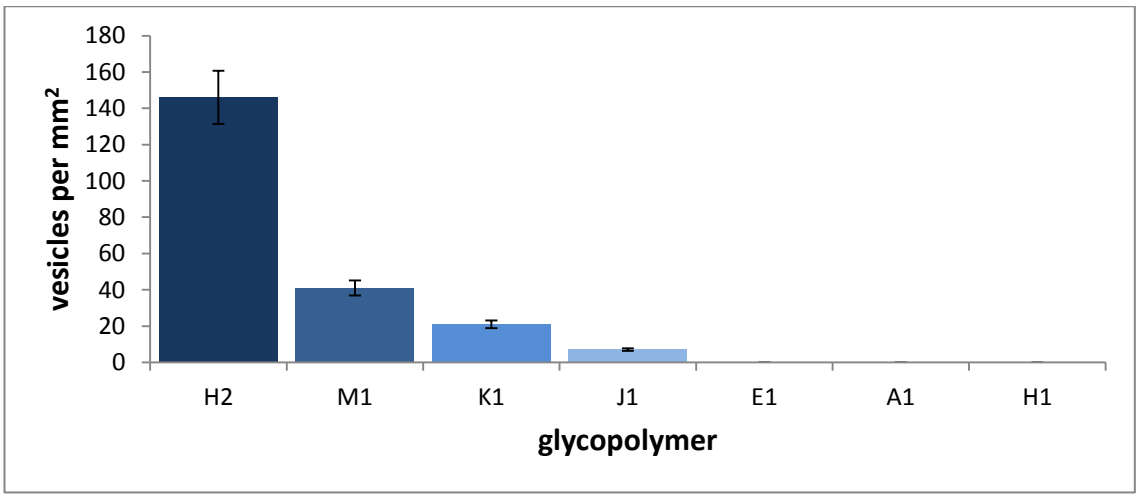

Figure 3-9. Density of vesicles in glycopolymer samples after initial electroformation experiments on glycopolymers PNGEA - b - BA using procedure "B".

3.3.4. Glycopolymersome electroformation from glycopolymer M1

Data collected and presented in Chapter 2, suggest that the electroformation time has a significant influence on vesicle size and morphology. For that reason, electroformation experiments on glycopolymer M1, under procedure "B", were performed with varying time: 0.5 h, 2 h and 3h.

Experiments were initiated with an electroformation time of 0.5 h in order to examine the impact of procedure "B" on glycopolymer M1 self-assembly. These initial parameters were deemed to be successful, due to the formation of stable, giant polymersomes with an average density of 30 ± 3 vesicles per square mm. An average diameter of 24.0 ± 2.0 µm was determined over a population of 30 vesicles. The distribution of vesicle diameters shows a tendency to form polymersomes with diameters from 10 µm to 20 µm as presented in Figure 3-10 (blue bars). Vesicles with

diameter smaller than 20 µm form 60 % of all population. The largest observed GUV size was 54.1 µm.

A further increase in electroformation time to 2 h resulted in stable GUV formation with a yield more than 2 times higher than at 0.5 h. The density of self-assembled structures was 77 ± 8 vesicles per square mm. A slight decrease in average diameter from 24.0 ± 2.0 µm to 20.0 ± 2.0 µm was observed; however, the total number of vesicles with average size from 20 µm to 30 µm increased more than 5 times as presented in Figure 3-10 (red and blue bars). The general tendency in vesicle diameter distribution remained the same as before; vesicles with diameter smaller than 20 µm formed the majority of the whole population. The largest observed GUV diameter was 45.2 µm. Typical images of this electroformation sample are presented in Figure 3-12.

Experiments with an additional increase in electroformation time to 3 h resulted in stable GUV formation with a significantly lower yield 24 ± 3 vesicles per square mm; however, the average diameter of vesicles increased to 25.5 ± 3.0 µm. The general tendency in the distribution of vesicular diameters has changed as presented in Figure 3-10 (green bars). Vesicles with diameter from 20 µm to 30 µm form 50 % of the population.

The collected data demonstrate that length of the electroformation time has a strong influence on polymersome yield and average diameter. Experiments with an electroformation time of 2 h resulted in the formation of vesicles with the highest yield as presented in Figure 3-11 (typical sample images are presented in the Figure 3-12); however, a further increase in the experiment time gave a significant decrease in GUV yield and average size.

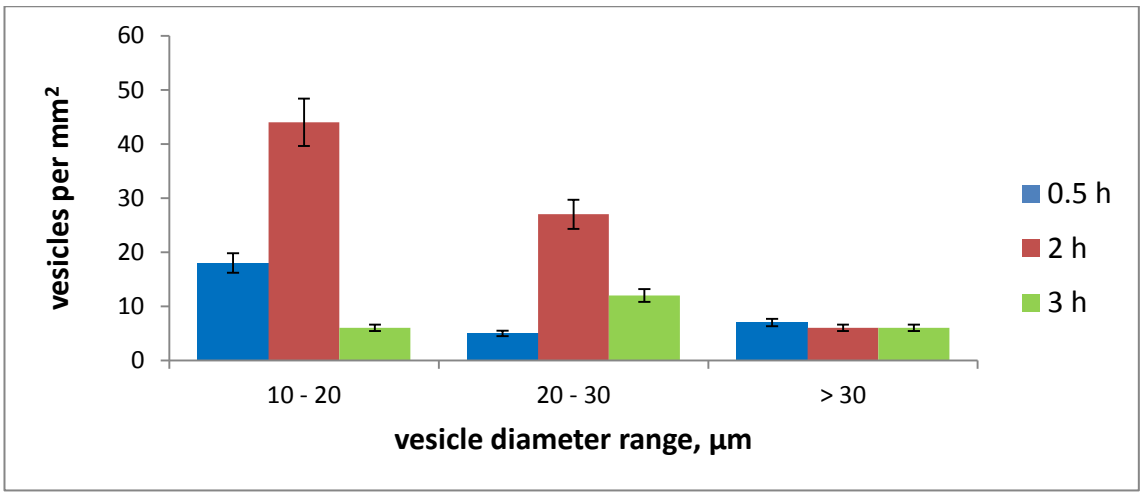

Figure 3-10. Distributions of M1 vesicles diameters dependence on electroformation time (formed using procedure B). Only vesicles with diameter larger than 10 µm were included in the statistics.

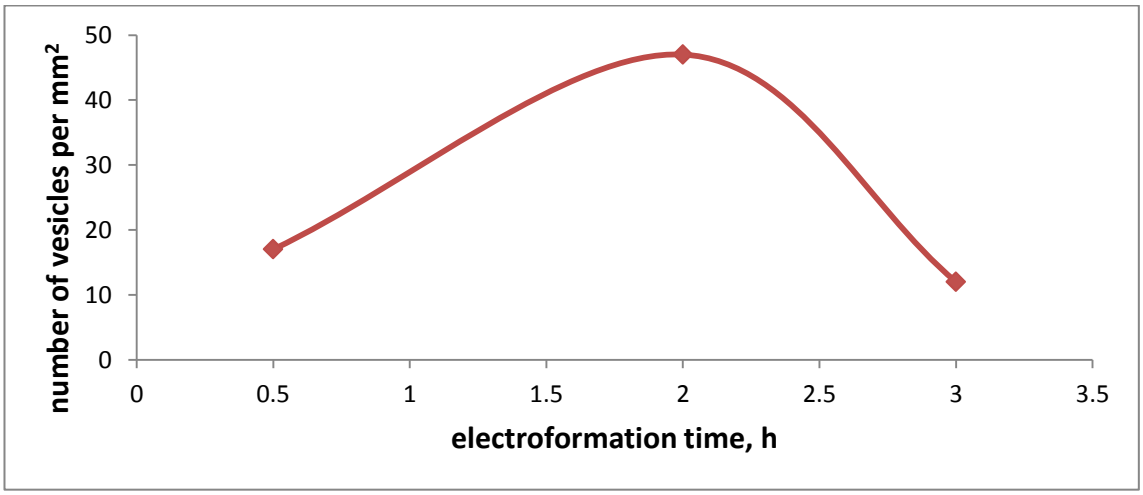

Figure 3-11. Change in amount of vesicles from polymer M1 upon varying electroformation time. Only vesicles with diameter larger than 10 µm were included.

The shape of the graph presented in Figure 3-11 indicates that the optimal electroformation time is 2h and further adjustments in the length of experiment resulted in a significant decrease in the number of produced GUVs. A shorter experiment time is not sufficient for GUV formation in high yield, while longer

self-assembly time (than optimal) results in giant polymersome fission to large and medium units, which are not desirable for further experiments. Polymersomes created under the most suitable conditions were applicable for further internalisation studies as reported in the Chapter 4.

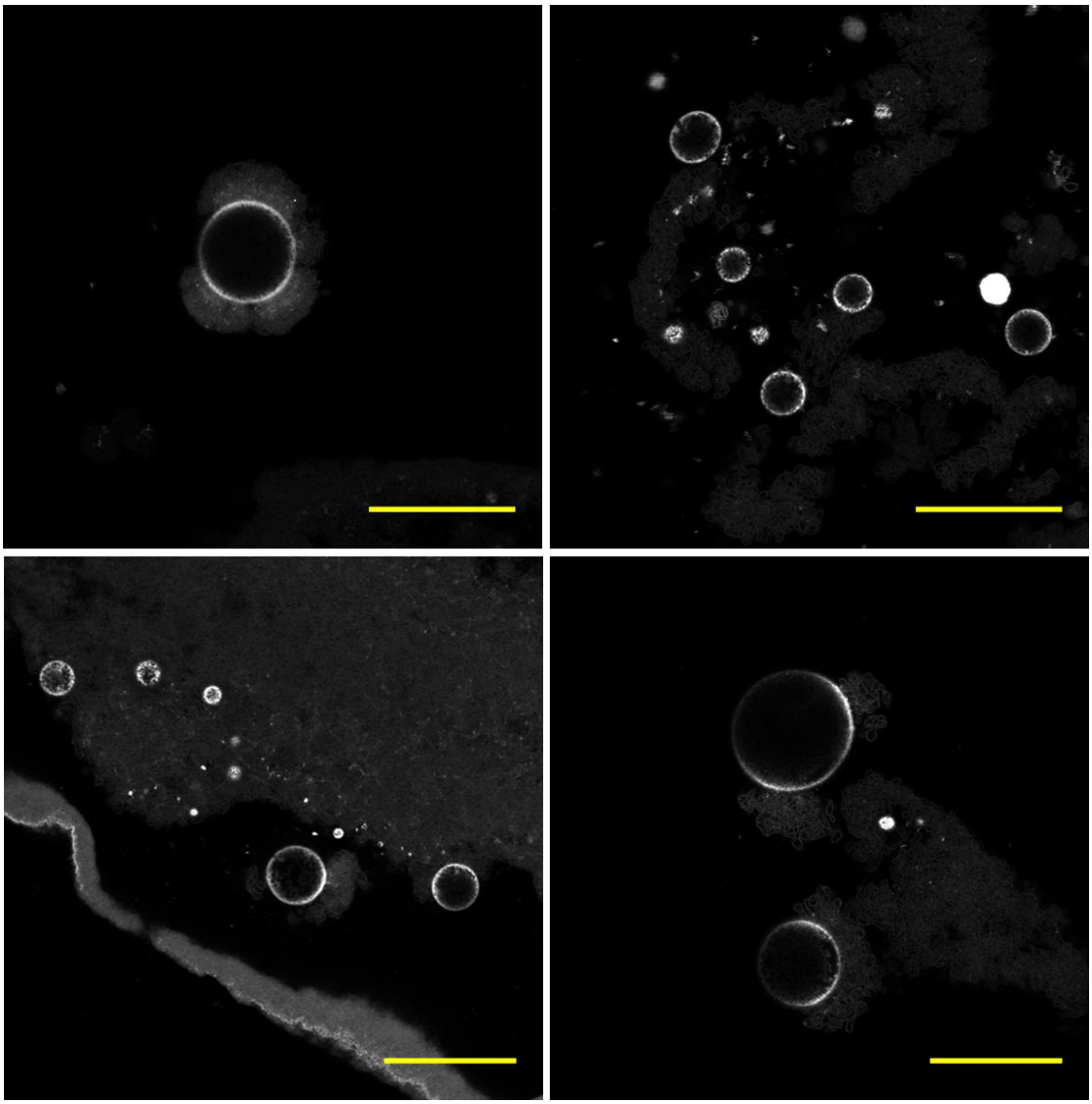

Figure 3-12. Confocal images of polymersomes M1 formed under procedure "B" with electroformation time of 2 hours. Hydrophobic fluorescent dye Rhodamine B octadecyl ester perchlorate was used for sample visualisation. Scale bar size is 40 µm.

3.3.5. Glycopolymersome electroformation from glycopolymers H2

Initial electroformation experiments based on procedure “B” revealed that glycopolymer H2 is also able to form giant vesicles in high yield. Therefore it was decided to perform a more detailed study on the polymer H2 self - assembly process. The electroformation experiments were carried out with varying time: 0.5 h, 2 h and 3 h (analogous as for glycopolymer M1 as described in 3.3.3.1).

Studies were initiated with an electroformation time of 0.5 h in order to examine the possible differences in self-assembled structures from glycopolymers H2 and M1. These initial experiments were deemed to be successful, due to the formation of stable, giant polymersome clusters with an average density of 1160 ± 50 vesicles per square mm; however only one GUV with size larger than 10 µm was observed in the sample as presented in the Figure 3-13 (blue bar). The majority of polymersomes were of size from 3 µm to 6 µm assembled into vesicle clusters (from 9 to 100 polymersomes in one cluster) as presented in the Figure 3-15 a) and Figure 3-15 b).

A further increase in electroformation time to 2 h resulted in a minor rise in the average density of GUVs of diameter 10 to 20 µm, to 19 ± 2 vesicles per square mm (Figure 3-13 red bar); however GUVs larger than 20 µm were not detected in the specimen and the polymersome clusters, analogous to observed ones after a 0.5 h electroformation, were still present in the sample (Figure 3-15 c) and Figure 3-15 d)).

Experiments with an electroformation time of 3h resulted in a further increase in the number of formed single vesicles, moreover, the average diameter (21.3 ± 2.2 µm) of

the formed structures also rose, as presented in Figure 3-15 (green bars). Polymersomes with an average diameter from 10 µm to 20 µm were recorded with an average density of 30 ± 3 units per square mm and constituted 53 % of the whole population. Vesicles with an average size from 20 µm to 30 µm were obtained with an average density of 9 ± 1 vesicles per square mm. Structures larger than 30 µm were observed with an average density of 5 ± 1 vesicles per square mm. Typical polymersome images obtained after the experiment are presented in Figure 3-15 e) and Figure 3-15 f).

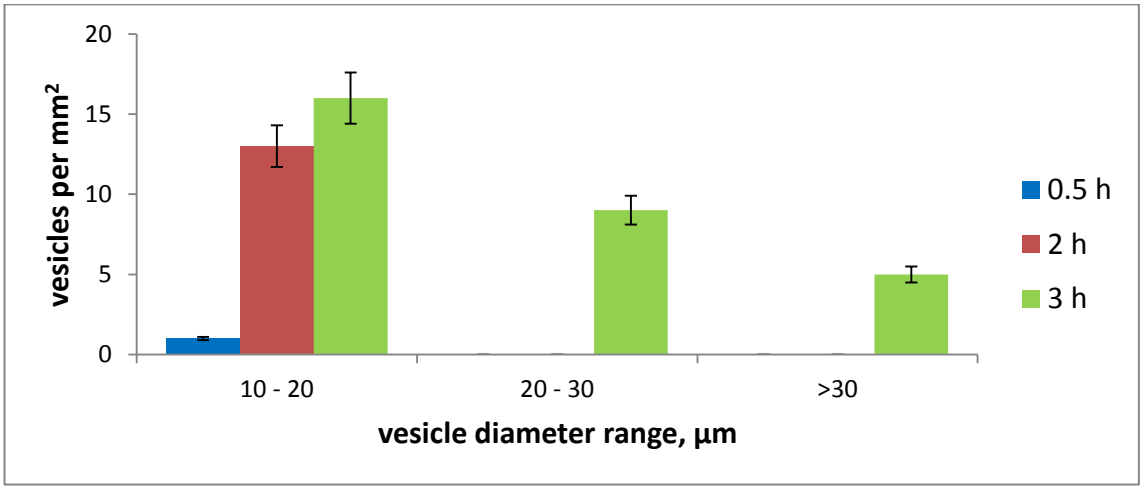

Figure 3-13. Distributions of H2 vesicles diameters dependence on electroformation time (formed using procedure "B"). Only vesicles with diameter larger than 10 µm were included in the statistics.

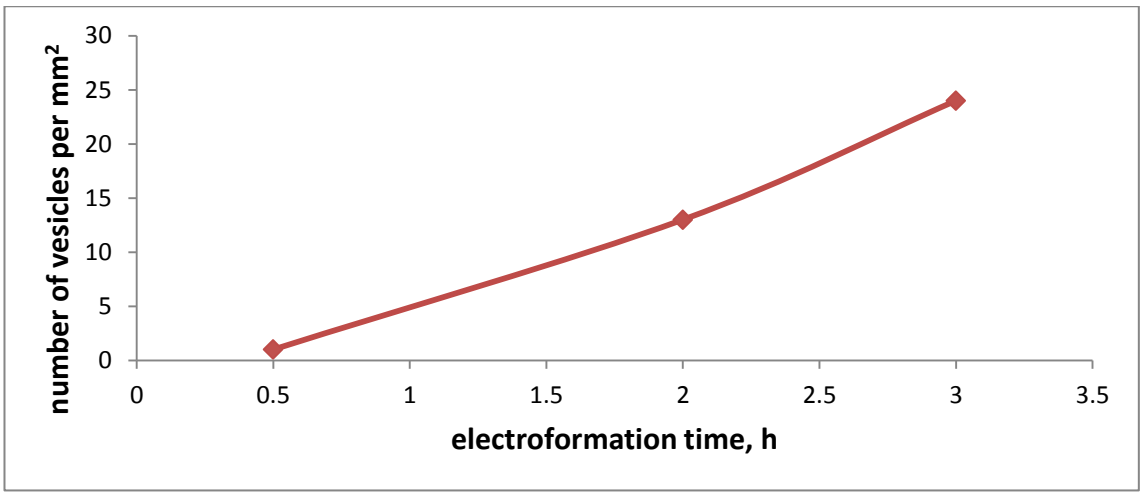

Figure 3-14. Change in amount of vesicles from polymer H2 upon varying electroformation time. Only vesicles with diameter larger than 10 µm were included.

Increasing the electroformation time to 3 h enhanced notably the number of produced giant vesicles and their average size; however, adjustments in the experiment time have not reduced the number of vesicular clusters which were still commonly observed in the sample. The polymersome assemblies were not desirable in specimens due to the high possibility of inducing distortion and misinterpretation of data on polymersome properties collected in further studies. The profile of the graph presented in Figure 3-14 suggests that the optimal electroformation time for glycopolymer H2 has not been reached. According to the observed tendency a further rise in electroformation time could trigger formation of giant polymersomes and reduce amount of vesicular clusters; however, additional increase in experiment length would make the process time consuming and inefficient for further research, consequently an additional study of glycopolymer H2 self - assembly properties was discontinued.

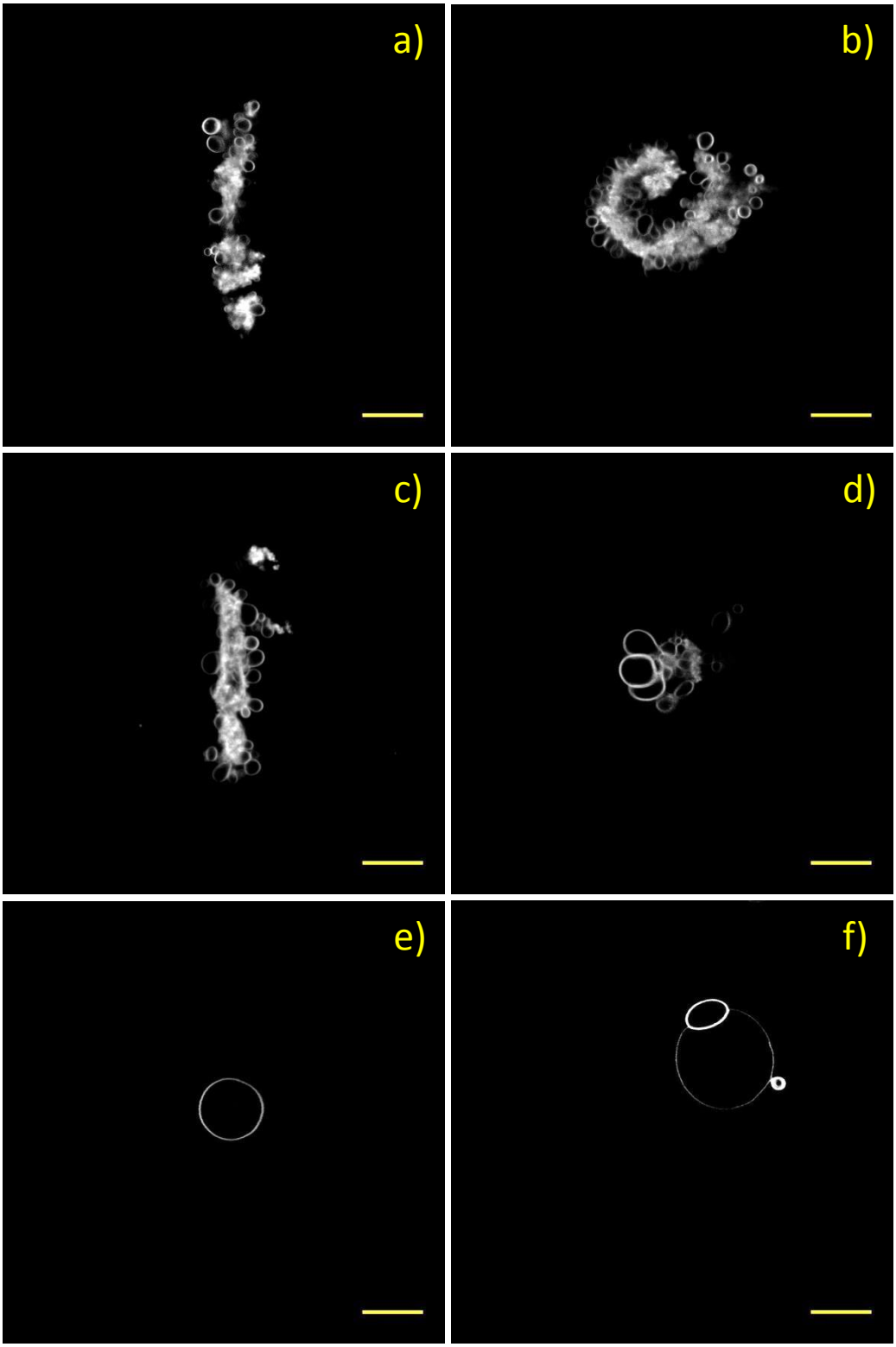

Figure 3-15. Confocal images of polymersomes formed from polymer H2 under procedure "B" with varying electroformation time: 0.5 h (a, b), 2 h (c, d) and 3 h (e, f). Hydrophobic fluorescent dye rhodamine B ctadecyl ester perchlorate was used for sample visualisation. Scale bar size is 20 µm.

3.4. Conclusions

Initial experiments on glycopolymer PE - b - (Glu) PEG giant glycopolymersomes were accomplished. The most suitable solvent mixture for the polymer layer preparation on the ITO covered glass slides was reported to be chloroform and methanol in the ratio 4 : 3. Conditions suitable for reproducible GUVs electroformation were determined (conditions #5 in Table 3-3). The GUVs were formed in high yield with a broad size distribution. The oval shape of the structures suggests that they remain in the semi - solid state due to the high melting transition temperature of the used polymer.

Glycopolymer $PNGEA_n$ - b - BA_m was synthetised with a systematically varied molar block ratio n to m (as presented in Table 3-4) in order to adjust packing parameter value to a range from ½ to 1 which is reported in literature as suitable for vesicle formation. It was expected that with an increase in size of hydrophobic tail block (m) in comparison to a size of hydrophilic head block (n), the molecular packing parameter (P) would increase and therefore the type of aggregates formed during the self-assembly process will change from micelles to vesicles respectively.

Data collected during the initial research on glycopolymersome electroformation under two different protocols (procedure “A” and procedure “B”) revealed that glycopolymers with a molar block ratio of 1 to 10 and higher (n to m; glycopolymers M1 and H2) characterise with a strong tendency to self - assemble into giant vesicles. Glycopolymers with a molar block ratio lower than 1 to 10 self-assemble into GUVs with a significantly lower yield (K1 and J1) or do not form giant vesicular structures at all which is congruous with initial expectations based on packing parameter

predictions. Furthermore, those glycopolymers with packing parameter lower thank ½ are likely to create nanoscale structures such as spherical micelles and rod - like micelles; however, those structures are not clearly detectable in prepared specimens due to visualisation technique utilised in the present study.

Glycopolymer M1 is the most promising polymer for formation of vesicles with a broad size range and high yield. Under conditions “A” GUVs from glycopolymer M1 were assembled with an average density of 37 ± 4 vesicles per square mm and with an average diameter of 19.7 ± 2.0 μm. Upon applying conditions “B” polymersomes M1 were created with significantly higher yield (77 ± 8) and average diameter (24.0 ± 2.0 μm). The electroformation protocol “B” was also suitable for GUV formation from the glycopolymer H2. Giant glycopolymersomes were assembled with an average density 30 ± 3 per square mm and average diameter of 21.3 ± 2.2 μm. The yield and size of electroformed vesicles are strongly dependent on the length of the self-assembly experiment, and is specific for every glycopolymer.

The created self - assembled structures from glycopolymer M1 under optimal conditions of procedure “B” were deemed to be suitable for further studies on polymer membrane behavior and properties, and synthetic cell model creation.

4. Studies on Giant Glycopolymersomes

4.1. Introduction

In the last few years there has been a growing interest in developing synthetic models of cells with the ability to mimic processes occurring within the cell and the cellular membrane.[108-110] Quite recently, considerable attention has been paid to reproducing the naturally occurring processes phagocytosis and endocytosis in purely synthetic systems.[111-113] This research is focused on creating a physical system which is able to perform receptor mediated endocytosis (RME).

RME is a process by which cells selectively absorb molecules and other species such as viruses located in the external medium by utilising vesicles containing proteins with receptor sites exclusive for the absorbed molecules as a delivery and selectivity mechanism. Binding of a required molecule to the receptor site triggers a series of events which result in an invagination of the target particle by the plasma membrane and opsonisation in a vesicle by the host cell as presented in Figure 4-1. RME plays an important role in cell life and functionality; it participates in a variety of cellular processes such as the uptake of specific substances required by the cell, transduction and downregulation of the transmembrane signals.

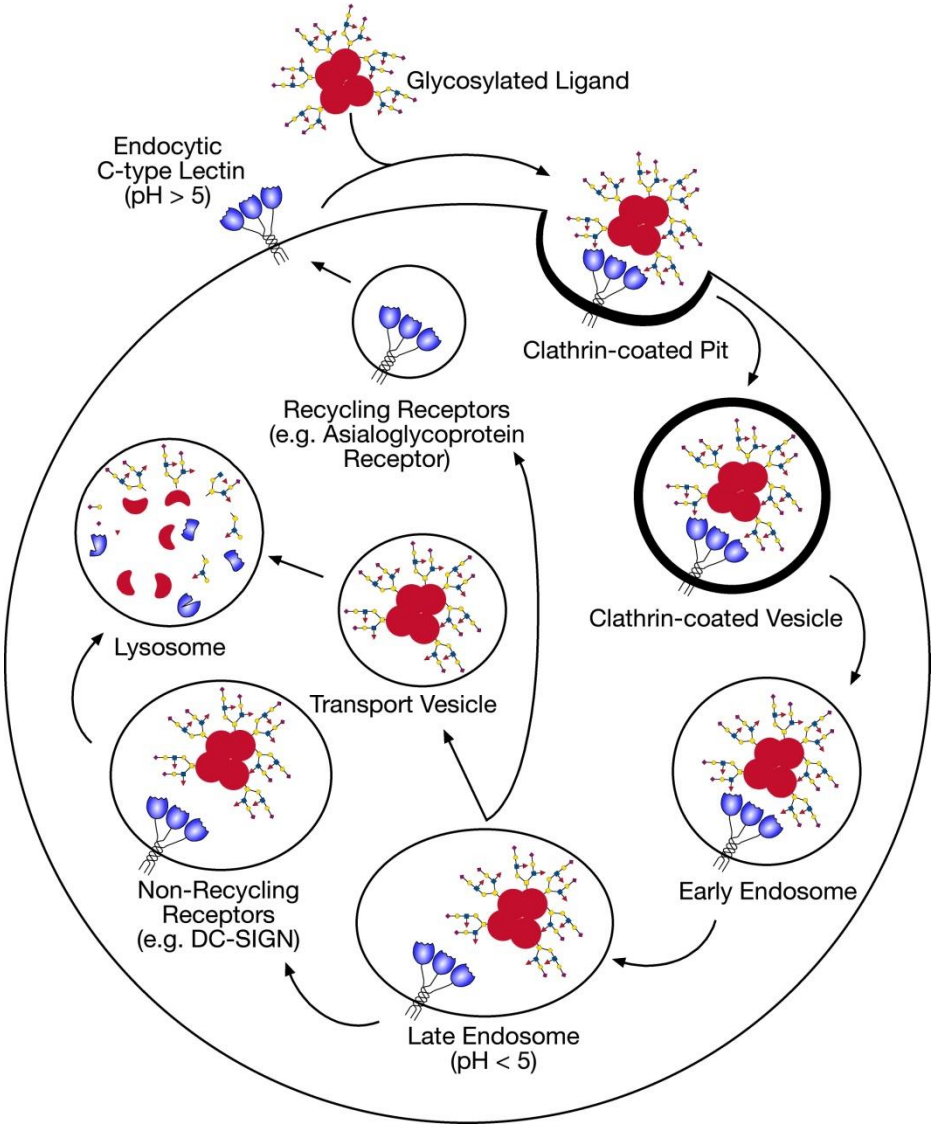

Figure 4-1. C-type lectins that function as endocytic receptors.[114]

In order to create a reliable RME model it is essential to choose a suitable material to mimic the cellular membrane and to select a convenient ligand - receptor pair which could be easily employed in the study. For several years much effort has been devoted to the study of interactions between lectins and polymers decorated with different sugar moieties.[115-117] Lectins are carbohydrate - binding proteins with high specificity for sugar functional groups; they are spread ubiquitously in nature with a variety of carbohydrate selectivity which has been of interest to scientists for more than twenty

years.[116, 118-120] Even though the function of some plant lectins is unknown, the role of animal lectins is well understood. Animal lectins play a vital role in a variety of recognition and bridging events.[121] One of the widely known superfamily of animal lectins is the C - type lectins. The family includes collectins, selectins, endocytic receptors, and proteoglycans. The function of many of the C - type lectins in RME is to initiate the endocytosis process by recognising and binding with specific ligands; examples of the endocytic C - type lectins are asialoglycoprotein receptor (ASGPR) in hepatocytes, dendritic cell - specific intercellular adhesion molecule - 3 - grabbing non - integrin (DC - SIGN) in myeloid cells and P - selectins in endothelial cells. Inspired by nature, we have decided to utilise lectin - sugar selective interactions in our study as a receptor - ligand pair (as presented in Figure 4-2). However, even if the receptor - ligand pair can introduce the required selectivity in a physical RME model, is it possible to perform selective encapsulation of external particles into a polymersome?

Calculations performed by Balazs et al. suggest that encapsulation of nanoscopic particles into polymersomes is achievable in a purely synthetic system.[113] The authors modelled the interaction of giant liposomes with spherical nanoparticles in solution utilising dissipative particle dynamics (DPD). Studies were performed with the aim of understanding the mechanism of the external objects' passage through the vesicular membrane. Modelling parameters were chosen accordingly to induce unified favorable adhesive interactions between the membrane and the nanoparticle. The results obtained by the authors suggest that under these conditions a homogeneous membrane is unable to fully wrap the particle if the adhesion strength is below a threshold (see Figure 4-2 b) - d)); moreover, this phenomenon is observed even if the membrane tension is limited to zero. When the adhesion strength is increased above a

certain value, the vesicular membrane fully wraps the particle; however, the engulfed structure remains attached to the membrane (as presented in Figure 4-2 e)). To overcome this challenge, the authors proposed creating a system based on a nonadhesive vesicular membrane with adhesive rafts. Studies confirmed that adhesive rafts promote fission allowing the vesicle with the engulfed cargo to detach from the larger membrane (see Figure 4-2 f)).

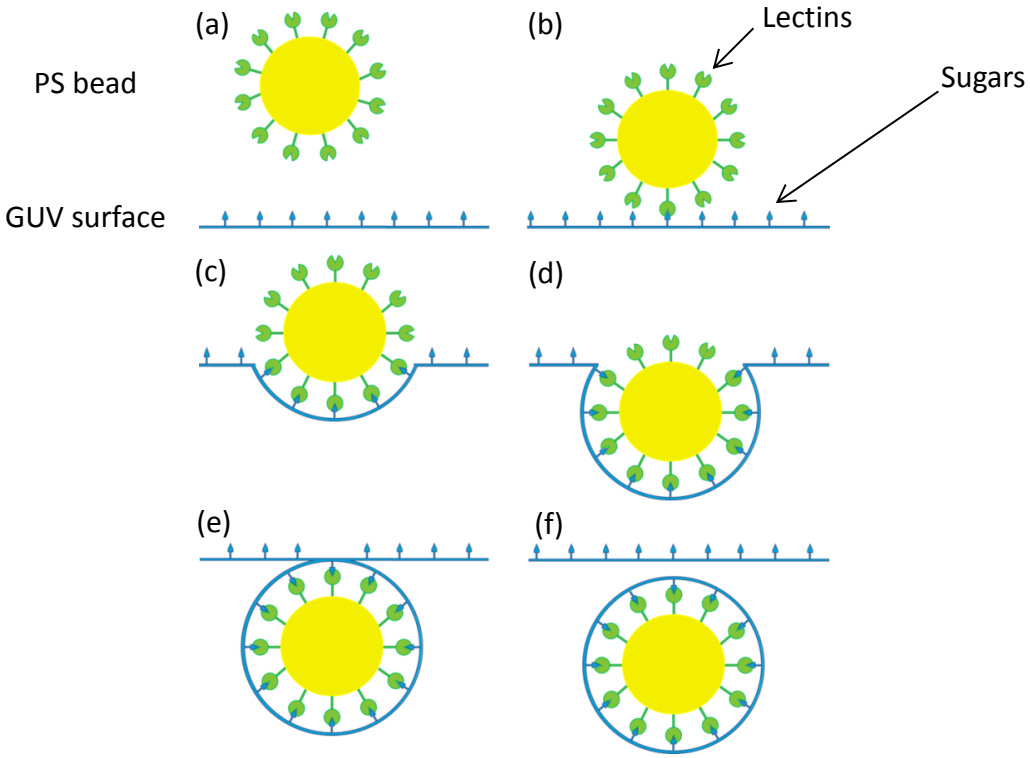

Figure 4-2. Schematic representation of a physical RME model based on selective sugar - lectin interaction. Respectively: a) a PS bead functionalised with the lectin and approaches the surface of a GUV, b) Con A lectins present on the PS bead surface interact with glucose pendent units present on the GUV surface, c) membrane invagination appears in the interaction site, d) PS bead is engulfed by membrane, e) PS bead is fully coated by the membrane, f) PS bead is opsonised by the polymersome.

4.2. Studies on glycopolymersome properties

Initial electroformation studies on the glycopolymer PNGEA - b - BA presented in Chapter 3, revealed that glycosylated block copolymer M1 with a block ratio 1 : 10 (hydrophilic block to hydrophobic block ratio) reproducibly generates GUVs upon applying the electroformation method with conditions described as procedure “B” (as presented in 3.3.3.1). In order for the polymersomes from M1 to serve as an effective artificial cell prototype, their response to changing environmental conditions and their permeability to various substances must be well - understood. Therefore, osmotic shock and pH stress approaches were utilised as simple and versatile methods to obtain information on the polymersome membrane permeability and stability (as presented in 4.2.1. and 4.2.2). Following studies of vesicular properties, a development of a physical RME model is described in detail in Chapter 4.3.

4.2.1. Osmotic Shock

The osmotic shock approach presents a straightforward method to gather data on polymeric membrane permeability and stability. Optical microscopy was employed to observe the response of aqueous solution - filled polymersomes to osmolality changes in the external solution. The rate of vesicle size change is dependent on the permeability of its membrane. Due to difficulties in observation of freely floating structures within a restricted field of view before and after adjustment in the osmolality of the peripheral solution, an average diameter of GUVs present in the sample of > 10 μm was chosen as a threshold parameter on which to monitor changes in the vesicular morphology induced by osmotic pressure. The osmotic pressure

gradient between an internal vesicular medium and the external (surrounding) medium separated by the semi - permeable polymersome membrane is related to the difference in osmolality:

$$\Delta \boldsymbol{\Pi} = \boldsymbol{RT}(\boldsymbol{c_{int}} - \boldsymbol{c_{ext}}) = \boldsymbol{RT\Delta c} \qquad \textbf{(4-1)}$$

Where: $\boldsymbol{\Delta\Pi}$ - osmotic pressure gradient (atm), $\boldsymbol{R}$ - gas constant (L × atm × K $^{-1}$ × mol $^{-1}$), $\boldsymbol{T}$ - temperature (K), $\boldsymbol{c_{int}}$ - molar concentration of internal solution (M), $\boldsymbol{c_{ext}}$ - molar concentration of external solution (M).

GUVs were prepared using an electroformation method based on procedure “B” (as described in 6.3.4.3.) and their initial average diameter was determined for samples that were diluted by an isotonic aqueous solution. The second measurement of the average diameter was performed 2 h after applying the osmotic shock by adjusting the molar concentration of NaCl (hypertonic shock) or sucrose (hypotonic shock) in the external aqueous solution. The GUVs were subjected to systematically varied osmotic pressures as presented in Table 4-1 and a time delay of 2 h was sufficient to observe changes in GUV diameter induced by the osmotic pressure gradient created between the internal polymersome medium and the external solution present in the sample.

Table 4-1. Compound utilised to adjust osmotic pressure, osmotic shock values expressed in molar concentration gradient and osmotic pressure gradient, and percent change in average diameter of vesicles upon applied conditions.

#	Utilised compound	Δc (mM)	ΔΠ (atm)	Δ in average diameter (%)
1	NaCl	-750	-36.6	-20 ± 2.0
2	NaCl	-500	-24.4	-20 ± 2.0
3	NaCl	-250	-12.2	-10 ± 1.0
4	NaCl	-125	-6.1	-4.3 ± 0.4
5	NA	0	0.0	0.7 ± 0.0
6	sucrose	250	6.1	2.1 ± 0.2
7	sucrose	500	12.2	3.8 ± 0.4

The evolution of GUV average diameter upon hypertonic and hypotonic osmotic shock presented in Figure 4-3 confirmed that negative osmotic pressure results in shrinking and positive osmotic pressure in swelling of polymersomes. The GUVs are more susceptible to hypertonic conditions than hypotonic. Upon creating - 12.2 atm osmotic gradient a decrease in the vesicle average diameter was observed by 10.0 ± 1.0 %; however, upon applying + 12.2 atm osmotic pressure a slight increase in the polymersome average diameter was recorded by 3.8 ± 0.4 %.

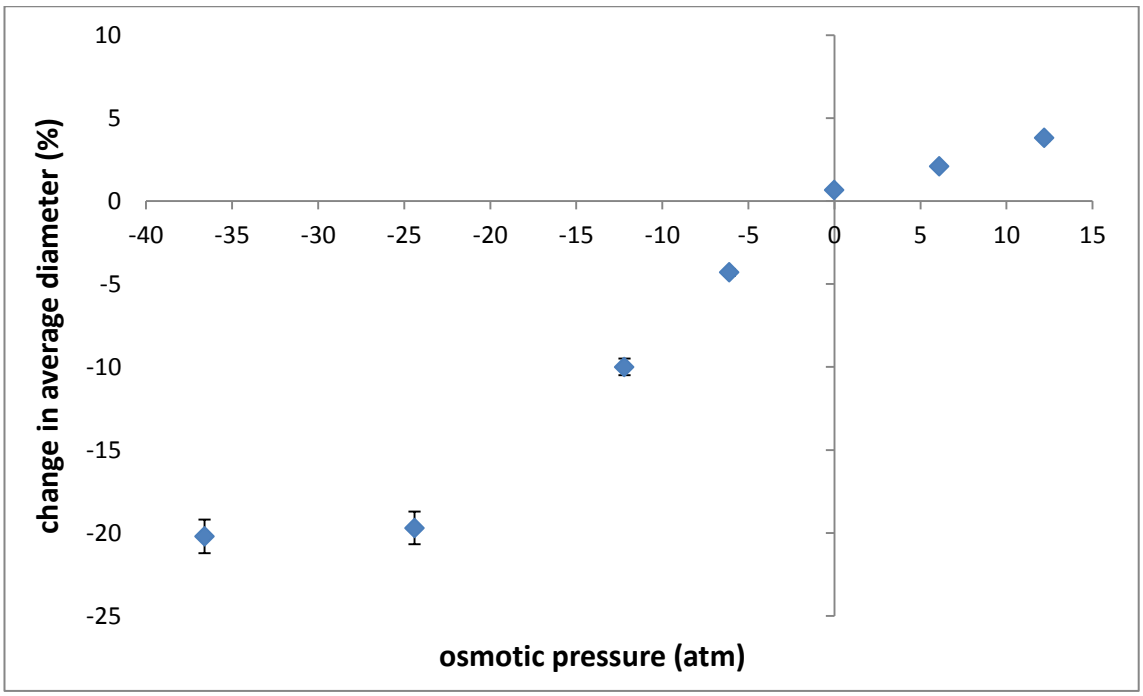

Figure 4-3. Percent change in GUVs diameter after applied various osmotic shocks. Only vesicles larger than 10 µm were included in the statistics.

The average diameter of vesicles decreased linearly by 20 ± 2.0 % upon gradual increase in negative osmotic pressure to 24.4 atm; however, no significant decrease by was recorded upon a further increase in negative osmotic pressure to 36.6 atm. The observed phenomena can be related to the stability and permeability of the created structures. Polymersomes from M1 are able to withstand a hypertonic shock with values lower than 24.4 atm; upon applying a negative osmotic pressure, gradual shrinkage of the structures is observed - the pressure between inner polymersome media and the surrounding solution is equalised. GUVs are not able to withstand without damage a hypertonic shock pressure higher than 24.4 atm; the majority of the largest polymersomes collapse and only the most stable GUVs remain undamaged. Following initial shock, the sample osmolality reduces and the vesicles which survived accordingly reduce their diameter to equalise the osmotic pressure.

The data collected during hypertonic osmotic shock experiments performed on GUVs electroformed from glycopolymer M1 suggests that those microstructures are resistant to osmolality changes in surrounding solution. For comparison, Carlsen et al. reported that vesicles prepared from polymers PDMS - g - PEO (surfactant Dow Corning 5329) and PB_{46} - b - PEO_{30} in hypertonic conditions reduces their diameter more than 40 % (at pressure of 6 atm) and 30 % (pressure of 2.5 atm) respectively.[122] Those microstructures are significantly more susceptible to hypertonic shock that GUVs utilised in our study. Shum et al. studied properties of polymersomes generated from polymer PEG_{5000} - b - PLA_{5000} and showed that under severe hypertonic conditions (pressure of 24.4 atm) those microstructures reduce their diameter by 18 %, which are comparable to data obtained for GUVs M1.[123] Even higher resistance to hypertonic conditions was reported for polymersomes generated from triblock copolymer PEO - b - PDMS - b - PEO. Salva et al. demonstrated that in hypertonic conditions (at pressure of 18.3 atm) those vesicles adjust their diameter by only 10 %.[124]

The average diameter of the vesicles increased linearly by 3.8 ± 0.4 % upon applying a positive osmotic pressure of 12.2 atm. The absolute value of the average diameter percent change was significantly lower in comparison to the hypertonic shock (3.8 ± 0.4 % vs. - 10 ± 1.0 %). A plateau point was not observed in the hypotonic pressure region possibly due to the limitations of the self - assembly method employed in this study; the electroformation of glycopolymersomes can only be successfully performed in aqueous solutions under certain conditions. Control electroformation experiments on glycopolymer M1 revealed that this self - assembly method is inefficient with a sucrose concentration above 1 M, possibly due to a significant increase in the solution

viscosity (approximately 3 times higher in comparison to the viscosity of ultrapure water).

4.2.2. pH Shock

A pH shock approach was utilised as a straightforward method to observe the response of giant polymersomes to changing proton concentration in the external solution. It can be assumed that the pH shock approach is a specific type of osmotic shock induced by H^+ ions. Optical microscopy was employed to observe the response of aqueous solution - filled polymersomes to pH changes in the external solution. An average polymersome diameter was chosen as a threshold parameter to monitor changes in the vesicular population induced by a pH switch. The samples of GUVs from M1 were prepared utilising procedure “B” (as described in 6.3.4.3.) in ultrapure water and their average diameter was determined immediately after preparation. The second measurement of polymersome average diameter was performed 2 h after applying a pH shock by adding the required amount of 1 M HCl or 1 M NaOH solution. The GUVs were observed under systematically varied pH values as presented in Table 4-2.

Table 4-2. pH shock parameters and percent change in average diameter of vesicles.

#	Utilised compound	Δ pH	final pH value	Δ in average diameter (%)
1	HCl	- 6	1	-14 ± 1.4
2	HCl	-4	3	2.3 ± 0.2
3	HCl	-2	5	1.6 ± 0.2
4	NA	0	7	0.7 ± 0.0
5	NaOH	2	9	-3.8 ± 0.4
6	NaOH	4	11	-4.1 ± 0.4
7	NaOH	6	13	-13 ± 1.3

The variation of GUV average diameter under various pH values showed that polymersomes are more susceptible to a basic environment than an acidic environment as presented in Figure 4-4. Upon adjusting the pH value to 11 (higher by 4 units from starting pH 7 value), the average polymersome diameter decreased by 4.1 ± 0.4 %, while adjusting the pH value to 3 (lower by 4 units from starting value pH 7) increased the vesicle average diameter by 2.3 ± 0.2 %, which is two times lower than was observed under basic conditions.

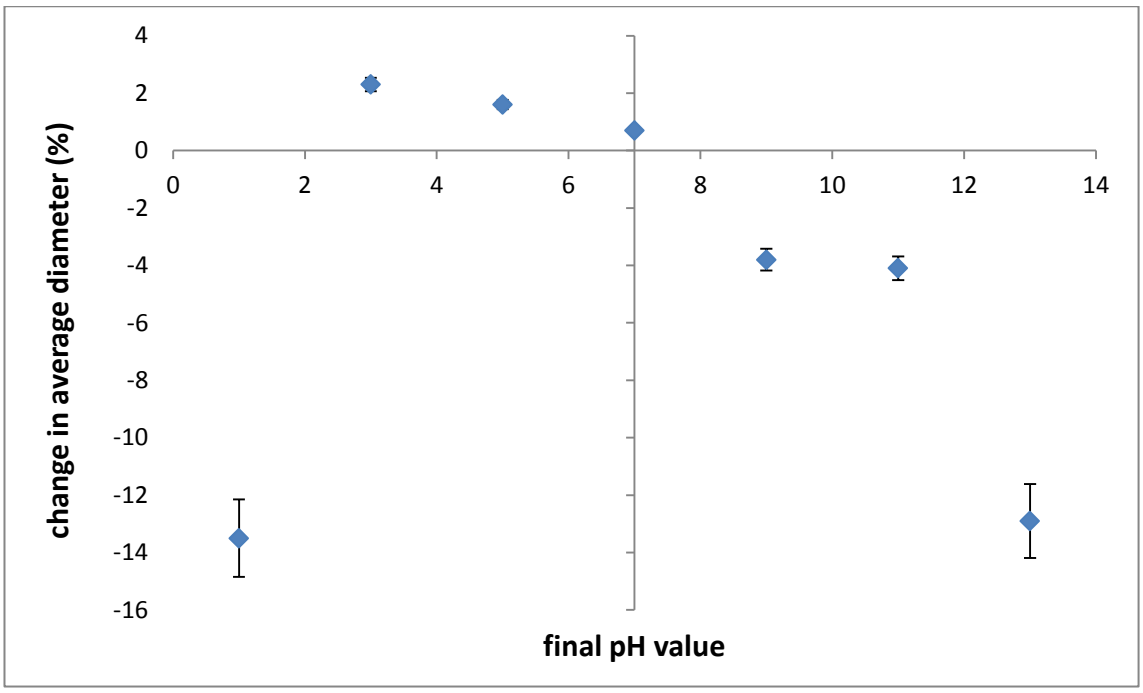

Figure 4-4. Percent change in GUV diameter with change in pH value. Only vesicles larger than 10 µm were included in the statistics.

At pH 13 a significantly larger decrease in the GUV average diameter was observed than is recorded at pH 11; the average diameter of the vesicles changed by - 13 ± 1.3 % (- 4.1 ± 0.4 % at pH 11).

Giant polymersomes in response to an acidic shock increased in average diameter; however, an exceptional phenomenon was observed at pH 1. The GUVs did not increase in diameter further following the trend determined between pH 5 and pH 3; moreover the average polymersome diameter decreased notably by 14 ± 1.4 %. The observed occurrence is possibly related to the stability and permeability of the polymersomes. The vesicles are susceptible to H^+ concentration changes in the environment due to the proton gradient created by the semi - permeable polymersome membrane. GUVs are not able to withstand the stress generated by the reduction of pH by 6 units (from starting pH 7 to final pH 1); the majority of the largest

vesicles collapse. The most stable GUVs which endured an initial pH shock increased their diameter; however, the average diameter of vesicles decreased significantly as presented in Table 4-2 and Figure 4-4 due to the GUVs rearrangement. An analogous process might occur during the experiment at pH 13 which is created by increasing the pH by 6 units (from starting pH 7 to final pH 13); the majority of the largest vesicles are not able to withstand the proton gradient and collapses - only the most stable (smaller) GUVs remain undamaged. Hence, a significant decrease in polymersome average diameter is observed in comparison to the values recorded after pH 9 and pH 11 shocks.

4.3. Interactions between glycopolymersomes and particles

Initially turbidity measurements of a solution containing GUVs from glycopolymer M1 and the lectin *Concanavalin A* (Con A; specific for mannosyl and glucosyl residues) were performed over a fixed period of time to examine if pendent glucose units present on the polymersomes' surface are able to interact with the water soluble lectin Con A and trigger aggregation. Once this assessment was accomplished, the research was redirected towards non - selective and selective interactions between GUVs formed from M1 and polystyrene (PS) beads functionalised with different lectins. Control experiments were performed with non - functionalised PS beads and the lectin *Ricinus communis Agglutinin* (RCA_{120}; specificity for Galβ1 - 4GalNAcβ1 - R) functionalised PS beads (PS - RCA_{120}) to investigate non - selective interaction between beads and GUVs from M1. Following initial analysis, research on selective interactions was performed utilising polymersomes from M1 and Con A - functionalised PS beads (PS - Con A).

4.3.1. Glycopolymersome interactions with the water soluble lectin Con A

Upon initial preparation of a mixture containing GUVs and lectin Con A (as described in subsection 6.3.6.3.) changes in visible light (λ = 450 nm) were recorded for the first 60 minutes every 5 minutes (as presented in Figure 4-5).

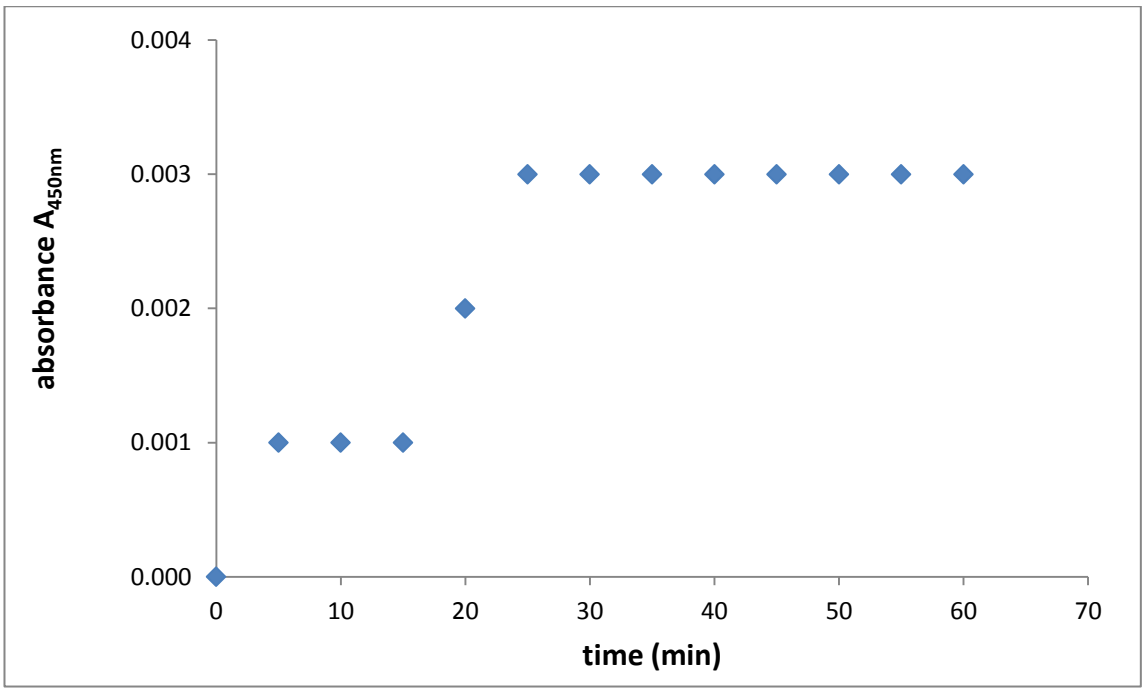

Figure 4-5. Change in visible light (λ = 450 nm) absorbance with time for mixture of GUVs and Con A (1 : 10 ratio).

Between 15 and 25 minutes from the start of the experiment the absorbance increased from 0.001 to 0.003; however, from 30 minutes of experiment onwards no further changes in absorbance were observed. The final recorded turbidity value for the lectin - sugar interactions was considered very low; possibly due to insufficient amount of glycopolymersomes present in the sample and/or a lack of interactions between the lectin and pendent sugar units present at the polymersome surface caused by steric factors. In order to explain the observed phenomenon, it was decided to repeat the performed experiment with a higher GUV concentration. A sample was prepared with an increase in volume of vesicular solution to 240 µl (giving a volume ratio 5 : 2). A_{450nm} was recorded for the first 60 minutes every 5 minutes. Collected data are presented in Figure 4-6.

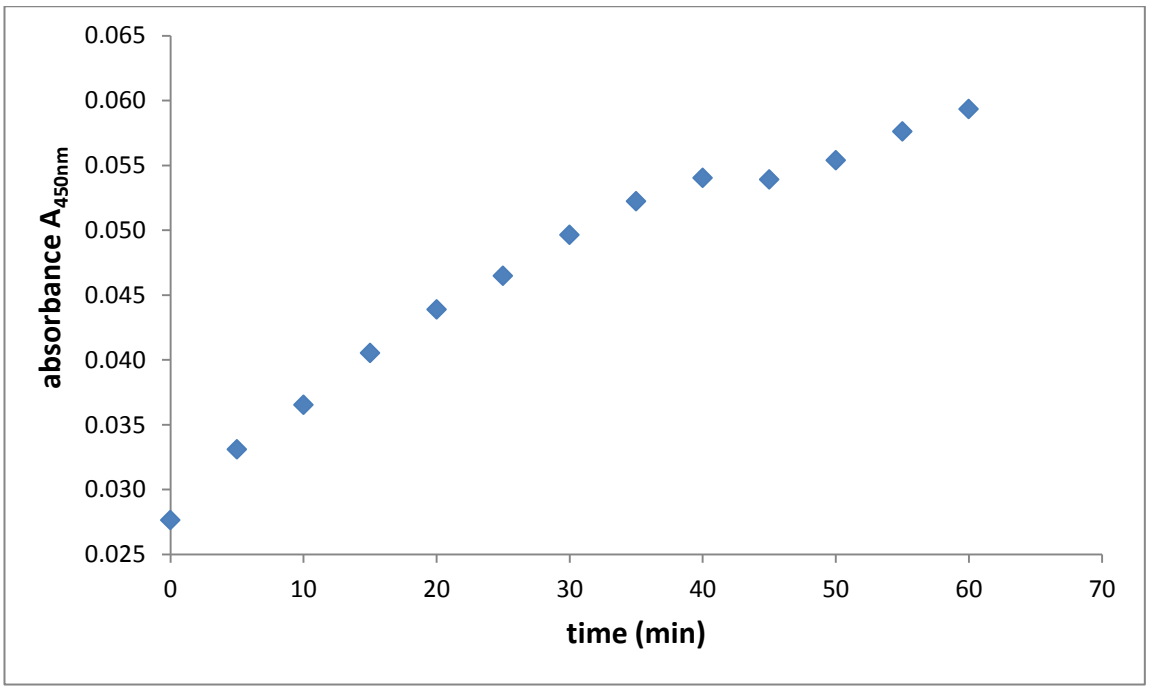

Figure 4-6. Change in visible light (λ = 450 nm) absorbance with time for mixture of GUVs and Con A (2 : 5 ratio).

A steady increase in light absorbance was observed for the first 40 minutes until it reached a value of A_{450nn} = 0.054. During the next 20 minutes a further increase in absorbance value was recorded to a value of A_{450nn} = 0.059, which is more than 20 times higher than the final absorbance obtained in the experiment with the lower amount of glycopolymersomes present in the sample. The collected data indicates that the amount of polymersome solution used in the initial turbidity experiment was too low. The turbidity experiment with an adjusted volume ratio of vesicle to lectin solutions confirmed that pendent glucose units are present on the polymersome surface and are able to interact with the lectin present in the sample. Due to the high avidity from the multivalency of the glycosylated hydrophilic copolymer blocks, giant glycopolymersomes are able to overcome the low affinity of carbohydrate ligands for their protein receptors and the cluster glycoside effect is observed as an increase in

the sample turbidity. Therefore it was concluded that GUVs from polymer M1 are suitable for use in interaction studies with solid PS particles functionalised with lectins.

4.3.2. Interactions with PS beads

Interaction studies were performed in a strictly controlled manner in order to minimalise any potential errors and misinterpretations of data produced by non – lectin mediated interactions. Considering that, two types of control experiments were performed: GUVs incubated with non – functionalized PS beads and GUVs incubated with PS beads functionalised with RCA_{120}, a lectin selective for galactose. Initial experiments involving incubation of glycopolymersomes with Con A - functionalised PS beads were performed under analogous conditions to study the selectivity of interaction between the macrostructures.

4.3.2.1. Non selective interactions between giant vesicles formed from glycopolymer M1 and carboxylate - modified PS beads

Experiments on glycopolymersomes and carboxylate - modified PS beads were replicated three times in order to obtain significant data on non - specific interactions between species. According to the collected data, vesicles and PS beads do not indicate any specific attraction. Upon overnight incubation of the microstructures, only a few beads were observed adhered to the vesicular membrane; however, the

majority of the PS beads were distributed randomly and remained attached to the bottom of the visualization chamber as presented in Figure 4-7 and Figure 4-8.

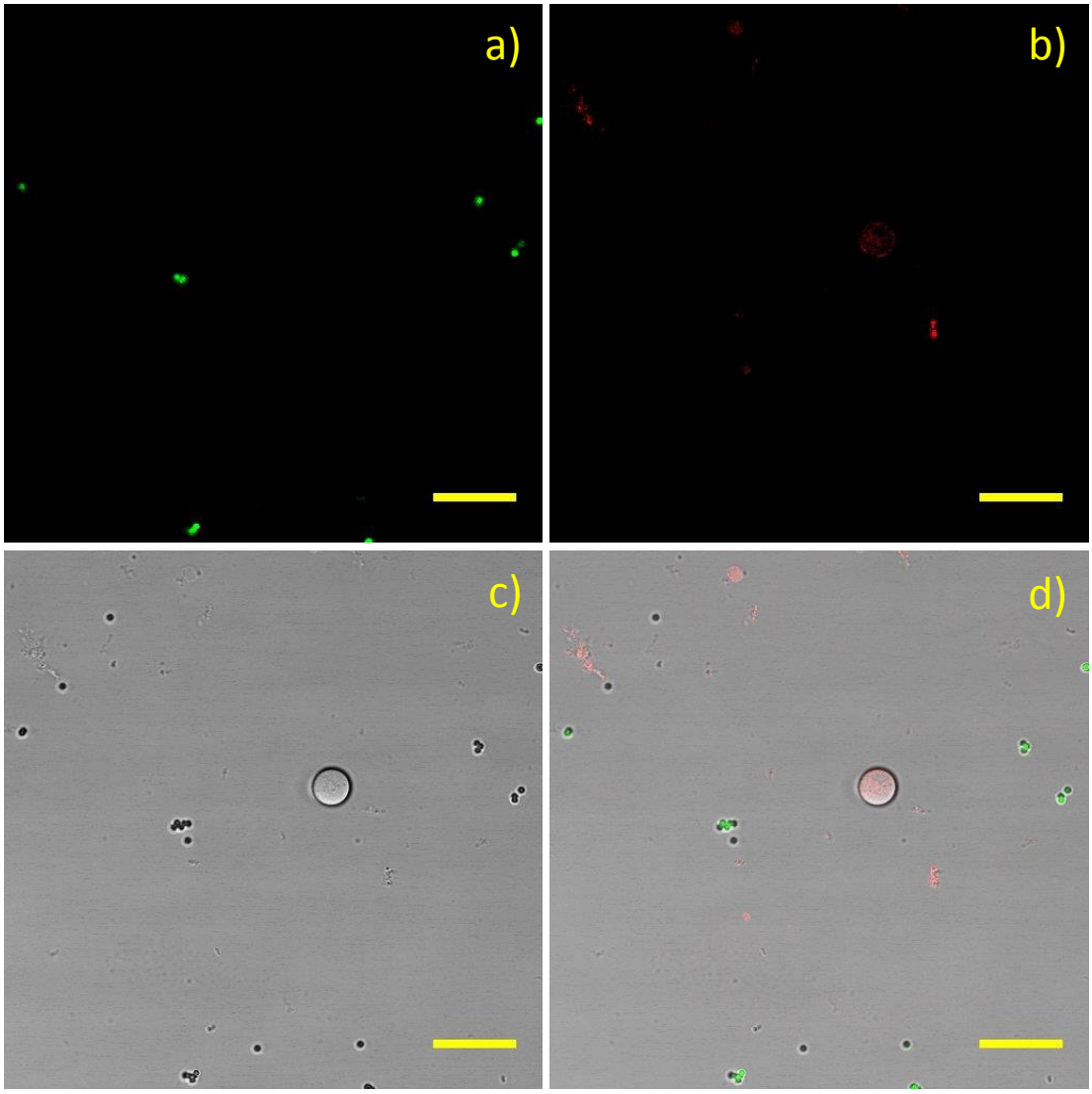

Figure 4-7. Confocal microscopy image of green dye (Fluorescein, λ_{ex} = 494 nm) labelled carboxylate - modified 1 µm PS beads a), red dye (Rhodamine B octadecyl ester perchlorate, λ_{ex} = 554 nm) stained micro - sized giant vesicles b), light microscopy image c) and overlaid green channel, red channel and light microscopy channel images d). Scale bar size is 20 µm.

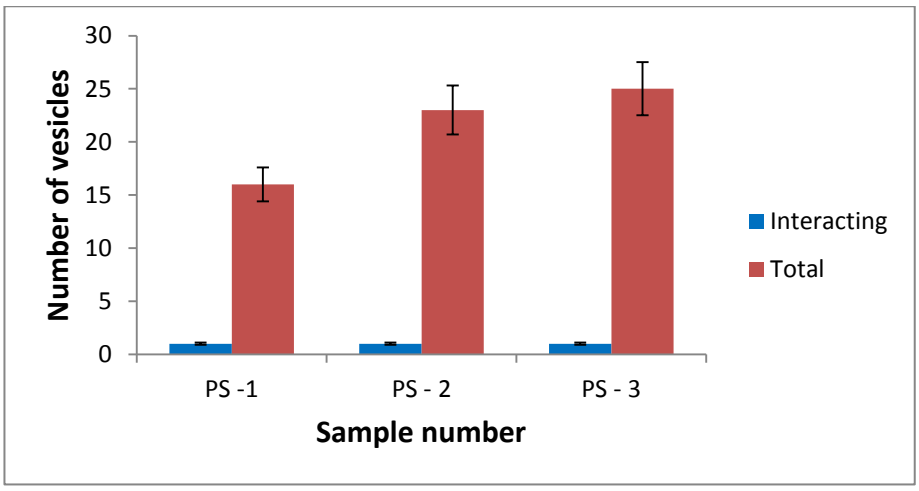

Figure 4-8. Number of GUVs interacting with carboxylate - modified 1 µm PS beads (blue bars) and total number of giant polymersomes observed in each sample (red bars).

The percent interaction of GUVs with carboxylate - modified beads did not exceed 6.5 % in each of the observed samples (see Figure 4-9). Based on the collected data, the average percent of non - specific interactions of the glycopolymer vesicles with PS beads was determined to be 4.9 ± 1.0 %.

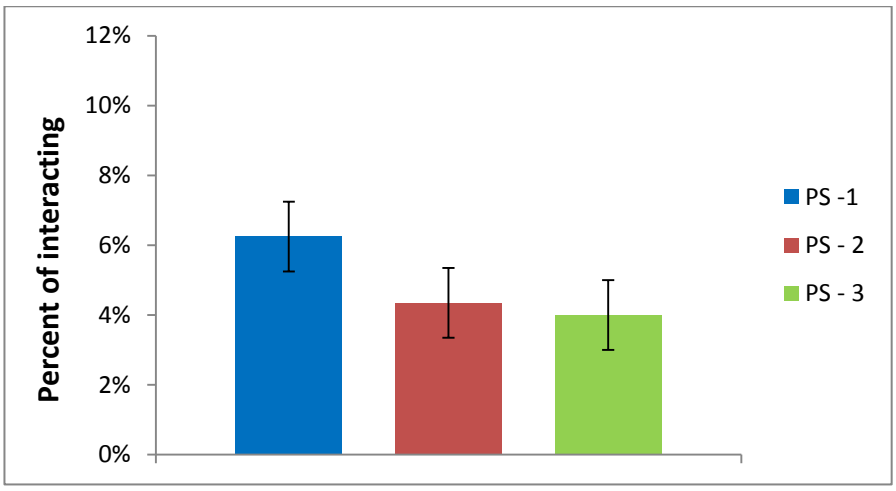

Figure 4-9. Percent interaction of the vesicles with carboxylate - modified 1 µm PS beads.

4.3.2.2. Vesicles and RCA_{120} - functionalised 1 µm PS Beads

Experiments on glycopolymersomes and RCA_{120} - functionalised PS beads (PS - RCA_{120}) were replicated three times in order to obtain significant data on interactions between the species. Upon overnight incubation of the microstructures a small number of interactions between the species were observed; however the majority of PS - RCA_{120} beads were dispersed randomly in the sample as presented in Figure 4-10 and Figure 4-11. The percent interaction of vesicles with PS - RCA_{120} varied from 6 % to 9 % (Figure 4-12), which is insignificantly higher than for carboxylate - modified beads (Figure 4-12 blue bars; 4 % - 6 %). The increase observed in the percent of interaction was possibly induced by the surface modification of PS particles with water - soluble lectin RCA_{120}, which could possibly interact non - selectively with the hydrophilic block on the surface of the vesicular membrane and remain attached during the interaction studies.

Based on the collected data, an average percent of interactions between glycopolymer vesicles and PS - RCA_{120} was determined to be 8.2 ± 1.4 %.

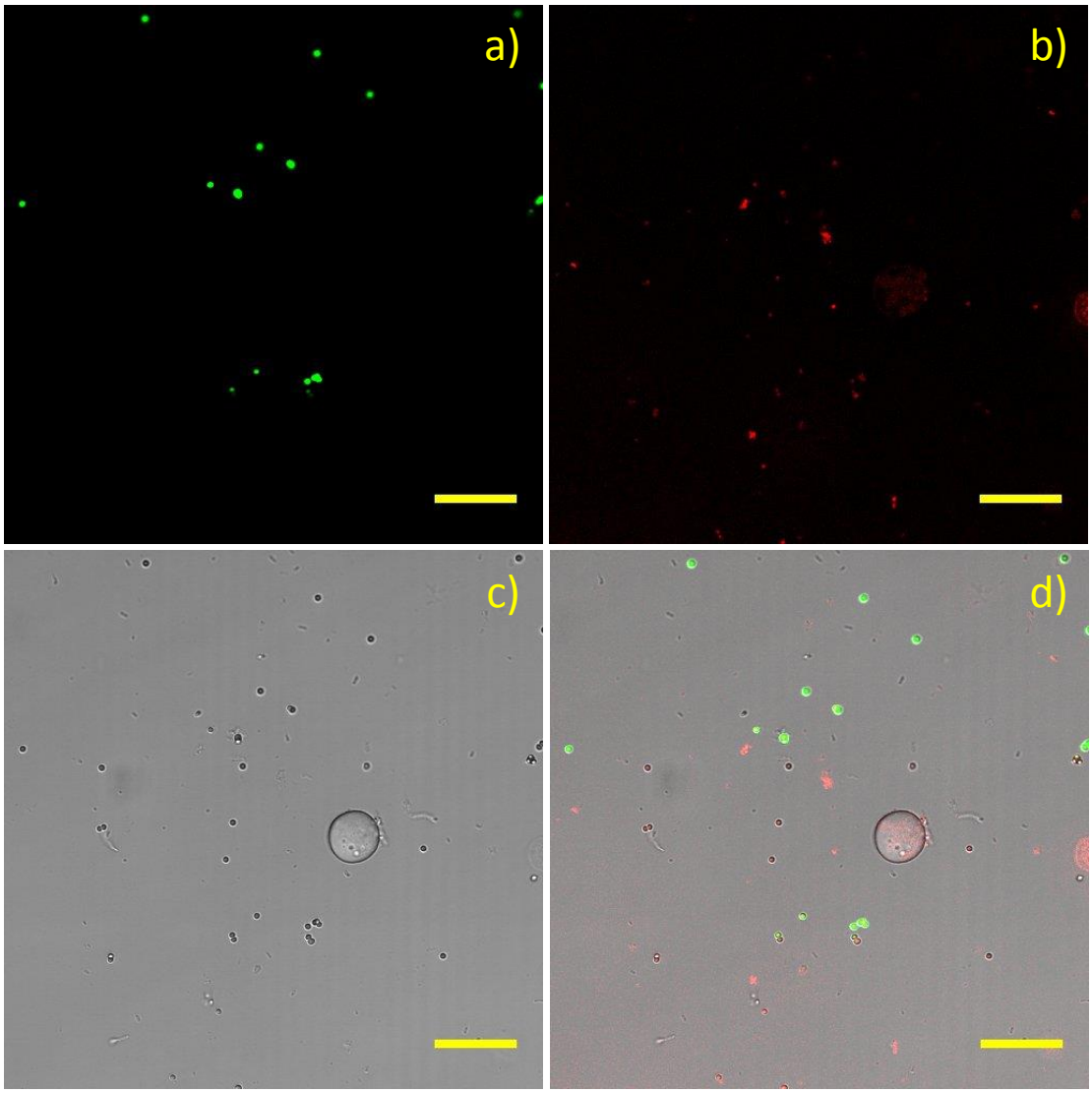

Figure 4-10. Confocal microscopy image of green dye (Fluorescein, λ_{ex} = 494 nm) labelled 1 µm PS - RCA_{120} beads a), red dye (Rhodamine B octadecyl ester perchlorate, λ_{ex} = 554 nm) stained micro - sized giant vesicles b), light microscopy image c) and overlaid green channel, red channel and light microscopy channel images d). Scale bar size is 20 µm.

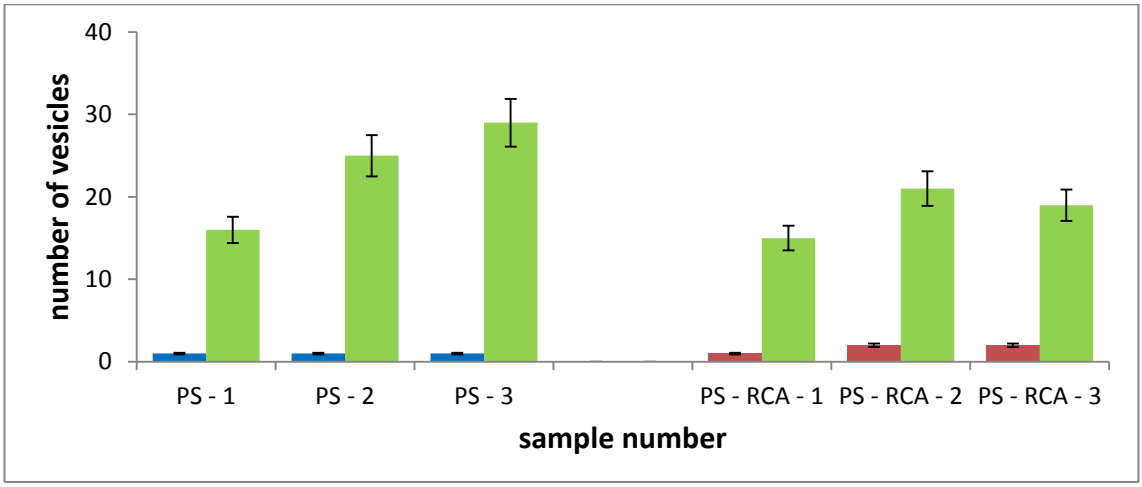

Figure 4-11. Number of GUVs interacting with carboxylate - modified 1 µm PS beads (blue bars) and 1 µm PS - RCA_{120} (red bars), and total number of giant polymersomes observed in each sample (green bars).

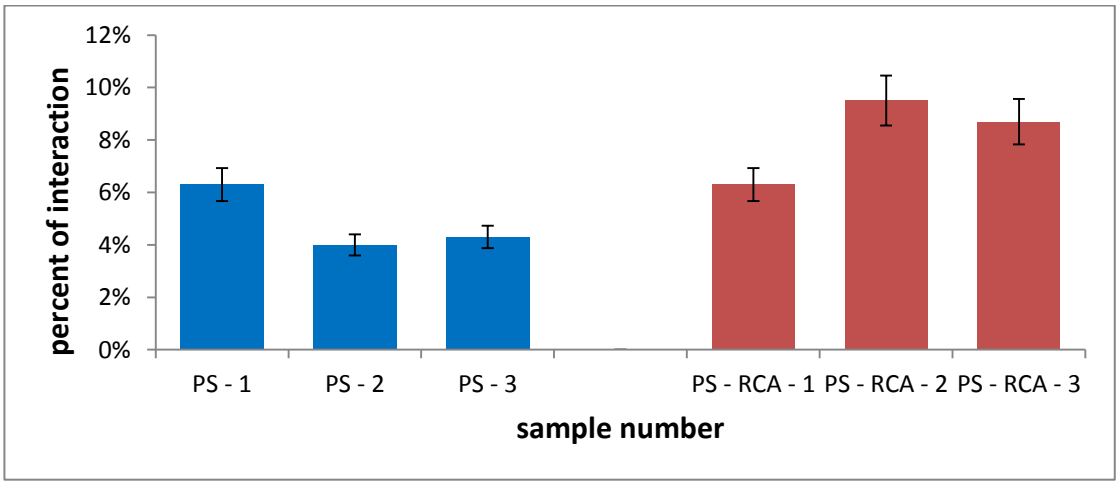

Figure 4-12. Percent interaction of the vesicles with carboxylate - modified 1 µm PS beads (blue bars) and 1 µm PS - RCA_{120} (red bars).

4.3.2.3. Vesicles and Con A - functionalised 1 µm PS beads

Initial control experiments on non - selective interactions between glycopolymersomes and PS beads confirmed that such events occur sporadically, and do not affect more than 10 % of the GUV population in a sample (as described in subchapter 4.3.2.1 and 4.3.2.2). Following the initial control experiments, research on selective interactions between glycosylated polymersomes and PS - Con A beads was initiated. Procedures were strictly controlled and performed under analogous conditions to the control experiments. Incubation experiments were repeated four times in order to increase the reliability of the collected data. The majority of lectin - functionalised beads remained dispersed in the sample randomly, as was observed in the control experiments (as presented in Figure 4-13). In comparison to initial control experiments the number of interactions increased significantly; the obtained results are presented in Figure 4-14. The selective interactions between GUVs and PS - Con A varied from 38 % to 57 % as presented in Figure 4-15.

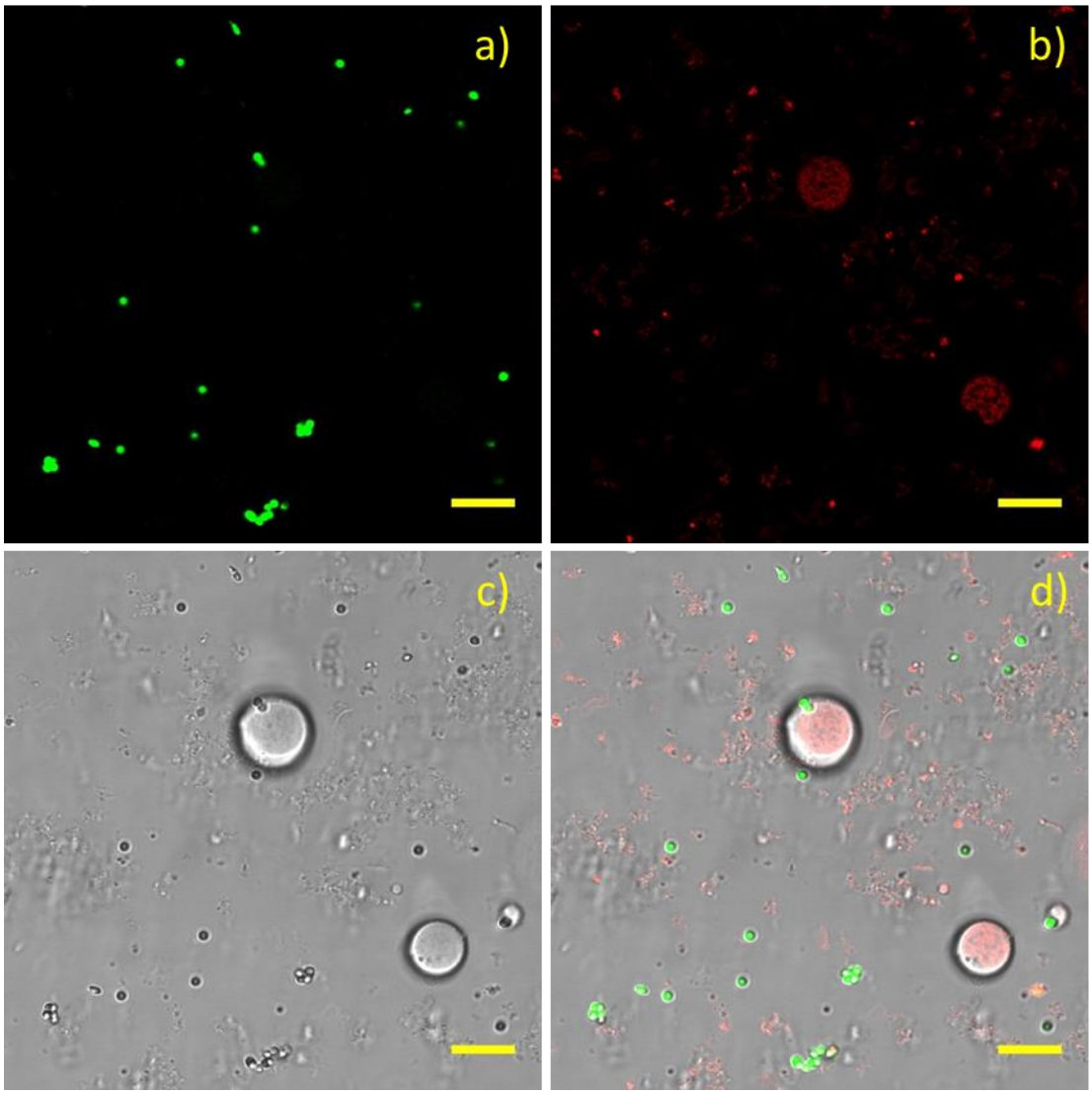

Figure 4-13. Confocal microscopy image of green dye (Fluorescein, λ_{ex} = 494 nm) labelled 1 µm PS - Con A beads a), red dye (Rhodamine B octadecyl ester perchlorate, λ_{ex} = 554 nm) stained micro - sized giant vesicles b), light microscopy image c) and overlaid green channel, red channel and light microscopy channel images d). Scale bar size is 10 µm.

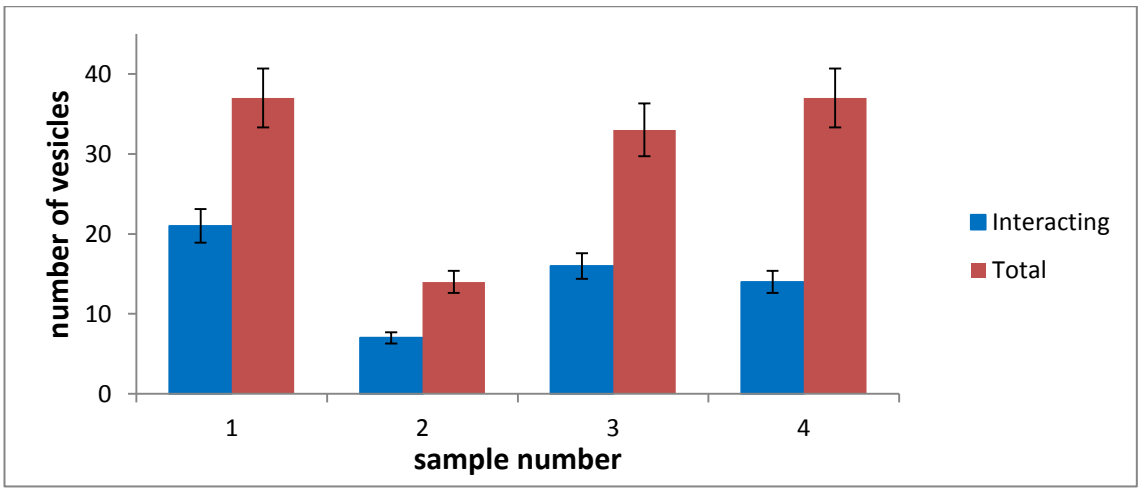

Figure 4-14. Number of GUVs interacting with 1 µm PS - Con A (blue bars) and total number of giant polymersomes observed in each sample (red bars).

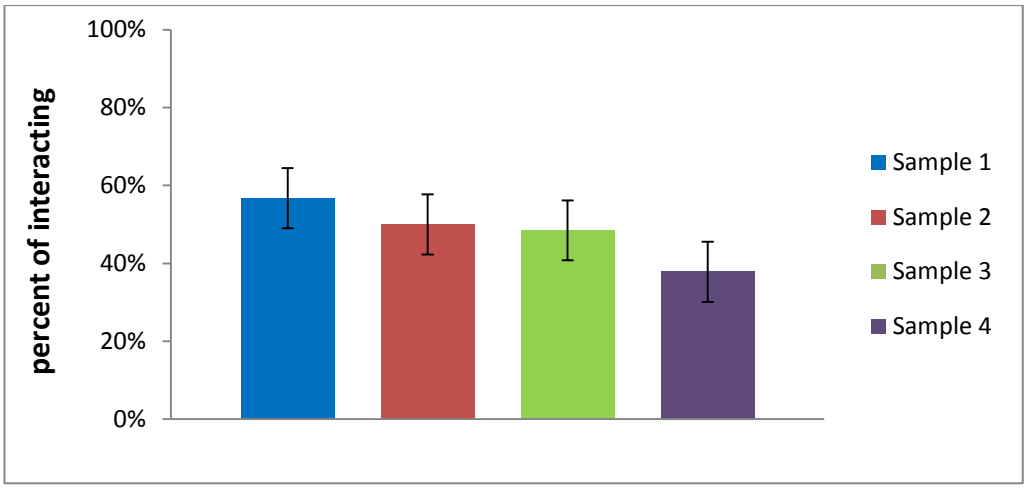

Figure 4-15. Percent interaction of vesicles M1 with 1 µm PS - Con A.

Based on the collected data, an average percent of the selective interaction between glycopolymer vesicles with PS - Con A beads was determined to be 42.0 ± 7.8 % as presented in Figure 4-16 (blue bar) which is approximately five times higher than the non – selective interactions with PS - RCA_{120} (Figure 4-16 red bar) or carboxylate - modified PS beads (Figure 4-16 green bar).

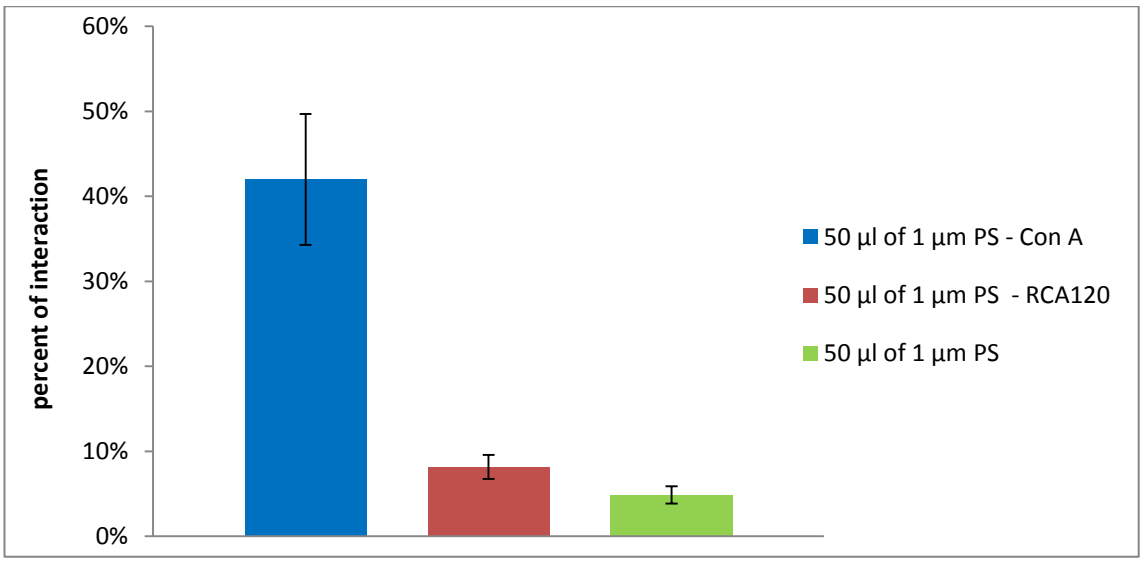

Figure 4-16. Data comparison - percent of interaction of different types of PS beads with GUVs prepared from glycopolymer M1.

To support the statistical data, glycosylated GUVs and PS - Con A beads were observed over a 20 second time period to assess the strength and stability of the connection between ligand and receptor (Figure 4-17 and Figure 4-18). The GUV presented in Figure 4-17 remains stable at the bottom of visualization chamber during observation; the attached cluster of PS - Con A beads fluctuates accordingly with solution vibrations. The vesicle presented in Figure 4-18 oscillates in the visualization chamber along with a selectively attached cluster of PS beads; the connection remains undamaged and is preserved at the observation period. The selective link between the observed species was reported to be stable and was sufficiently strong to remain intact during the sample fluctuations.

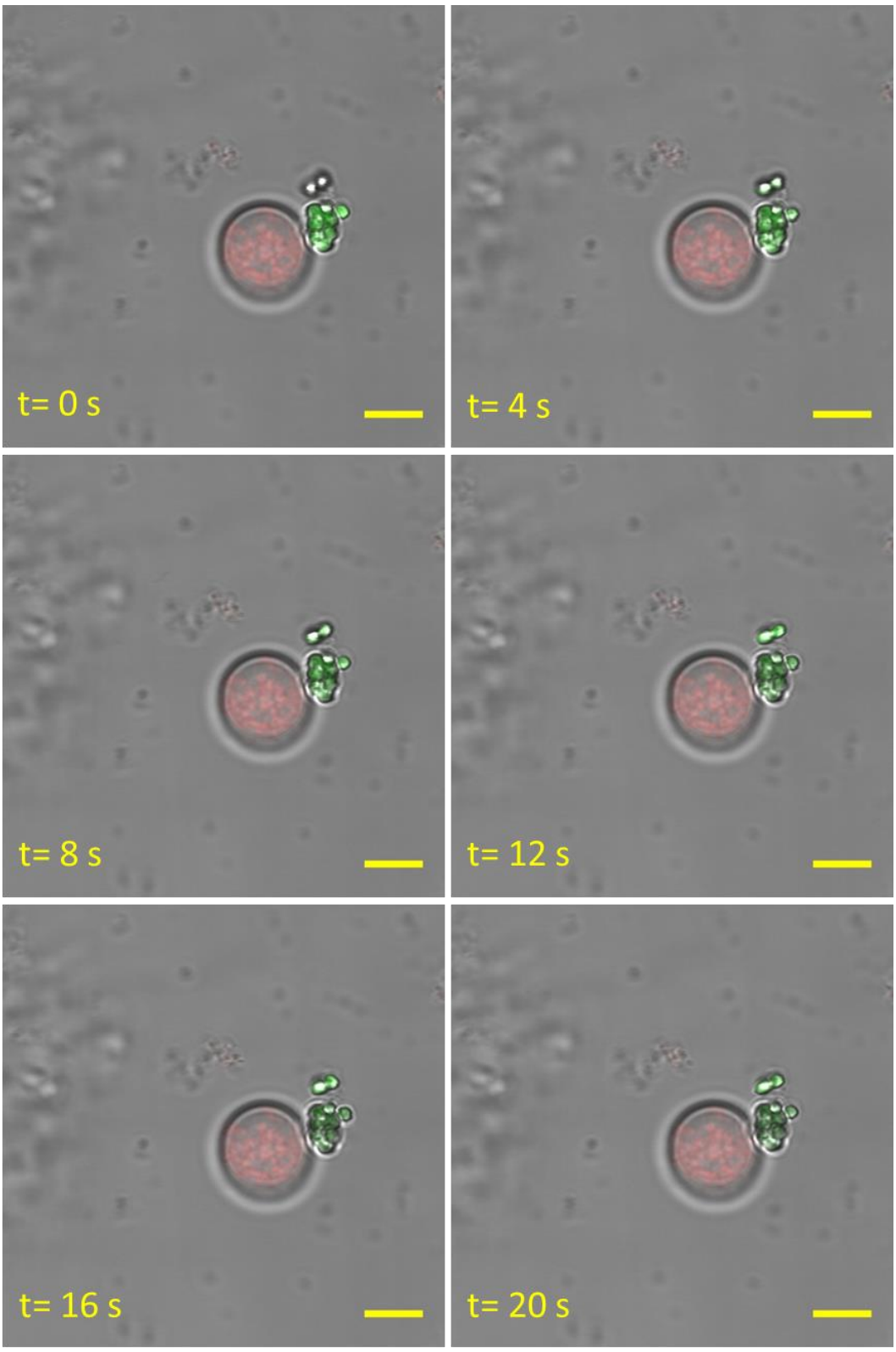

Figure 4-17. Movement of PS - Con A beads selectively attached to a stable giant glycosylated polymersome. Images present overlaid channels of confocal green channel (Fluorescein 494 nm, PS beads), red channel (Rhodamine B octadecyl ester perchlorate 554 nm, micro size giant vesicles) and light microscopy. Scale bar size is 5 µm.

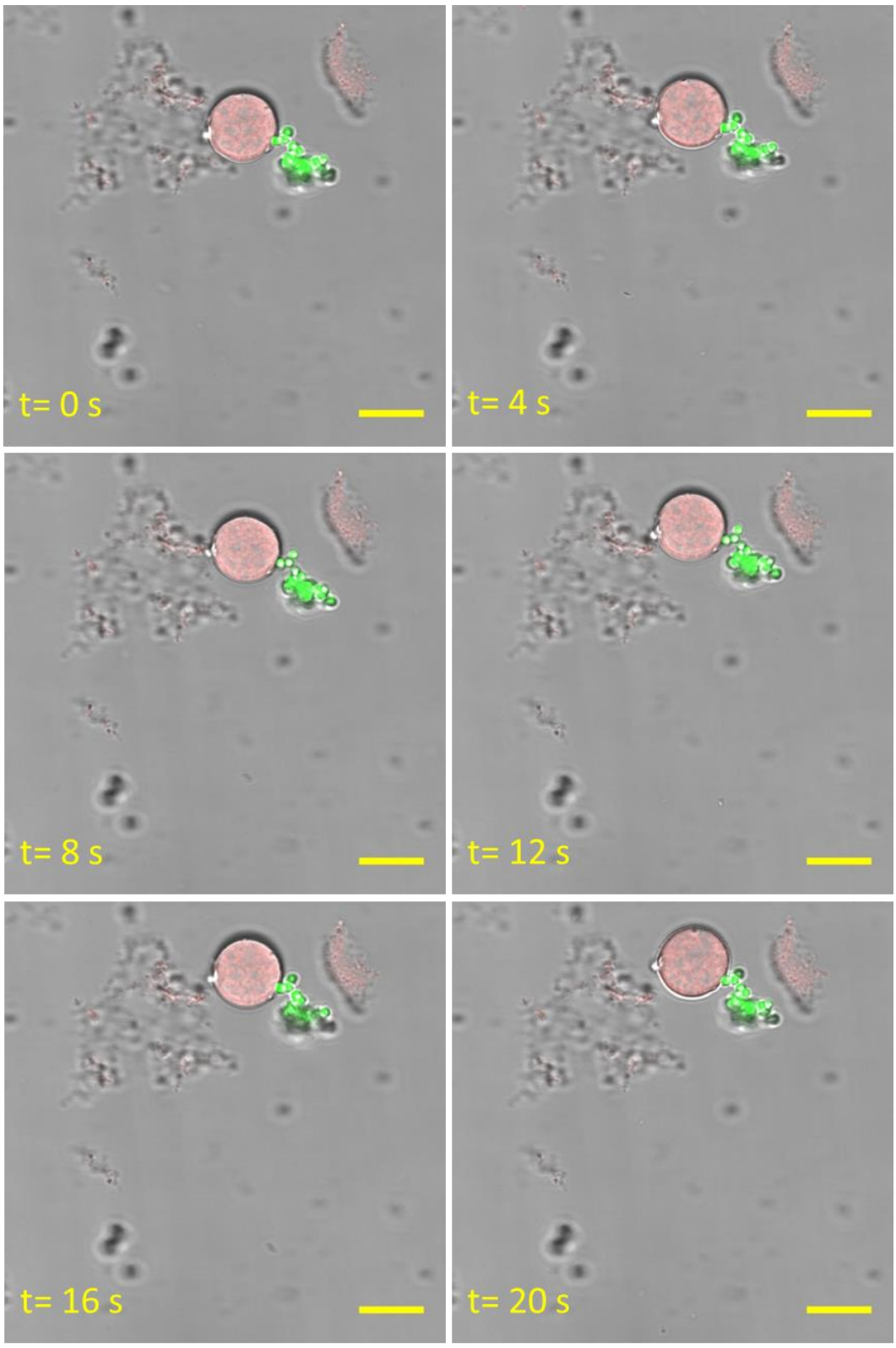

Figure 4-18. Movement of giant glycosylated polymersome with selectively attached PS - Con A beads. Images present overlaid channels of confocal green channel (Fluorescein 494 nm, PS beads), red channel (Rhodamine B octadecyl ester perchlorate 554 nm, micro size giant vesicles) and light microscopy. Scale bar size is 10 µm.

Despite the selective interactions between GUVs and PS - Con A beads, evidence of uptake of nanoparticles by the glycopolymersome was not observed (schematic representation in Figure 4-19 b)). A significant number of the PS - Con A beads attached to and/or incorporated into the vesicular membrane were detected during the statistical data processing; however, additional studies were required to determine if the beads remained attached to the vesicular membrane outside the vesicle (as schematically presented in Figure 4-19 c)) or entrapped inside the polymersome membrane (see Figure 4-19 d)). A series of z - scans of confocal fluorescent microscopy were performed to obtain detailed information on the arrangement of structures during the interaction. Images of typical z - scans are presented in Figure 4-20 and Figure 4-21.

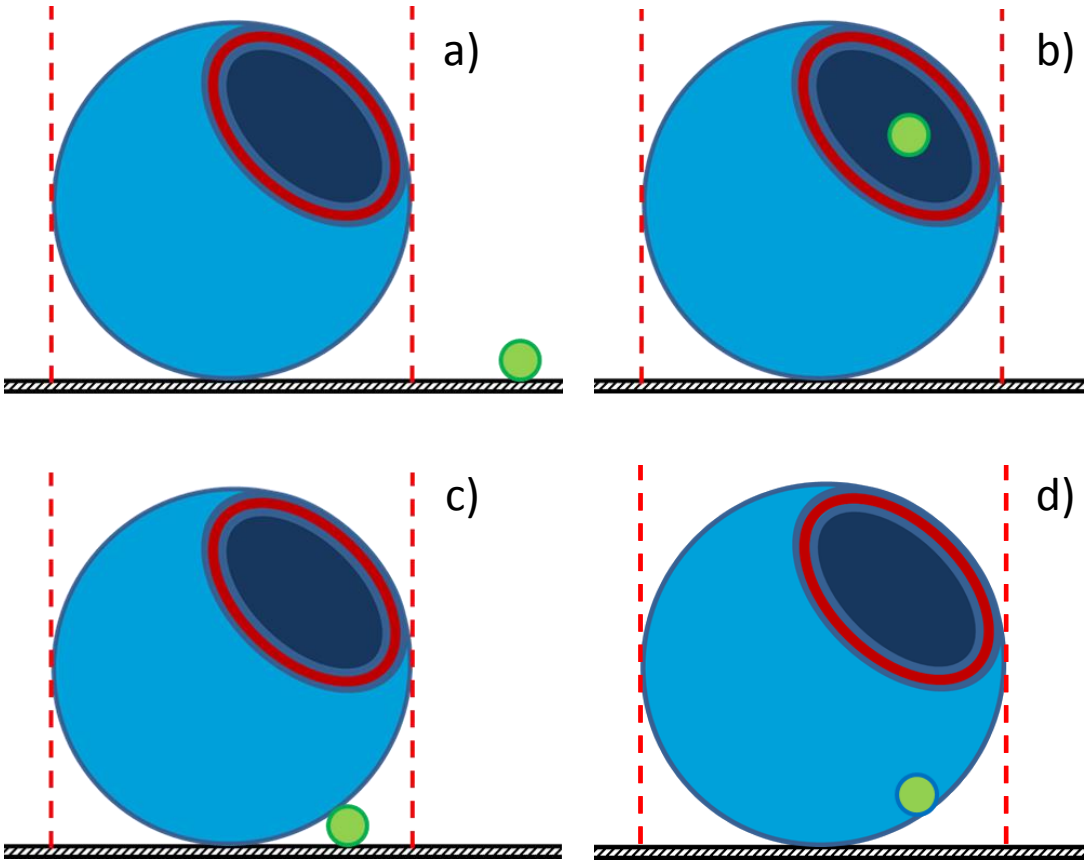

Figure 4-19. Schematic representation of possible arrangements of GUVs and PS - Con A beads: a) outside the GUV, b) inside the GUV, c) under the GUV between membrane and surface, d) inside the GUV remain attached to the internal membrane.

The z - scans were performed from the top to the bottom of a chosen GUV. Initial images suggested that microparticles might be entrapped inside the glycopolymersome (see Figure 4-20 a) - d) and Figure 4-21 a) - d)); however, further scans rejected initial hypothesis. It is clearly visible in the lowest z - slices that the image of polymersome (red channel) does not overlay the image of PS - Con A bead (green channel; see Figure 4-20 f) and Figure 4-21 f)) and therefore confirmed that PS - Con A beads attached to the GUVs remain outside the structure in the position schematically visualised in Figure 4-19 c).

Interaction experiments were also performed under alternative incubation conditions: variation of time, temperature and sample agitation. An increase in incubation time (from overnight to 24 h), temperature (from 19 °C to 37 °C) and inducing sample agitation were hoped to increase the percent of interaction between the glycosylated GUVs and Con A functionalised PS beads; however, none of the listed parameters had a significant effect. Therefore, it was decided to perform interaction studies with smaller, 0.5 μm, PS - Con A beads and determine the particle size influence on the percent of interaction with GUVs.

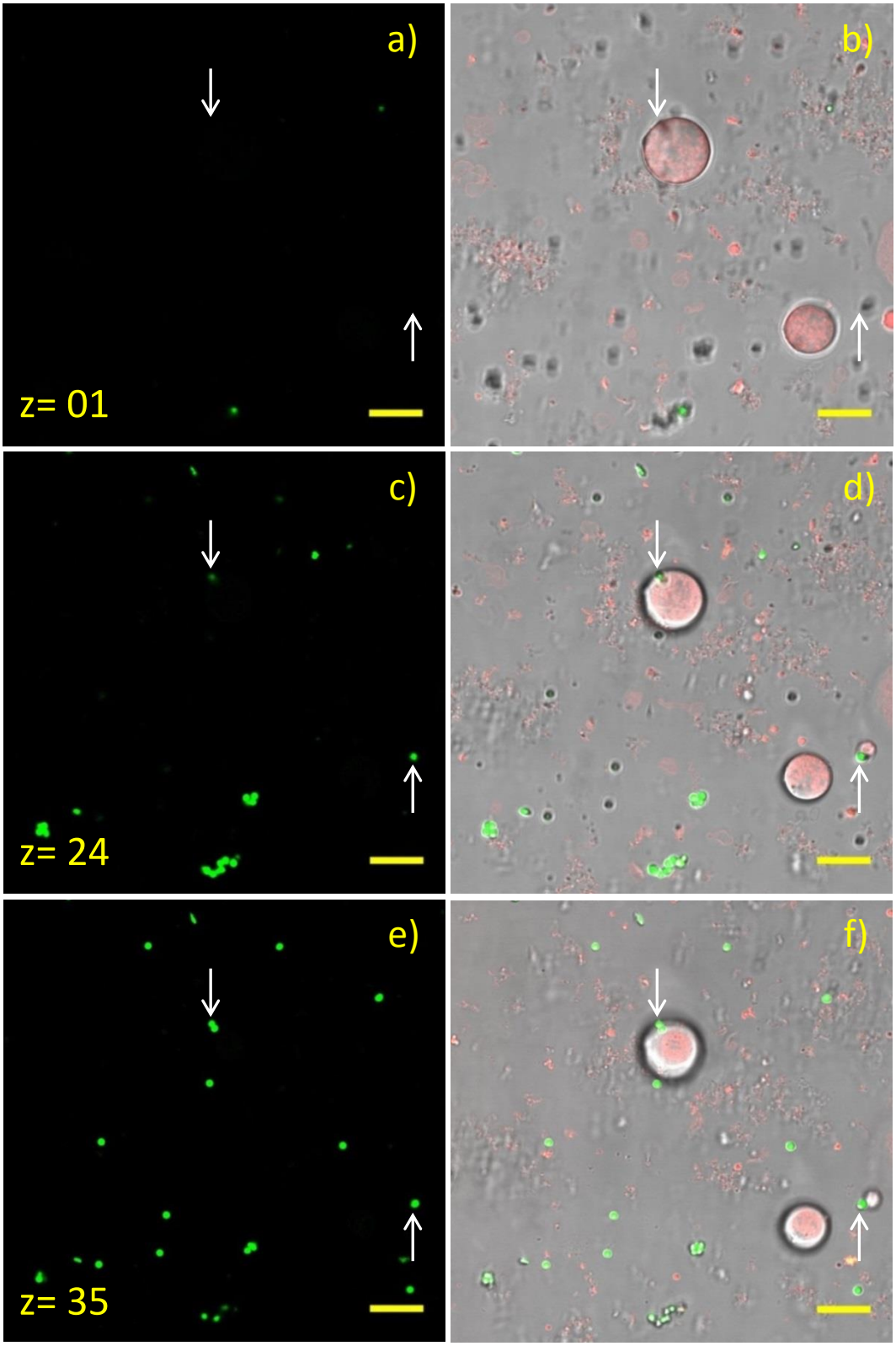

Figure 4-20. Chosen confocal microscopy images of z - stack: green dye (Fluorescein, λ_{ex} = 494 nm) labelled 1 µm PS - Con A beads at the left (a),c),e)) and overlaid red channel (Rhodamine B octadecyl ester perchlorate, λ_{ex} = 554 nm stained micro - sized giant vesicles), green channel and light microscopy channel images (b),d),f)). Scale bar size is 10 µm.

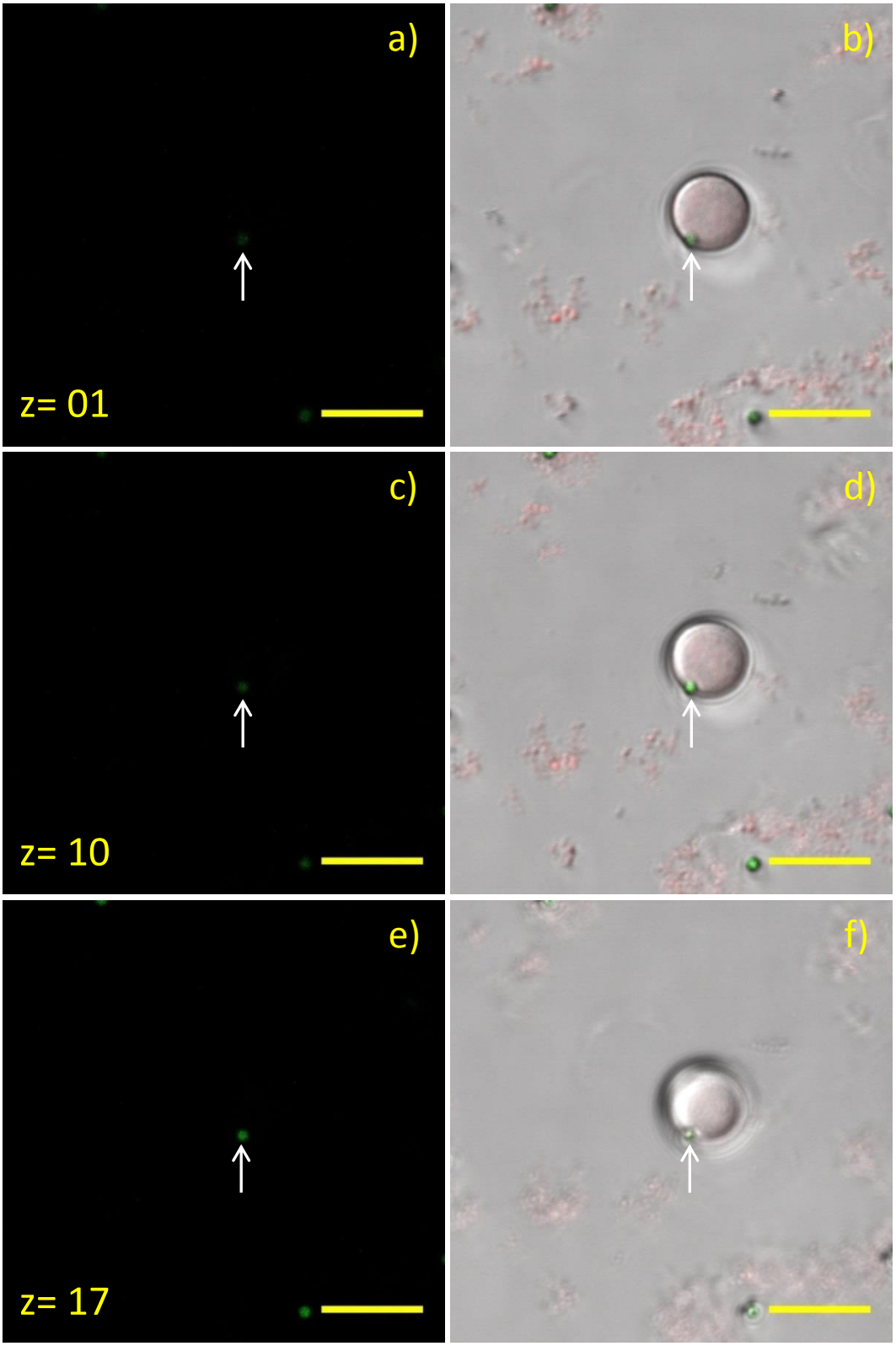

Figure 4-21. Chosen confocal microscopy images of z - stack: green dye (Fluorescein, λ_{ex} = 494 nm) labelled 1 µm PS - Con A beads (a),c),e)) and overlaid red channel (Rhodamine B octadecyl ester perchlorate, λ_{ex} = 554 nm stained micro - sized giant vesicles), green channel and light microscopy channel images (b),d),f)). Scale bar size is 10 µm.

4.3.2.4. Vesicles and Con A - functionalised 0.5 µm PS beads

Research on interactions between vesicles and Con A - functionalised 0.5 µm PS beads was performed in order to investigate the influence of particle size on the selective interactions between the species of interest.

Experiments were initiated using analogous conditions as with Con A - functionalised 1 µm PS beads. The majority of 0.5 µm PS - Con A beads remained dispersed in the sample randomly (as was observed in the previous experiments with 1 µm PS - Con A beads; described in 4.3.2.3.) or connected in clusters (as presented in Figure 4-22); however some of them interacted with giant polymersomes as presented in Figure 4-23. The analysis of the collected data concluded that smaller nanoparticles interact with significantly lower percent of interaction than larger ones. Upon overnight incubation of polymersomes with 50 µl of PS - Con A 0.5 µm beads, between 7 % and 13 % of glycopolymersomes selectively interacted with the external species (Figure 4-24 blue bars); the obtained value of 8.2 ± 1.4 % is approximately four times lower than for analogous experiments performed with 1 µm beads (42.0 ± 7.7 %). A further increase in the volume of 0.5 µm PS - Con A beads to 100 µl (double volume than used initially) resulted in a linear increase in the percent of interaction which ranged from 16 to 23 % (approximately twice higher than the value recorded for 50 µl) as presented in Figure 4-24 (red bars).

Despite the observed increase in the percent of interaction for 0.5 µm beads at 100 µl volume, the obtained value of 19.1 ± 4.1 % was approximately 50 % lower in comparison to the value obtained for 1 µm PS - Con A beads (42.0 ± 7.8 %). The significantly lower percent of interaction of 0.5 µm PS - Con A beads than 1 µm

PS - Con A beads with giant polymersomes could be possibly explained by differences in reactivity of functionalised particles with small, medium and large vesicles; smaller vesicles are more accessible to smaller PS - Con A beads to bind with lectins present on their surface. Furthermore, glucose units present on the smaller vesicle's surface trigger the cluster glycoside effect for a significant number of 0.5 μm PS - Con A beads, the sugar ligands attach selectively to lectins and make the beads unable to interact with giant polymersomes. The interaction results presented in subchapter 4.3.2 are based on GUVs with diameter > 10 μm; therefore 0.5 μm PS - Con A beads interacting with polymersomes smaller that the set threshold (< 10 μm) are not included in the statistics. Hence, the total number of interacting vesicles appears lower. Summing up, it is likely that many of the 0.5 μm PS - Con A beads mixed with the GUVs were inactivated by the smaller glycosylated structures.

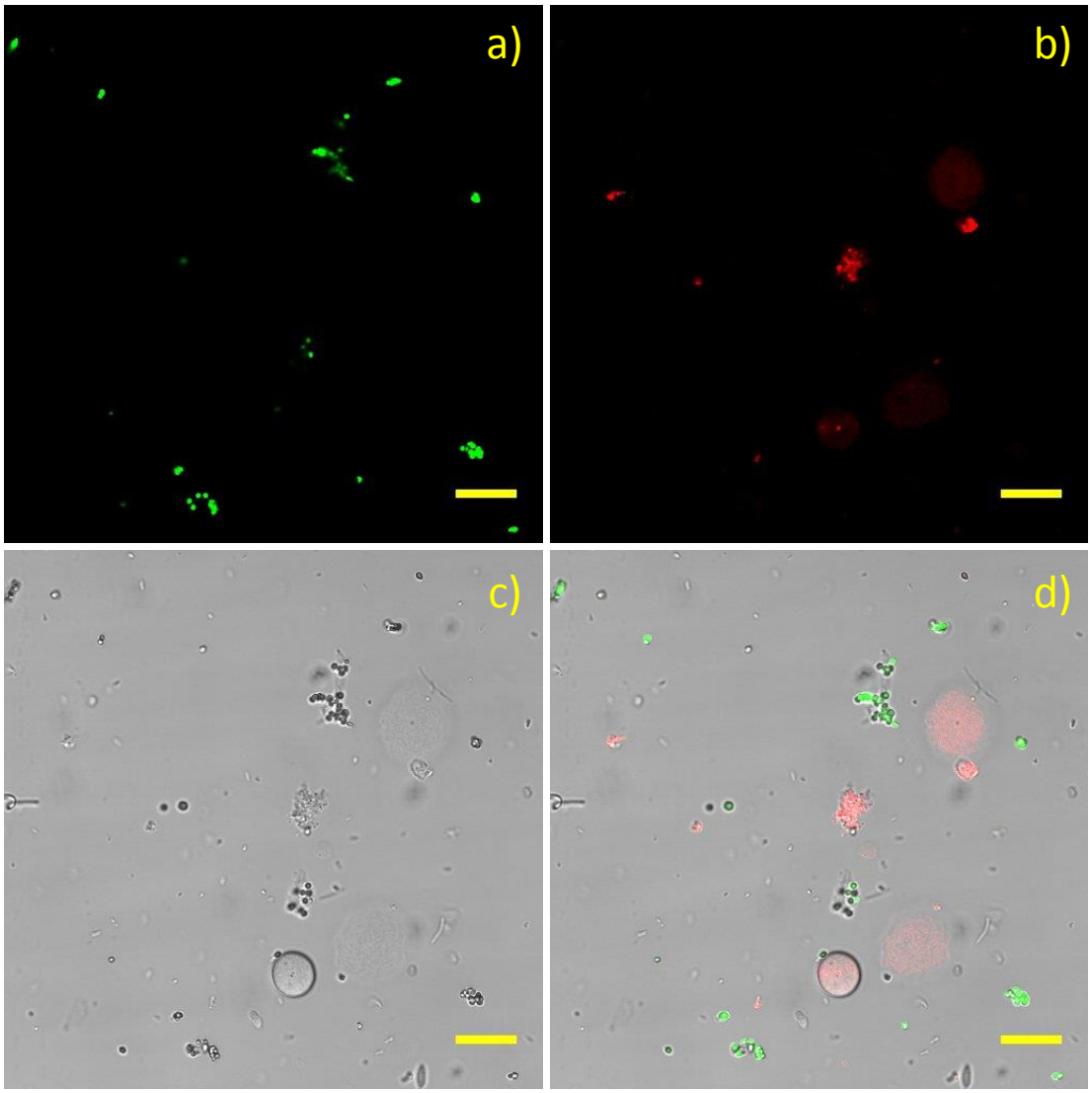

Figure 4-22. Confocal microscopy image of green dye (Fluorescein, λex = 494 nm) labelled 0.5 µm PS - Con A beads a), red dye (Rhodamine B octadecyl ester perchlorate, λex = 554 nm) stained micro - sized giant vesicles b), light microscopy image c) and overlaid green channel, red channel and light microscopy channel images d). Scale bar size is 15 µm.

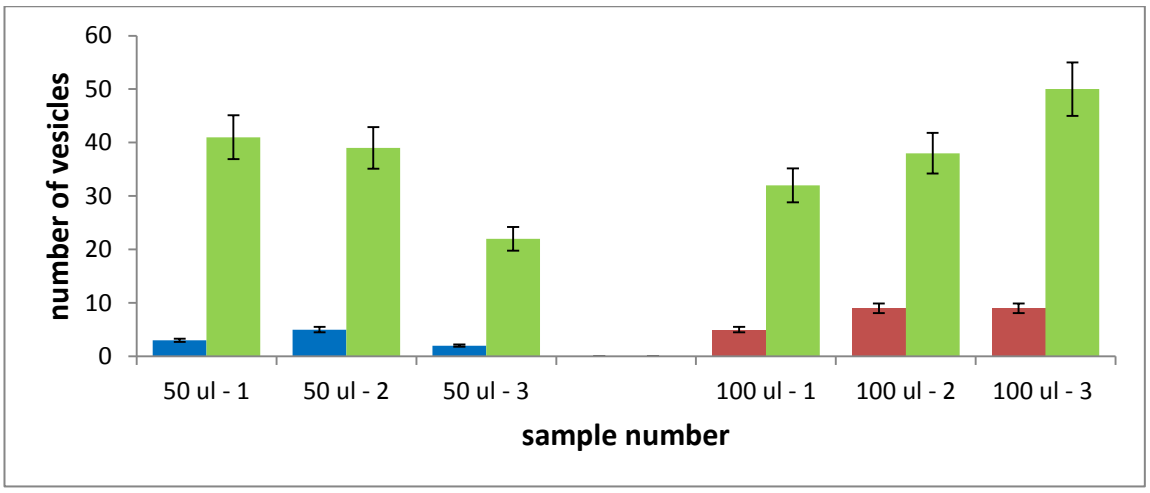

Figure 4-23. Number of GUVs interacting with 0.5 µm PS - Con A upon addition of 50 µl (blue bars) and 100 µl (red bars) of particles, and total number of giant polymersomes observed in each sample (green bars).

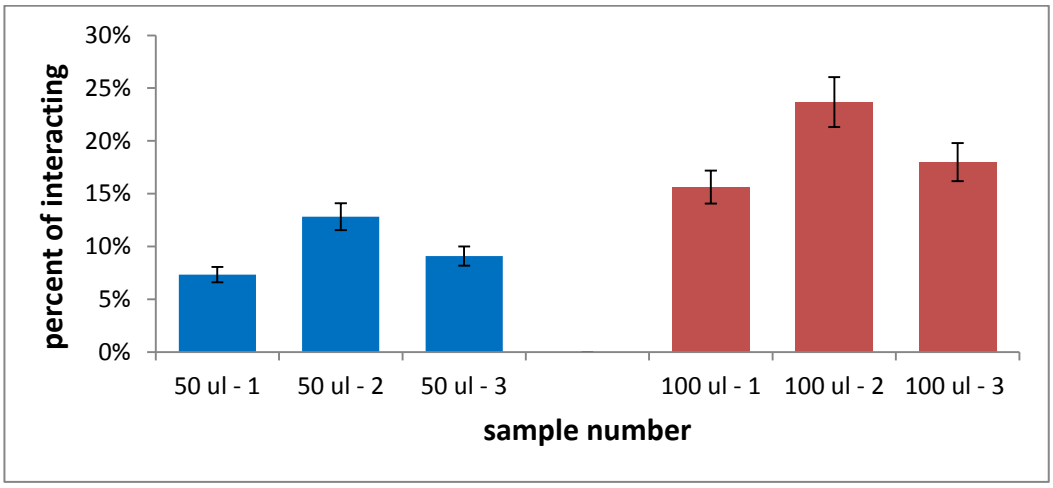

Figure 4-24. Percent interaction of the vesicles M1 with 0.5 µm PS - Con A upon addition of 50 µl (blue bars) and 100 µl (red bars) of particles.

4.3.3. Conclusions

Studies on the properties of giant glycopolymersomes from polymer M1 were performed. The analysis of data collected during osmotic shock studies (presented in 4.2.1.) concluded that GUVs respond to changeable osmotic pressure; hypertonic conditions trigger shrinking of vesicles while hypotonic conditions induce swelling of microstructures. The GUVs are approximately 2.5 times more susceptible to negative osmotic pressure than positive. The percent change of the polymersome average diameter decreases linearly to - 20 ± 2.0 % with an increase of osmotic shock pressure to - 24.4 atm; however a further decrease in osmotic pressure does not facilitate major changes in the average diameter of vesicles. Polymersomes are able to withstand a negative osmotic shock higher than -24.4 atm and adapt to the altered osmolality; however upon applying an osmotic shock lower than - 24.4 atm the majority of the GUV population collapses and the remainder adjusts their average diameter to reduce the osmotic gradient.

The pH shock assay (presented in 4.2.2.) revealed that giant polymersomes M1 are more susceptible to an acidic environment than basic; upon increasing pH by 4 (from pH 7 to pH 11) the average diameter of polymersomes decreased by 4.1 ± 0.4 %, while a pH reduction by 4 units (from pH 7 to pH 3) initiated an increase in the average diameter of polymersomes by 2.3 ± 0.2 % (as presented in Figure 4-3). GUVs are sensitive to pH changes larger than 4 units (from pH 7 to lower than pH 3 and from pH 7 to higher than pH 11), which possibly initiate structural rearrangements in the whole population.

Research on interactions between giant glycopolymersomes and particles was fulfilled. It has been demonstrated that glycosylated polymersomes are able to interact selectively with lectin Con A solubilized in HEPES buffer.

Based on the results presented in 4.3.2., it can be concluded that the glycosylated GUVs are able to interact selectively with lectin Con A - functionalised PS beads. The highest average percent of the selective interactions between polymersomes and PS - Con A beads was achieved utilising 50 µL of 1 µm size microparticles and was determined to be 42.0 ± 7.8 % (as presented in Figure 4-25, blue bar). It has been demonstrated, that by reducing the bead size to 0.5 µm (and using the same volume of beads, 50 µl), the percent of interaction decreases to 9.8 ± 2.8 % (Figure 4-25, red bar), moreover, utilising double the amount of beads employed in the study (100 µl) increases the percent of interaction to 19.1 ± 4.1 % (Figure 4-25, green bar) which is significantly lower than that reported for 1 µm PS - Con A beads. Control experiments revealed that non - functionalised PS beads are able to non - selectively interact with GUVs M1; however such interactions occurs sporadically and the percent of interaction is as low as 4.9 ± 1.0 % (Figure 4-25, orange bar). 1 µm PS beads functionalised with lectin RCA_{120}, which does not bind to glucosyl residues, increases non - selective percent of interaction to 8.2 ± 1.4 % (Figure 4-25, purple bar). Summing up the interaction statistical results, it is evident that glycosylated GUVs from polymer M1 interact selectively with PS - Con A beads.

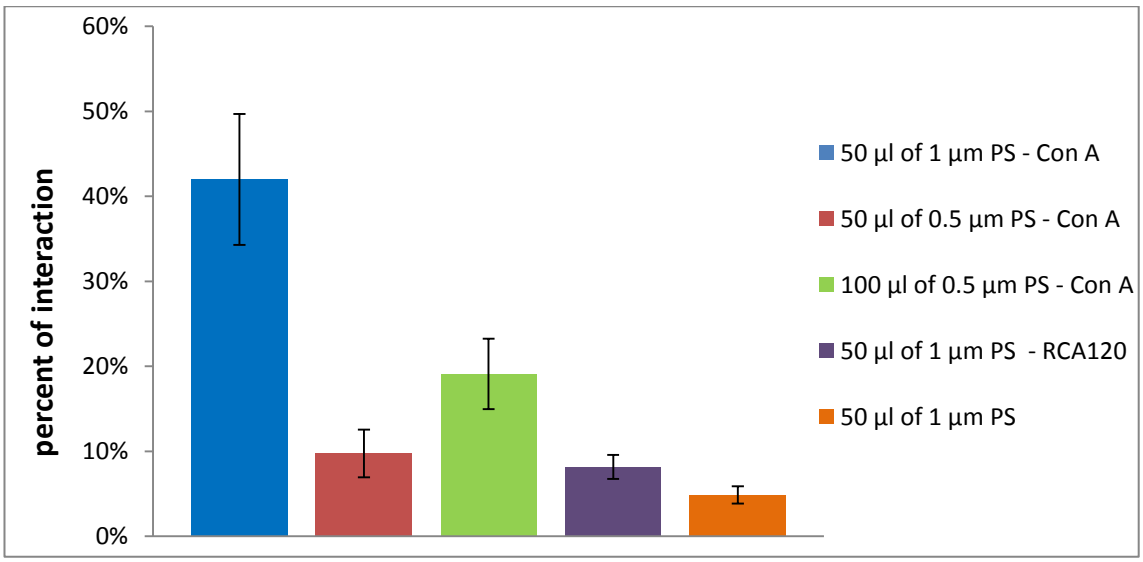

Figure 4-25. Data comparison - percent of interaction of different types of PS beads with GUVs prepared from glycopolymer M1.

The statistical calculations were supported by microscopy observations which concluded that interaction between GUVs and PS - Con A are stable and durable enough to withstand fluctuations of the surrounding media, and maintain an intact connection.

According to the computational simulations performed by Balazs et al. further encapsulation of PS - Con A beads could appear only if adhesion between protein and ligand would be sufficiently strong to induce the membrane deformation (as presented in Figure 4-2 (c)).[113] Due to the membrane incurvation the amount of glucose units available to interact with protein would gradually increase (as presented in Figure 4 - 2 (d)) and full particle internalisation could appear (as presented in Figure 4-2 (e)).

Despite the selective interactions between GUVs and PS - Con A beads present in system described in subchapter 4.3, an evidence of uptake of nanoparticles into the glycopolymersomes was not observed. The confocal fluorescent microscopy z- scans confirmed that PS - Con A beads are attached to the GUVs and remain outside the

structure in a surrounding media without any sign of encapsulation (as presented in Figure 4-2 (b)).

The influence of different experimental conditions on the binding of PS - Con A and glycopolymersomes was explored. Collected data concluded that an increase in incubation time (from overnight to 24 h), temperature (from 19 °C to 37 °C) and/or inducing gentle sample agitation did not result in any favourable effect on the microstructure binding.

The findings presented in this chapter are promising and convincing that RME could be performed in a purely synthetic system; however, we have not observed such an event in the present study. In compliance with the findings reported by Balazs et al. we hypothesise that the glucose - lectin adhesion energy is not sufficient to induce deformation of rigid vesicular membrane self - assembled from glycopolymer M1, leading to invagination of PS - Con A bead. To overcome this potential problem a mechanism allowing adjustment of membrane physical properties should be incorporated into synthetic cell.

4.4. Modifications of the physical RME model

4.4.1. GUV probing by micromanipulation

Studies performed on the creation of a synthetic RME model described in subchapter 4.3 revealed that GUVs electroformed from glycopolymer M1 are able to selectively interact with external species; however they are unable to internalise them. We hypothesise that the membrane is too rigid to allow internalisation. Investigating polymersome membrane elasticity using a micromanipulation method (micropipette) may help to understand the observed lack of evidence for internalisation.

Figure 4-26 presents images from the micromanipulation performed on a single GUV, while Figure 4-27 demonstrates manipulation studies performed on a GUV attached to polymeric membrane. The main goal of the micromanipulation study was to investigate the rigidity of the GUV membrane created from glycopolymer M1 and to assess whether it would permit invagination of solid beads present in the polymersome surrounding solution.

Both GUVs utilised in our study retained their shape and size during all micromanipulation procedures. Initially, the vesicular membrane was pierced several times with the micro - size needle (Figure 4-26 a) - c) and Figure 4-27 a) - c)); the vesicle remained visually unaffected by the performed procedures. Upon rapid movement of the needle, the polymeric membrane was pierced; however, if the motion was slower the needle could not penetrate the vesicular barrier and the GUV was propelled away from the needle tip (as presented in Figure 4-26 d) - f)). The polymersome was probed this way several times with gradually increased speed of

needle movements until the vesicle was pierced; however, no membrane deformations (i.e. bending, swelling or vibrating) were observed, which suggests that the polymeric lamina covering the polymersome is relatively rigid and tough.

Another micromanipulation test was performed on a giant polymersome still attached to a fragment of freely floating polymeric membrane. It was hoped to either separate the GUV from the polymeric lamina or to destabilise the vesicle by placing the micromanipulation needle inside the structure and changing its position rapidly. It was found that the GUV remained stable and undamaged over the performed experimental procedures. Moreover, the polymersome remained attached to the polymeric membrane and drifted according to movements of the micromanipulation needle (as presented in Figure 4-27 d) - f)). The giant vesicles are rigid, tough and stable which most likely makes them unsuitable to serve as an efficient and reliable synthetic model of RME with the current (unchanged) polymer composition.

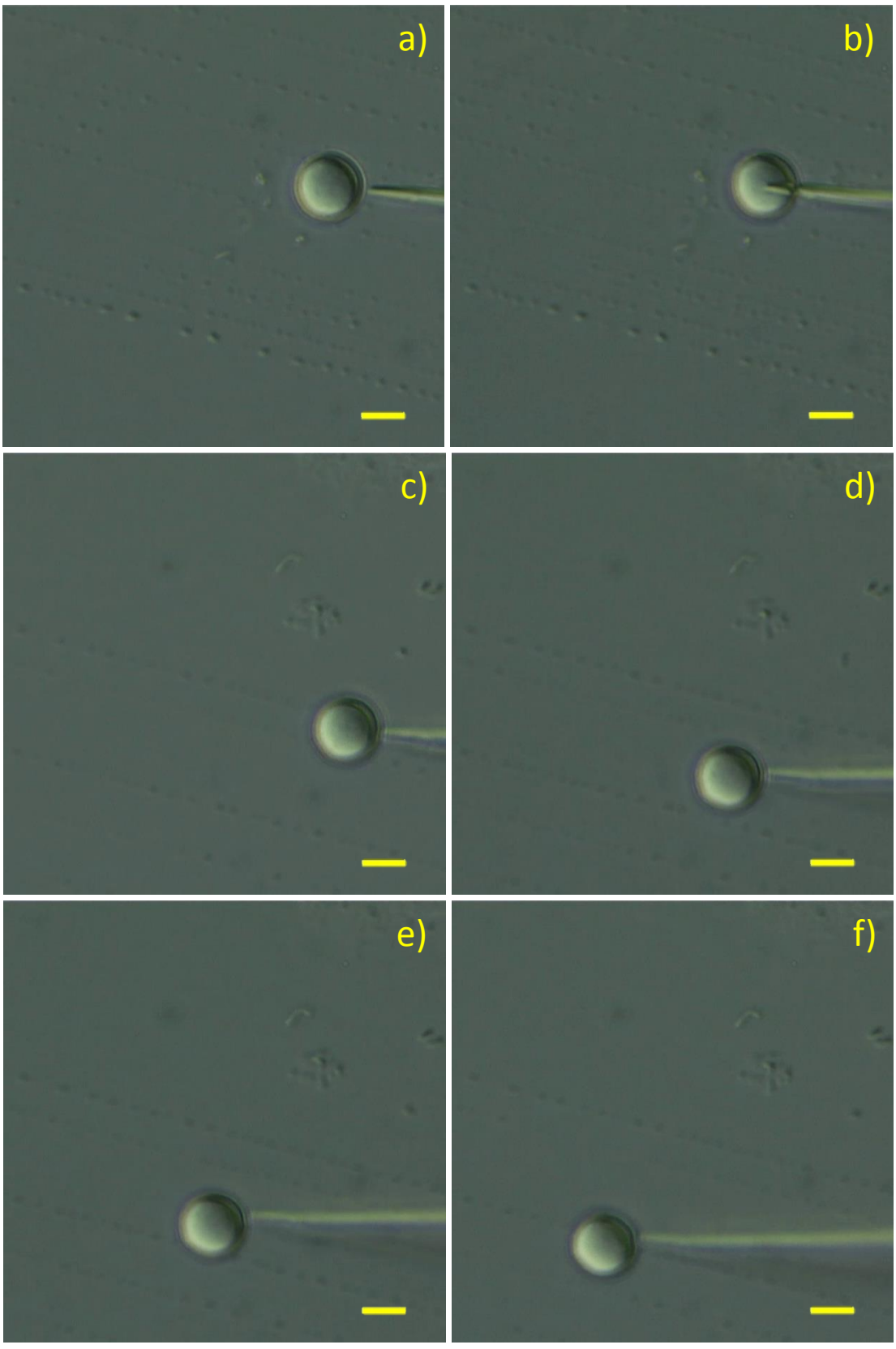

Figure 4-26. Micromanipulation experiment performed on a single GUV. a) - c): presents movement of the needle which pierces the GUV; d) - f): show movement of the needle which propels the GUV away from the needle tip. All images were recorded with the same focus position. Scale bar size is 10 µm.

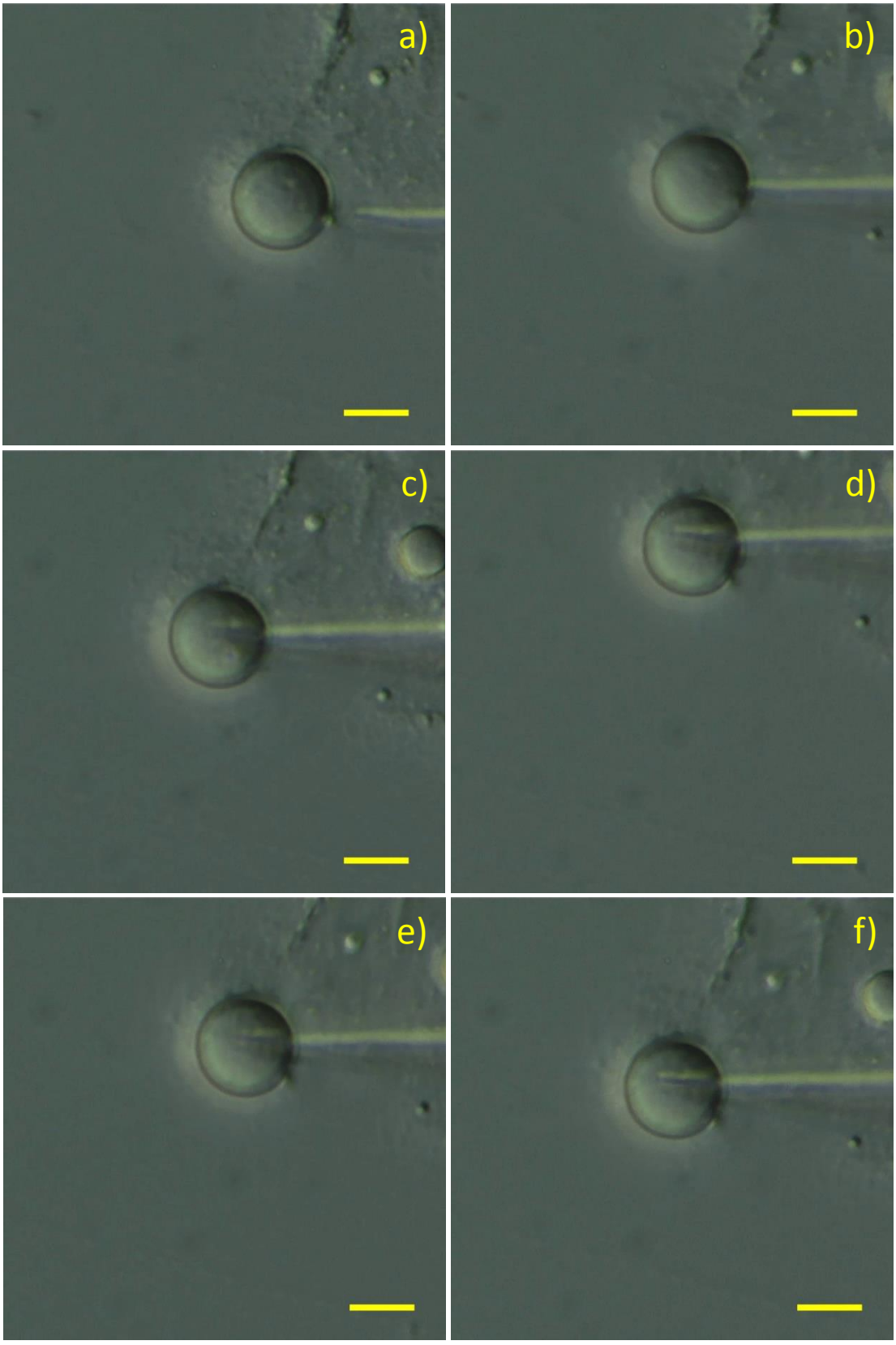

Figure 4-27. Micromanipulation experiment performed on GUV attached to a polymeric membrane. a) - c): presents movement of the needle which pierces the GUV; d) - f): show movement of the needle which propels the GUV away from needle tip. All images were recorded with the same focus position. Scale bar size is 15 µm.

4.4.2. Polymer - lipid mixed GUVs

Initial micromanipulation experiments on GUVs electroformed from glycosylated polymer M1 confirmed that the polymersome membrane is too tough and rigid to be utilised as a synthetic RME model. The high mechanical stability and low permeability of the polymersome membrane (as demonstrated in subchapter 4.2 and 4.4.1) are possibly limiting factors to create a synthetic RME model from GUV, electroformed from glycopolymer M1, even thorough they are able to selectively encapsulate external species (as described in 4.3). To overcome this potential problem it was decided to design a mixed polymersome system which would allow the control of the toughness and permeability of the self - assembled structures.[125]

Table 4-3. Ratios of amphiphilic materials utilised in the mixed vesicles study.

#	Mass of polymer M1 used (mg)	Mass of lipid DOPC used (mg)	Mass ratio	Amount of polymer M1 used (mmol)	Amount of lipid DOPC used (mmol)	Molar ratio
1	0.40	1.60	1 : 4	4.09E-05	2.04E-03	1 : 50
2	1.00	1.00	1 : 1	1.02E-04	1.27E-03	1 : 12
3	1.60	0.40	4 : 1	1.64E-04	5.09E-04	1 : 3

Experiments were initiated with amphiphilic materials mixed in a mass ratio of 1 : 4 (M1 to DOPC; described as #1 in Table 4-3). However, the initial ratio of materials used was found to be unsuitable for the formation of mixed structures. The samples obtained were analogous to pure liposome samples observed during initial electroformation studies on the model lipid DOPC as described in subchapter 2.2. Upon detailed analysis of the prepared electroformation samples using light and

fluorescence microscopy it was concluded that the structures were liposomes without any detectable traces of polymer M1. It was decided to continue studies with an increased amount of polymer in comparison to the lipid mass used for film preparation.

Following initial experiments, another attempt of mixed vesicle formation was performed with amphiphilic materials mixed in a mass ratio of 1 : 1 (M1 to DOPC; described as #2 in Table 4-3). These conditions however were also deemed to be unsuccessful, due to the sample failing to form any hybrid structures. The prepared electroformation samples were analogous to those obtained using mass ratio #1 (see Table 4-3). The self - assembled structures discovered in the prepared samples were classified as DOPC liposomes without any indication of the presence of glycopolymer M1. The structures formed had the same size range and were formed with a similar density as in initial experiments with mass ratio of 1 : 4 (#1 in Table 4-3); however, a large amount of unsymmetrical aggregates and detached film pieces were detected during examination of the samples using light and fluorescence microscopy which suggests that the amount of polymer used for the film preparation was still insufficient to form hybrid GUVs.

Further experiments were performed with a significantly increased amount of glycopolymer M1; amphiphilic materials were mixed in a mass ratio of 4 : 1 (M1 to DOPC; described as #3 in Table 4-3). Electroformation experiments with this ratio of vesicle - forming materials resulted in the formation of stable mixed GUVs as presented in Figure 4-28 and Figure 4-29, and confirmed the assumption that the amount of polymer used in previous experiments (with mass ratio #1 and #2) was insufficient to form hybrid GUVs.

The hybrid giant vesicles were produced at a significantly lower yield than liposomes during initial experiments (with mass ratio #1 and #2) or glycopolymersomes from M1 obtained during studies presented in subchapter 3.3. Moreover a large amount of asymmetrical aggregates and detached film pieces were present in the samples.

The lipid DOPC has a strong tendency to accumulate on the outer surface of the created structures as presented in Figure 4-28 and Figure 4-29. Furthermore, vesicles present in the samples look like polymersomes covered or entrapped by larger liposomes; however, there are no visible gaps between the lipid and polymeric membranes, lipid/polymer domains within the vesicle or phase separation induced - fission of the structures.

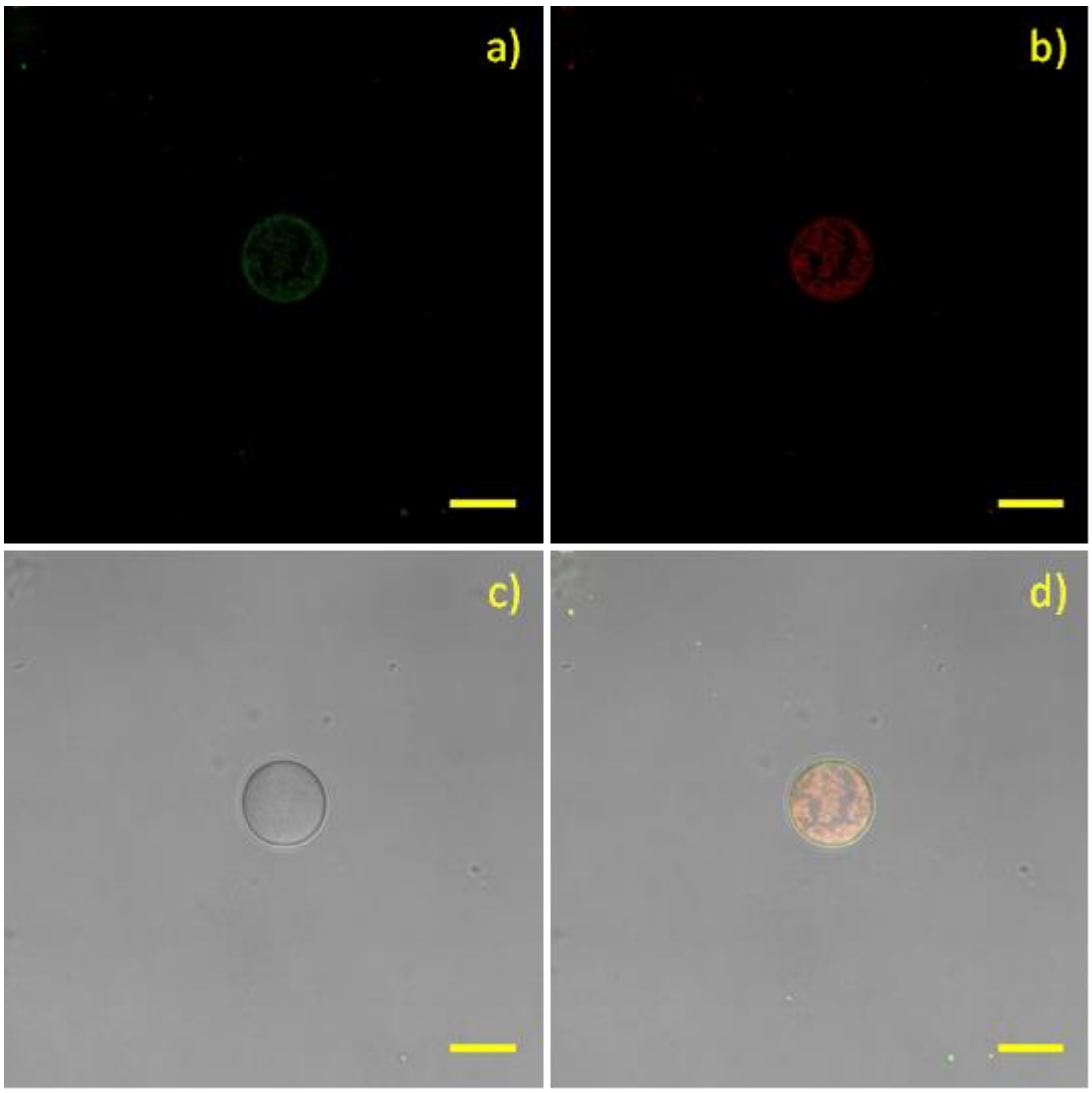

Figure 4-28. Confocal microscopy image of green dye (Fluorescein, λ_{ex} = 494 nm) labelled DOPC lipid layer a), red dye (Rhodamine B octadecyl ester perchlorate, λ_{ex} = 554 nm) stained polymeric shell b), light microscopy image c) and overlaid green channel, red channel and light microscopy channel images d). Scale bar size is 10 µm.

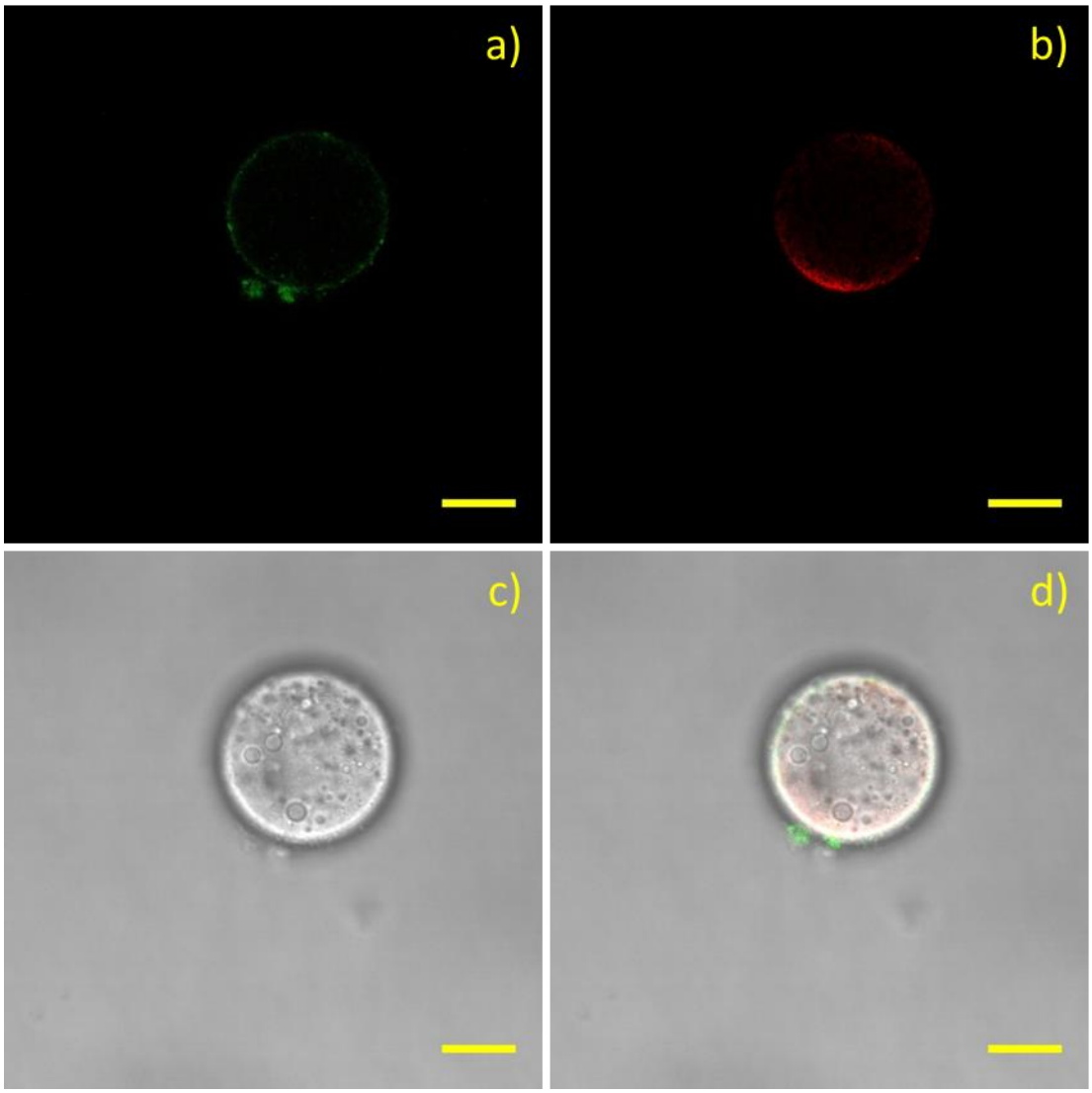

Figure 4-29. Confocal microscopy image of green dye (Fluorescein, λ_{ex} = 494 nm) labelled DOPC lipid layer a), red dye (Rhodamine B octadecyl ester perchlorate, λ_{ex} = 554 nm) stained polymeric shell b), light microscopy image c) and overlaid green channel, red channel and light microscopy channel images d). Scale bar size is 10 µm.

4.4.3. Conclusions

The brief micromanipulation studies (as presented in 4.4.1.) confirmed that GUVs electroformed from glycopolymer M1 have a high stability, which probably arises from the polymeric membrane properties i.e. low elasticity and permeability, and high rigidity. This makes them unsuitable to serve as an efficient and reliable synthetic model of RME with the current (unchanged) polymer composition.

Studies on mixed vesicles (as presented in 4.4.2.) were initiated in order to introduce modifications to the previously developed self - assembly system based on glycopolymer M1, providing a regulation mechanism to tune the membrane properties i.e. toughness and permeability of the created structures. Initial experiments revealed that hybrid structures can be obtained from a mixture of glycopolymer M1 and lipid DOPC in the mass ratio of 4 : 1 (described as #3 in Table 4-3). The electroformation experiments with mixtures containing a higher amount of lipid (described as #1 and #2 in Table 4-3) resulted in standard DOPC liposome formation.

The experimental data presented in subchapter 4.4.2. are clearly promising and might overcome the current problems in the synthetic RME model creation. Clearly, further research will be required to increase the efficiency of the hybrid structures electroformation. More research into a systematic comparison of glycopolymeric and mixed giant vesicle membrane properties is still necessary before obtaining a definitive answer if the prepared hybridised giant vesicles could be applied for the creation of a synthetic RME model.

5. Conclusion and Future Work

The overall conclusion from this study is that despite the observed selective interactions between GUVs and PS - Con A beads, an evident uptake of nanoparticles in the polymersome was not recorded during this research project. The collected data suggests that the stiffness of the glycopolymersome membrane does not allow membrane deformation and engulfment of the particle to occur and therefore no clear internalisation is observed. More research on artificial membranes (made from different type of polymers, polymers and lipids or polymers and peptides) is necessary to develop a more viscoelastic artificial membranes which we believe will be essential in creating a synthetic membrane that could perform RME.

The application of the electroformation technique on model compounds was initiated in order to become familiar with this self - assembly method and perform systematic characterisation of the created structures. The initial electroformation studies expanded enormously knowledge of the self - assembly process and the created structures, developed practical skills in the electroformation technique as well as various microscopy techniques.

Conditions suitable for the production of GUVs from the lipid DOPC and polymer PBd - b - PEO were obtained; liposomes were electroformed with an average density of 143 ± 14 units per square mm and average diameter of 26.0 ± 2.0 μm, while polymersomes were formed as expected in a lower density of between 37 ± 4 (procedure “A”) to 40 ± 4 (procedure “B”) and with an average diameter from 20.9 ± 2.1 μm (procedure “A”) to 28.8 ± 2.9 μm (procedure “B”).

Upon familiarisation with the electroformation technique and characterisation methods, the research was then shifted to novel glycopolymers PE - b - (Glu) PEG and PNGEA - b - BA with different block ratios and molar masses.

It was found that glycopolymer PE - b - (Glu) PEG has limited solubility and requires different electroformation conditions from those utilised for the model polymer PBd - b - PEO; therefore, an additional solubility assessment in a mixture of organic solvents was performed and electroformation experiments were carried out step by step (instead of using stabilised procedure "A" or "B"). Overall, conditions suitable for reproducible GUV electroformation from glycopolymer PE - b - (Glu) PEG were determined (conditions #5 in Table 3-3); however, the oval shape of the created structures suggest that they remain in the semi - solid state and their membrane rigidity is likely to be very high due to the high Tg, and that makes the polymersomes inappropriate to utilise as a model cell membrane system to study biological processes mediated by carbohydrates. Therefore, studies were continued with the polymer containing the more liquid - like poly (butyl acrylate) hydrophobic block i.e. PNGEA - b - BA. Glycopolymers were reported to form GUVs with different size and yield; however, glycopolymer M1 (with a block ratio 1 : 10 hydrophilic to hydrophobic) is the most promising polymer for formation of giant vesicles with broad size and high yield (37 ± 4 vesicles per square mm with an average diameter of 19.7 ± 2.0 μm under procedure "A" and 77 ± 8 vesicles per square mm with an average diameter of 24.0 ± 2.0 μm under procedure "B").

Further research interest was concentrated on the glycosylated GUVs electroformed from glycopolymer M1. Studies on the properties of the created polymersomes revealed that they can withstand a pressure difference of up to 24.4

atm and pH fluctuations up to 4 units without visible changes in the membrane structure and rearrangements in the whole population.

Research performed on interaction between the giant glycosylated polymersomes and polystyrene particles functionalised with the lectin Con A concluded that those species are able to interact selectively and aggregate. The highest average percent of the selective interactions between Con A - functionalised PS beads and glycopolymersomes was determined to be 42.0 ± 7.8 %, while control experiments revealed that non - selective interactions occurs sporadically and the percent of interactions is as low as 4.9 ± 1.0 % for non - functionalised PS beads and 8.2 ± 1.4 % for lectin RCA_{120} functionalised PS beads (RCA_{120} does not bind to glucosyl residues). Despite the selective interactions between GUVs electroformed from glycopolymer M1 and PS - Con A, uptake of nanoparticle in the glycopolymersome was not observed exclusively; moreover, confocal fluorescent microscopy z - scans of interacting species confirmed, that PS - Con A beads remain attached to the GUVs membrane outside the structure.

Following interaction studies, the research then moved towards ways of overcoming the current problems in the synthetic RME model. The brief micromanipulation studies confirmed that GUVs electroformed from glycopolymer M1 have a high stability, which probably arises from the polymeric membrane properties i.e. low elasticity and permeability, which makes them unsuitable for the creation of a synthetic RME model. Studies on mixed vesicles created from glycopolymer M1 with addition of different amounts of the lipid DOPC were performed to introduce a regulation mechanism, allowing tuning of the membrane properties i.e. to decrease toughness and increase permeability of the vesicular membrane. Initial experiments revealed that hybrid

vesicles can be electroformed from a mixture of glycopolymer M1 and lipid DOPC mixed in the mass ratio 4 : 1; however further research is required to increase the efficiency of the hybrid vesicles electroformation. Additional studies on mixed membrane properties such as osmotic, pH shock and micromanipulation (as performed for pure polymeric membrane) are desirable to characterise the membrane. Moreover, a systematic comparison of glycopolymeric and mixed GUVs membrane properties is necessary to determine and quantify differences in membrane stability and rigidity before and after modifications. Another step might include binding studies with PS beads (analogous to studies carried out with glycopolymersomes) to compare binding percentage and selectivity, and finally answering the question if synthetic RME can be performed in the modified system.

6. General Experimental

6.1. Materials

6.1.1. Novel amphiphilic glycopolymers

6.1.1.1. PE - b - (Glu) PEG

The polyethylene - block - poly(ethylene glycol) β - D - glucoside block copolymer (PE - b - (Glu) PEG; see Figure 6-1) was synthetised by Dr. Ahmed M. Eissa under the supervision of Prof. Neil R. Cameron at Durham University, United Kingdom. The details of the synthesis and the characterisation procedures are given in the literature.[13]

The PE_{25} - b - PEG_3 - Glu, where the numbers refer to the number - average degree of polymerisation (see Figure 6-1), was prepared from commercially available hydroxyl - terminated polyethylene - block - poly(ethylene glycol) (PE - b - PEG; M_n ~ 875 g mol^{-1}, ethylene oxide ~ 20 wt %) using copper - catalysed azide - alkyne cycloaddition (CuAAC). The glass transition temperature (T_g) determined by differential scanning calorimetry (DSC) is 109 °C.

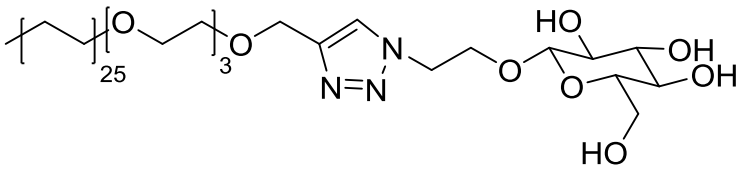

Figure 6-1. Structure of the block copolymer PE - b - (Glu) PEG.

6.1.1.2. $P(NGEA)_n$ - b - $(BA)_m$

The poly [N - 2 - (β - D - glucosyloxy) ethyl acrylamide] - b - (n - butylacrylate) glycosylated block copolymer (PNGEA - b - BA; see Figure 6-2) was synthesised by Dr. Ahmed M. Eissa and Mr. Ali Abdulkarim under the supervision of Prof. Neil R. Cameron at Durham University, United Kingdom.

The poly [N - 2 - (β - D - glucosyloxy) ethyl acrylamide] - b - (n - butylacrylate) glycosylated block copolymer $PNGEA_n$ - b - BA_m, where the n and m refer to the number - average degree of polymerisation, was synthesised through reversible addition - fragmentation chain transfer (RAFT) polymerisation. The initial block copolymer was functionalised with β - D - glucose as presented in the synthetic route shown in Figure 6-3. The chosen synthetic route allows formation of block copolymers with a varying block ratio and different molar mass as presented in Table 6-1. The $PNGEA_n$ - b - BA_m glycopolymers utilised in this study were synthesised with $Đ_M$ ranging from 1.18 to 1.30 and M_n varying from 2.5 kDa to 15.7 kDa. The details of the synthesis of glycopolymer $PNGEA_n$ - b - BA_m and the characterization are presented in supplementary information section 8.1.

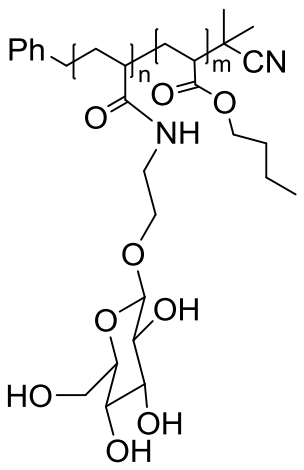

Figure 6-2. Structure of the block copolymer $P(NGEA)_n$ - b - $(BA)_m$.

Table 6-1. $P(NGEA)_n$ - b - $(BA)_m$ block copolymers used in the initial electroformation study.

#	Glycopolymer	$(NGEA)_n$ (n)	$(BA)_m$ (m)	Block ratio (n : m)
1	A1	16	38	1 : 2
2	E1	14	40	1 : 3
3	H1	13	77	1 : 6
4	H2	13	200	1 : 15
5	J1	8	10	1 : 1
6	K1	8	38	1 : 5
7	M1	6	62	1 : 10

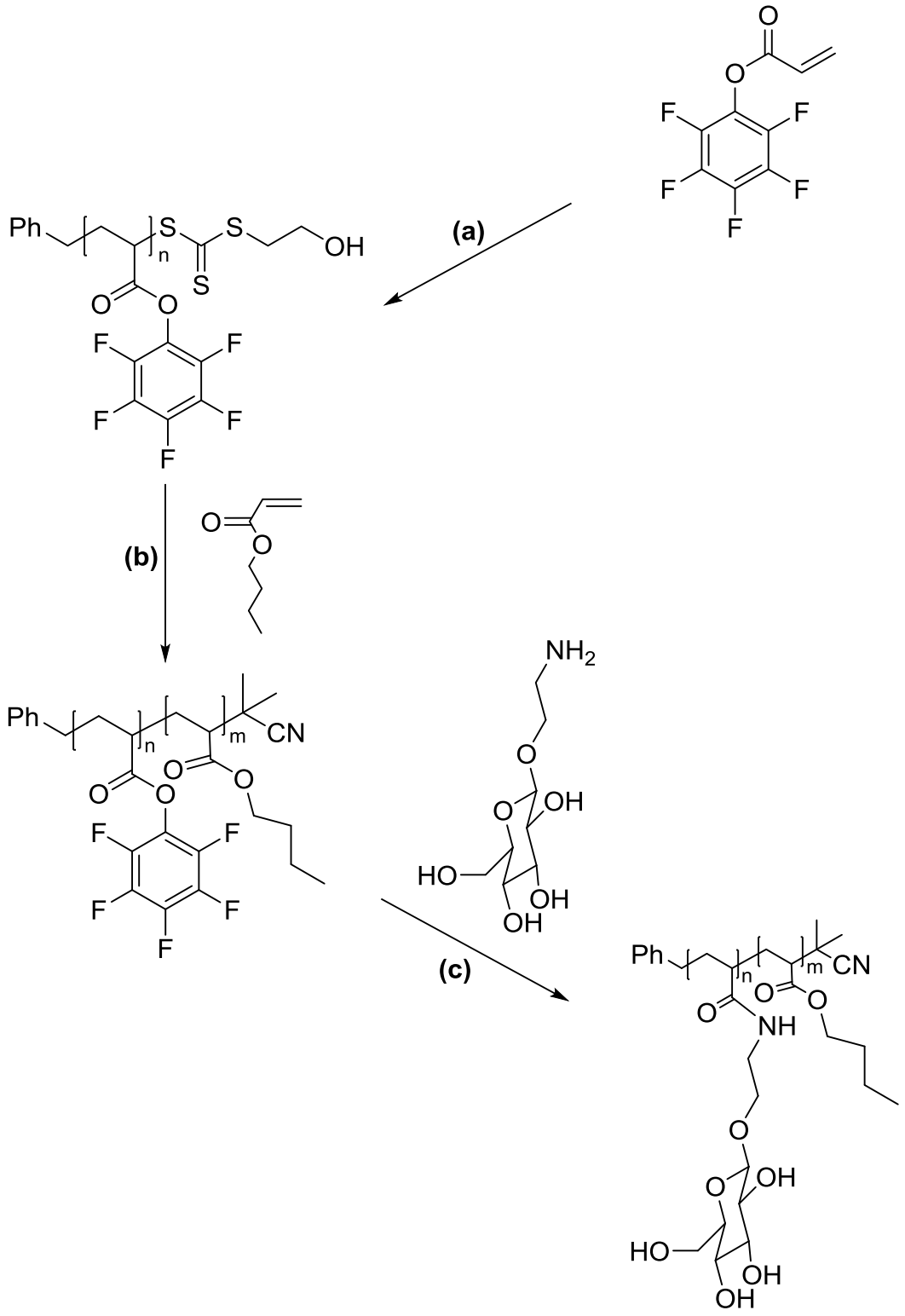

Figure 6-3. Synthesis scheme of the glycopolymer $P(NGEA)_n$ - b - $(BA)_m$. Respectively: (a) RAFT polymerisation; (b) chain extension with n - BA; (c) polymer functionalisation with β - D - glucose.

6.1.2. Commercially available amphiphilic materials used in the electroformation studies

6.1.2.1. DOPC

The commercially available lipid 1, 2 - dioleoyl - sn - glycero - 3 - phosphocholine (DOPC; see Figure 6-4) was purchased from Sigma - Aldrich UK in a lyophilised powder form. The lipid DOPC is a well - defined compound with molar mass of 786.11 g/mol. The melting temperature (T_m) value reported for DOPC is T_m = - 17 °C.[126]

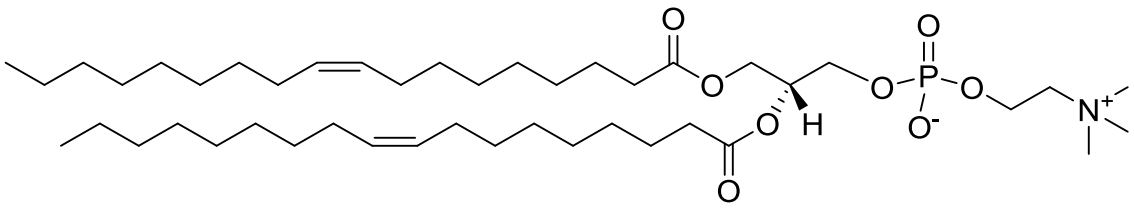

Figure 6-4. Structure of the lipid DOPC.

6.1.2.2. PBd - b - PEO

The commercially available polymer poly (butadiene - b - ethylene oxide) (PBd_{46} - b - PEO_{30}; see Figure 6-5) was purchased from Polymer Source (Canada). The polymer PBd_{46} - b - PEO_{30} is a well - defined block copolymer with $Đ_M$ = 1.04 and M_n = 3.8 kDa. The polymer's polybutadiene block contains 94 % 1, 2 microstructure. The weight fraction of ethylene oxide is 37.5 %. The thermal analysis performed by DSC revealed T_g values of - 31 °C (for Bd block) and - 64 °C (for PEO block).

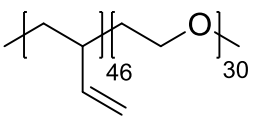

Figure 6-5. Structure of the block copolymer PBd - b - PEO.

6.1.3. Other Materials

Calcium (II) chloride (≥93.0 %), D - (+) - Glucose (≥99.5 %), manganese (II) chloride (≥99 %), N - (2 - hydroxyethyl) piperazine - N' - (2 - ethanesulfonic acid) (≥99.5 %), Nile Red (≥98.0 %; λ_{ex} 530 nm in methanol; λ_{em} 635 nm in methanol), Rhodamine B octadecyl ester perchlorate (≥98.0 %; λ_{ex} 554 nm in methanol; λ_{em} 575 nm in methanol), sodium chloride (≥99.5 %), α - D - Glucopyranosyl β - D - fructofuranoside (≥99.5 %) were purchased from Sigma - Aldrich, UK. 1,2 - Dioleoyl - sn - glycerol - 3 - phosphoethanolamine - N - (carboxyfluorescein) (> 99 %; λ_{ex} 500 nm in methanol; λ_{em} 523 nm in methanol) were purchased from Avanti Polar Lipids, US. Acetone (99.99 %), acetonitrile (>99.9 %), chloroform (>99 %), diethyl ether (>99 %) ethanol (99.8 %), hexane (95 %), isopropanol (>99.5 %), methanol (99.99 %) and THF (>99.5 %) were purchased from Fisher Scientific, UK.

6.1.3.1. HEPES buffer

HEPES buffer was utilised in internalisation studies described in subchapter 4.3. in order to maintain the stability and activity of the lectins present on the surface of PS beads. 250 mL of buffer was prepared by dissolving N - (2 - hydroxyethyl) piperazine - N' - (2 - ethanesulfonic acid) (HEPES, 0.596 g, 0.01 M), sodium chloride (NaCl, 2.192 g, 0.150 M), calcium (II) chloride ($CaCl_2$, 0.055 g, 0.002 M) and manganese (II) chloride

($MnCl_2$, 0.063 g, 0.002 M) in 230 mL of ultrapure water in volumetric flask. Upon full dissolution of the mixed chemicals, the required amount of ultrapure water was added to increase the total volume of buffer to 250 mL and the pH value was adjusted to 7.3 at ambient temperature. Prepared HEPES buffer was filtered using syringe filters with pore size 0.22 μm and stored at ambient temperature.

6.1.3.2. Lectin - conjugated PS beads

The lectin - conjugated PS beads were prepared by Dr. Ahmed M. Eissa under the supervision of Prof. Neil R. Cameron at Durham University, United Kingdom.

Commercially available carboxylate - modified PS latex beads, mean size 1 μm or 0.5 μm, (500 μL, aqueous suspension, 2.5 %) were activated by stirring for 2 h at ambient temperature in the presence of *N* - (3 - dimethylaminopropyl) - *N*'- ethylcarbodiimide hydrochloride (EDAC; 250 μL, 0.4 M) and *N* - hydroxysuccinimide (NHS; 250 μL, 2.8 M). Excess reagents were removed by dialysis (MWCO 3.5 - 5 kDa) against phosphate buffered saline (PBS; pH 7.4). The activated beads dispersion in PBS was added slowly into an Eppendorf tube containing Con A or RCA_{120} (5 mg) under continuous vortexing. The reaction was allowed to proceed overnight. The excess coupling sites were blocked by incubating the beads dispersion with glycine solution (0.5 mL, 200 mg/mL) for 1 h at ambient temperature. The beads dispersion was dialyzed (MWCO 12 - 14 kDa) against PBS and then bicarbonate - carbonate buffer (pH 9.5) to remove any unconjugated lectin. The buffer was replaced by ultrapure water. The lyophilized lectin - conjugated PS beads were stored at - 20 °C. Prior to usage the functionalised beads were suspended in HEPES buffer at a required concentration.

The details of the conjugated beads characterisation and post functionalisation validation are presented in supplementary information section 8.2.

6.2. Instrumentation

6.2.1. Electroformation cell

The electroformation cell was created by the Chemistry Department Electrical workshop Durham University, and its schematic representation is presented in Figure 6-6.

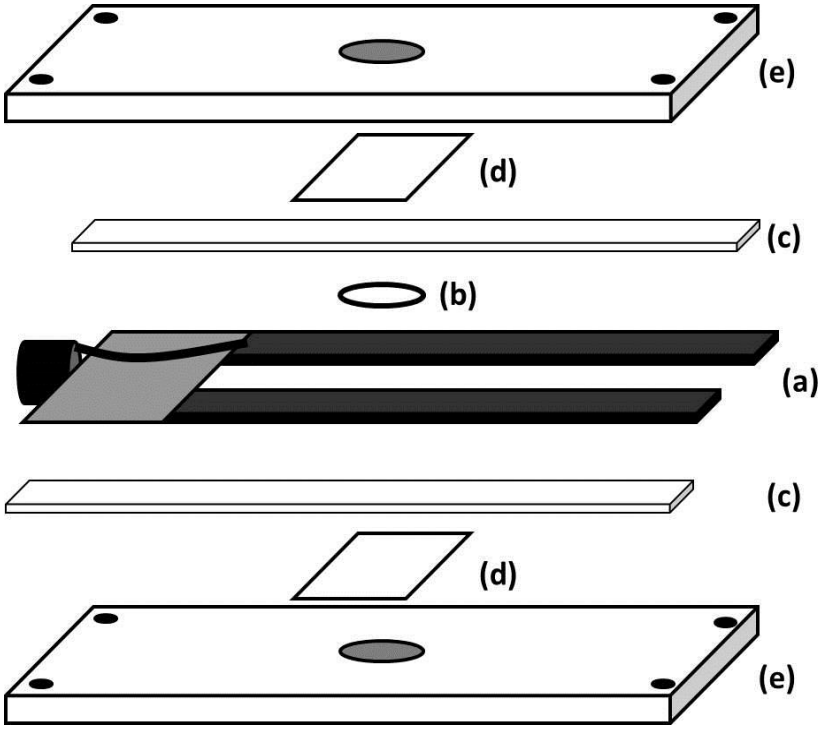

Figure 6-6. Schematic representation of the electroformation cell. Respectively: (a) electroformation cell housing; (b) rubber spacer; (c) isolating strips; (d) indium tin oxide (ITO) coated glass slide electrodes; (e) electro - conductive body connected to the AC source.

The device contains two copper slides which are connected to different electrical poles which operate as positive and negative electrodes. Two square glass slides, covered with indium tin oxide (In_2O_3/SnO_2, surface resistivity 8 - 12 Ω/sq) and polymer film are put one on top of another with a rubber ring (ø 10 mm) sandwiched between. The space in the rubber ring is filled with 150 µL ultrapure water (or ultrapure water - based solution with required additives) during the cell assembly. One glass slide is connected to the negative electrode and another to the positive electrode. The conductive glass slides are connected via the solution inside the rubber ring as presented in Figure 6-7.

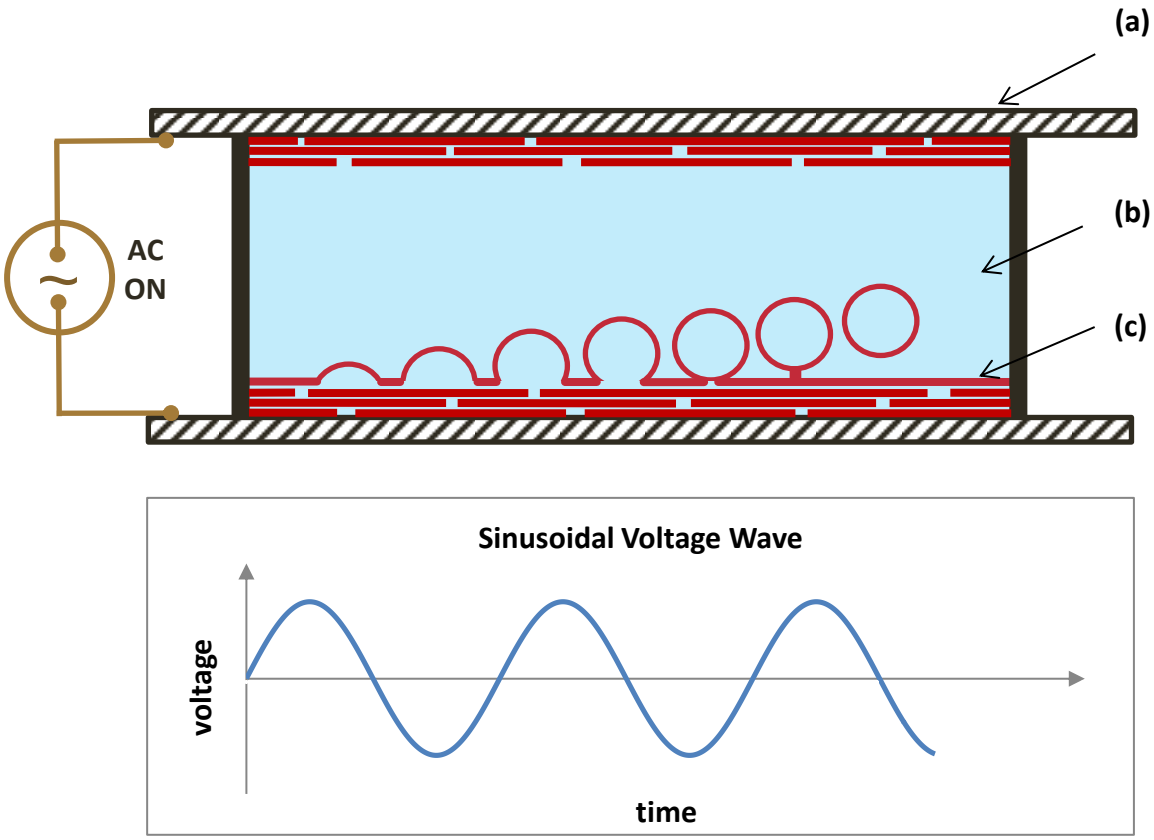

Figure 6-7. Schematic representation of vesicle electroformation process. Respectively: (a) ITO coated glass slide electrodes; (b) electroformation chamber filled with water based solution; (c) polymer film deposited on electrodes.

After applying an electric current, an electric field is induced through the copper electrodes, glass slides, polymer film and water based solution. The electric field initiates gentle film hydration and gradual detachment which facilitates vesicle formation (as presented in Figure 6-7).

6.2.2. Electroformation power supply

An Aim & Thurlby Thandar Instruments, UK, TG315 Function Generator 3MHz was used in this research project as an electrical signal generator. This device is suitable for the electroformation experiments, because it permits control of the main electrical signal parameters:

- Changeable electrical signal between alternating (AC) and direct (DC) current
- Output amplitude from 2 mV to 20 V
- Frequency range from 0.03 Hz to 3 MHz
- Changeable electrical signal form between *sinusoidal, square* and *triangle* waveforms for AC.

6.2.3. Microscopes

Confocal fluorescence microscopy observations were carried out on three types of microscopes: BioRad MicroRadiance Confocal Laser Scanning Microscope, Zeiss 510

Meta Confocal Laser Scanning Microscope and Leica SP5 Confocal Laser Scanning Microscope SP5.

BioRad MicroRadiance confocal scanning microscope is equipped with a Nikon 50x PL NA 0.85 oil - immersion objective. He - Ne laser with an excitation at 543 nm in combination with a photon multiplying tube (PMT) and emission filter at LP 570 was utilised for signal detection.

Zeiss 510 Meta confocal scanning microscope is equipped with Zeiss 40x NA 1.3 oil - immersion objective and Zeiss 63x NA 1.4 oil - immersion objective. He - Ne laser with an excitation 543 nm in combination with PMT and emission filter at BP 530 - 600 was utilised for signal detection.

Leica SP5 confocal laser scanning microscope SP5 is equipped with Leica 40x HCX PL APO oil - immersion UV objective and Leica 63x HCX PL APO oil - immersion UV objective. He - Ne laser with an excitation 543 nm and Ar laser with an excitation of 478 nm in combination with 2 PMTs were utilised for signal detection.

6.2.4. Micromanipulation system

Micromanipulation experiments were performed using Eppendorf TransferMan NK2 system connected to an Eppendorf FemtoJet injector and visualised using a Leica DMI3000 (Inverted) differential interference contrast (DIC) microscope equipped with Leica 40x N Plan L PH2 NA 0.55 objective.

Micro - pipettes of required size and shape were prepared using the Narishige PC - 10 Puller.

6.2.5. Spectrophotometer

Turbidity measurements were performed recording changes in the absorbance value of 450 nm light (A_{450nm}) at a constant temperature of 20 °C using a Varian Cary 100 Bio UV – Visible Spectrophotometer.

6.3. Methods

All the light, fluorescent and fluorescent confocal microscopy images presented in this thesis were processed using open source software ImageJ version 1.46r (used plugin: loci_tools) and/or Leica Application Suite Advanced Fluorescence Lite (LAS AF Lite, Leica Microsystems CMS GmbH) version 4.1.

6.3.1. Liposomes electroformation from DOPC

6.3.1.1. DOPC film preparation on glass slides

The lipid DOPC (see Figure 6-4) solution in chloroform with lipophilic dye Nile Red (in concentration of 0.001 mass %) was used for the film preparation on the electroformation glass slide. A required volume of the lipid solution was applied on the conductive side of electroformation slides and placed in the desiccator for solvent evaporation and lipid film formation.

6.3.1.2. Electroformation system preparation for lipid sample

Research on the GUV electroformation process started with vesicle formation using the lipid DOPC. All the experiments performed with DOPC are presented in Table 2-1.

It was found that the most optimal conditions for the GUVs electroformation from DOPC were found during the #13 experiment (see Table 2-1.). This experiment will be a

model sample for the standard electroformation procedure description. The lipid film covering the glass slide was created using DOPC solution in chloroform at a concentration of 10 mg/ml; applying 3 µl of the solution to the slide and leaving in desiccator for 2 hours for solvent evaporation. After evaporation, the electroformation process was performed using a voltage of 1.2 V, frequency of 10 Hz and a *sinusoidal* waveform for 4 hours. After that a voltage of 1.2 V, frequency of 5 Hz and a *square* waveform for another 1 hour allowed detachment. Electroformation was performed at 19 ^{o}C in 150 mM sucrose solution. After electroformation, the solution containing the vesicles was placed in the chamber with 150 mM equal osmotic glucose solution. The density difference between glucose and sucrose solutions cause the vesicles to sink to the bottom of chamber, where they are observed using light and confocal microscopy.

6.3.2. Polymersomes electroformation from PBd - b - PEO

6.3.2.1. PBd - b - PEO film preparation on glass slides

A required amount of polymer PBd - b - PEO was dissolved in chloroform along with the lipophilic dye Rhodamine B octadecyl ester perchlorate (in concentration of 0.001 mass %). A required volume of the polymer solution sample was applied to the conductive side of the glass slide and after initial polymer film formation in open air (from ten to fifteen minutes) was placed in the desiccator for at least 3 hours for further solvent evaporation and polymer film formation.

6.3.2.2. Electroformation procedure “A” for PBd - b - PEO polymer sample

Electroformation experiments with polymer PBd - b - PEO were performed in the order suggested by the DOE software. The most optimal conditions for polymersomes formation were achieved during the #8 experiment (see Table 2-3), for that reason the polymersome electroformation procedure will be described using that experiment.

The polymer film was created on the glass slide using PBd - b - PEO solution in chloroform at a concentration of 5 mg/ml; 30 µl of solution were placed onto the slide and left for at least 3 hours to allow solvent evaporation in the desiccator. After that the electroformation process was performed using a voltage of 15 V, frequency of 1 MHz and a *sinusoidal* waveform for 0.5 hour. After that a voltage of 1.2 V, frequency of 5 Hz and a *square* waveform was applied for another 0.5 hour in order to initiate vesicle detachment from the glass slide. Electroformation was performed in a 100 mM solution of sucrose at 19 ^{o}C. After electroformation, the solution containing vesicles was placed in the chamber with an equal osmolarity saline solution and was observed using light and confocal microscopy. The density difference causes the vesicles to sink to the bottom of the visualization chamber and makes them more static; light refraction difference makes them more visible through light microscopy.

6.3.2.3. Electroformation procedure “B” for PBd - b - PEO polymer sample

Following a thorough literature review it was decided to perform experiments on PBd - b - PEO polymersome electroformation using a procedure based on a protocol developed by Monroy *et al*.[38]

The polymer film was created on the glass slide using PBd - b - PEO solution in chloroform at a concentration of 2 mg/ml; 20 µl of solution were placed onto the slide and left for at least for 3 hours to allow solvent evaporation in the desiccator. After that the electroformation process in 100 mM sucrose solution was performed using a voltage of 9 V, frequency of 10 Hz and a sinusoidal waveform for 0.5 hour. Upon electroformation, the solution containing vesicles was placed in the chamber with an isotonic sodium chloride and was observed using light and confocal microscopy.

6.3.2.4. Full Factorial Design of Experiments

The SAS, US, statistical software JMP Pro 9.0.2 was utilized in a design of experiment approach to reduce cost and time required for the polymersomes electroformation study.

The chosen four continuous parameters were set up with two factor levels: minimum and maximum (see Table 6-2). A factorial design with only two level factors has a sample size that is equal to a power of two, thus it required sixteen experiments to perform a test of all possible combinations of the chosen electroformation conditions

as presented in Table 2-3. In order to improve the reliability of the statistical study, every set of parameters was tested three times (in total 48 experiments were performed).

Table 6-2. Chosen two levels of factors for the DOE study.

Factor level	Time (h)	Voltage (V)	Frequency (Hz)	Deposited Volume (µl)
Min (-)	0.5	0.2	10	5
Max (+)	5	15	1000000	30

Average Diameter Evaluation System

The electroformation output was assessed by measuring the diameter of the giant vesicles and calculating the average diameter. Data for every sample was collected on 20 randomly chosen regions of interest, each with an area of 0.05 square mm (total surface of 1 square mm). Due to research limitations, only vesicles with diameters larger than 5 µm were measured and included in the statistical study. Sample images were processed using the open - source software ImageJ version 1.46r (used plugin: loci_tools).

Blank samples or specimens containing only asymmetrical aggregates were assessed with an average diameter of 0 µm. Samples containing mostly spherical structures smaller than 5 µm were assessed with an average diameter of 1 µm; this assessment

methodology of the electroformation samples containing undesirable structures was found to be optimal (without losing any experimental data).

6.3.3. Glycopolymersomes electroformation from PE - b - (Glu) PEG

6.3.3.1. PE - b - (Glu) PEG film preparation on glass slides

The PE - b - (Glu) PEG polymer (see Figure 6-1) solution in chloroform and methanol in a ratio of 4 : 1 with lipophilic dye Nile Red (in concentration of 0.001 mass %) was used for the film preparation on the indium tin oxide coated glass slides. The required volume of polymer solution sample was applied to the glass slide in portions every 0.5 h and placed in the desiccator overnight to allow solvent evaporation.

6.3.3.2. Electroformation system preparation for glycopolymer sample

Starting conditions for the electroformation experiments with PE - b - (Glu) PEG were the same as optimal conditions for DOPC. The most optimal conditions for polymersomes formations were created during the #9 experiment (see Table 3-3), for that reason polymer electroformation procedure will be described using that experiment. Polymer film was created on the glass slide using PE - b - (Glu) PEG

solution in chloroform and methanol solution in a ratio of 4 : 1 with a concentration of 0.5 mg/ml; 5 layers of 20 µl of solution were placed onto the slide and left overnight to allow solvent evaporation in the desiccator. After that the electroformation process was performed at a temperature of 80 ^{0}C using a voltage of 10 V; frequency of 10 Hz and a *sinusoidal* waveform for 3 hours, followed by a voltage of 10 V, frequency of 5 Hz and a *square* waveform for another 1 hour.

6.3.4. Glycopolymersomes electroformation from $P(NGEA)_n$ - b - $(BA)_m$

6.3.4.1. $P(NGEA)_n$ - b - $(BA)_m$ film preparation on glass slides

The polymer PNGEA - b - BA (see Figure 6-2) solution in THF and methanol (mixed at a ratio of 3 : 1) with lipophilic dye Rhodamine B octadecyl ester perchlorate (in concentration of 0.001 mass %) was used for the film preparation on indium tin oxide coated glass slides. A required volume of the prepared polymer solution sample was applied on the conductive side of slide and placed in the desiccator overnight to allow solvent evaporation.

6.3.4.2. Electroformation procedure “A” for $P(NGEA)_n$ - b - $(BA)_m$ polymer sample

A polymer film was created on the glass slide using a solution of PNGEA - b - BA in THF and methanol at a concentration of 5 mg/ml; 30 µl of solution were placed onto the slide and left in the open air for 0.5 hour and after that in a desiccator overnight to allow solvent evaporation. After this initial step, the electroformation procedure was applied identically as described in 6.3.2.2.

6.3.4.3. Electroformation procedure “B” for M1 polymer sample

A polymer film was created on the glass slide using a solution of M1 in THF and methanol at a concentration of 2 mg/ml at a ratio of 3 : 1 with the lipophilic dye Rhodamine B octadecyl ester perchlorate (in concentration of 0.001 mass %); 20 µl of solution were placed onto the slide and left in the open air for 10 - 15 minutes and after that in a desiccator overnight to allow solvent evaporation. Following this initial step, the electroformation procedure was applied for 0.5, 2 or 3 hours identically as described in 6.3.2.3.

6.3.5. Electroformation of mixed vesicles from DOPC and glycopolymer M1

6.3.5.1. Mixed film preparation on glass slides

It was decided to use the well - known liposome - forming lipid DOPC along with glycopolymer M1 to test their compatibility and ability to form mixed GUVs. Initially, separate stock solutions of glycopolymer M1 and lipid DOPC were prepared in a mixture of THF and methanol (in ratio of 3 : 1) at a concentration of 5 mg/mL. A required volume of lipid and polymer solutions (as presented in Table 6-3) were mixed to obtain a solution with a desirable mass ratio of the amphiphilic materials; a hydrophobic dye Rhodamine B octadecyl ester perchlorate was added to the starting solution in concentration of 0.001 mass % to allow visualisation of samples using fluorescent microscopy. Moreover, a 5 % (wt.) additive of headgroup - labelled phospholipid 1,2 - dioleoyl - sn - glycerol - 3 - phosphoethanolamine - N - (carboxyfluorescein) (DOPEAN6 - FAM) was applied to the sample in order to be able to locate lipid accumulation zones in the electroformed structures.

Table 6-3. Composition of solutions used for the film preparation for the mixed vesicles study.

#	Volume of stock solution of M1(µL)	Volume of stock solution of DOPC (µL)	Mass of polymer M1 (mg)	Mass of lipid DOPC (mg)	Mass ratio	Molar ratio
1	80	320	0.4	1.6	1 : 4	1 : 50
2	200	200	1.0	1.0	1 : 1	1 : 12
3	320	80	1.6	0.4	4 : 1	1 : 3

6.3.5.2. Electroformation procedure “B” for mixed glycopolymer M1 and lipid DOPC sample

Following preparation of the mixed amphiphile solution, film preparation on indium tin oxide and electroformation experiments were performed following procedure “B” as described in subchapter 6.3.4.3.

6.3.6. Studies on GUVs from glycopolymer M1

6.3.6.1. Osmotic shock

Hypertonic shock

Electroformation of vesicles from glycopolymer M1 was performed in ultrapure water using procedure "B" as described in 6.3.4.3. 150 µl of electroformation solution was placed in the visualisation chamber filled with 600 µl of ultrapure water. Vesicles present in the sample were observed and characterised in detail. Following initial measurements, hyperosmotic shock was performed by adding to the solution the required amount of 5 M NaCl (as presented in Table 6-4) in order to increase the osmotic pressure in the vesicular environment. The prepared sample was left for 2 hours to stabilise and afterwards a new observation and characterisation of vesicles were performed.

Table 6-4. Hypertonic shock experimental solutions.

#	Δc (mM)	ΔΠ (atm)	V of sample (µL)	V of added 5M NaCl (µL)
1	-375	-18.3	750.0	60.8
2	-250	-12.2	750.0	39.5
3	-125	-6.1	750.0	19.2
4	-50	-2.4	750.0	7.6

Hypotonic shock

Electroformation of vesicles from glycopolymer M1 was performed in 1 M sucrose solution using procedure "B" as described in 6.3.4.3. 150 µl of electroformation solution was placed in the visualisation chamber filled with 600 µl of 1 M sucrose

solution. The vesicles present in the sample were observed and characterised in detail. Following initial measurements, hypoosmotic shock was performed by adding to the solution the required amount of ultrapure water (as presented in Table 6-5) in order to decrease the osmotic pressure in the vesicular environment. The prepared sample was left for 2 hours to stabilise and afterwards a new observation and characterisation of vesicles were performed.

Table 6-5. Hypotonic shock experimental solutions.

#	Δc (mM)	ΔΠ (atm)	V of sample (µL)	V of added ultrapure water (µL)
1	250	6.1	750.0	250.0
2	500	12.2	750.0	750.0

6.3.6.2. pH shock

Initially, electroformation of vesicles from glycopolymer M1 was performed in ultrapure water using procedure "B" as described in 6.3.4.3. The electroformation sample was diluted 5 times by placing 150 µl of the electroformation solution in the visualisation chamber filled with 600 µl of ultrapure water and left for approximately 0.5 h to stabilise. Vesicles present in the sample were observed and characterised in detail. Following initial measurements, pH adjustments were performed by adding the required amount of sodium hydroxide (NaOH) or hydrochloric acid (HCl) to the solution in order to increase or decrease the pH value. The prepared specimen was left for 2 hours to stabilise and afterwards a new observation and characterisation of vesicles were performed.

6.3.6.3. Turbidity measurements

The solution of lectin Con A was prepared in HEPES buffer at a concentration of 2 mg/ml (molar concentration is approximately 18.9 µM assuming that Con A molar mass is 106 kDa,). Then, 600 µl of lectin solution were placed in a cuvette and the required volume of vesicle solution (concentration 0.53 mg/ml) was added (to final volume ratio of 10 : 1 or 5 : 2). The absorbance of 450 nm light (A_{450nm}) was recorded using Varian Cary 100 Bio UV – Visible Spectrophotometer for the first 60 minutes every 5 minutes.

Control experiments were performed using an analogous protocol, utilising 2 mg/ml lectin Con A solution in HEPES buffer and solution of GUVs in HEPES buffer.

6.3.6.4. Interactions of polymersomes formed from glycopolymer M1 with PS beads

Polymersomes were prepared using the electroformation method following the procedure described previously in 6.3.4.2. PS beads were functionalised as described previously in 6.1.2.2.

The observation chamber was filled with 600 µl of HEPES buffer and 150 µl of electroformation sample, and left for 0.5 h to allow GUVs stabilisation. Subsequently, GUVs were observed using light and fluorescent confocal microscopy. Following initial observation on GUVs, 50 µl or 100 µl of required PS beads (for control experiments: non – functionalised and RCA_{120} functionalised; for selective interaction studies: Con A functionalised) were calculated. After 15 h of incubation the sample was observed

using light and fluorescent confocal microscopy. The collected images were processed using the open - source software ImageJ version 1.46r (used plugin: loci_tools).

6.3.6.5. GUV probing by micromanipulation

Initially, GUVs formed from glycopolymer M1 in a sucrose solution using electroformation procedure "B" (as described in 6.3.4.3) were transferred to the visualisation chamber with an isotonic glucose solution. The polymersomes were left for approximately 0.5 h to allow them to sink and stabilise at the bottom of the visualization chamber. Following the preparation procedure, initial micromanipulation testing was performed.

7. References

[1] Y. Y. Mai and A. Eisenberg, *Chemical Society Reviews* **2012**, *41*, 5969-5985.

[2] A. Jesorka and O. Orwar in *Liposomes: Technologies and Analytical Applications*, *Vol. 1* **2008**, pp. 801-832.

[3] J. N. Israelachvili, D. J. Mitchell and B. W. Ninham, *Journal of the Chemical Society-Faraday Transactions Ii* **1976**, *72*, 1525-1568.

[4] J. Israelechvili, *Intermolecular & Surface Forces*, Academic Press Limited, **1991**, p. 1-674.

[5] T. Headgordon, *Proceedings of the National Academy of Sciences of the United States of America* **1995**, *92*, 8308-8312.

[6] M. Antonietti and S. Forster, *Advanced Materials* **2003**, *15*, 1323-1333.

[7] P. Walde, K. Cosentino, H. Engel and P. Stano, *Chembiochem* **2010**, *11*, 848-865.

[8] D. E. Discher and A. Eisenberg, *Science* **2002**, *297*, 967-973.

[9] V. Malinova, S. Belegrinou, D. D. Ouboter and W. P. Meier, *Polymer Membranes/Biomembranes* **2010**, *224*, 113-165.

[10] P. L. Soo and A. Eisenberg, *Journal of Polymer Science Part B-Polymer Physics* **2004**, *42*, 923-938.

[11] A. D. Bangham, M. M. Standish and J. C. Watkins, *Journal of Molecular Biology* **1965**, *13*, 238-252.

[12] G. Gregoriadis, *Journal of Liposome Research* **2006**, *16*, 155-155.

[13] A. M. Eissa, M. J. P. Smith, A. Kubilis, J. A. Mosely and N. R. Cameron, *Journal of Polymer Science Part a-Polymer Chemistry* **2013**, *51*, 5184-5193.

[14] C. Nardin, S. Thoeni, J. Widmer, M. Winterhalter and W. Meier, *Chemical Communications* **2000**, 1433-1434.

[15] R. Stoenescu and W. Meier, *Chemical Communications* **2002**, 3016-3017.

[16] E. D. Gomez, T. J. Rappl, V. Agarwal, A. Bose, M. Schmutz, C. M. Marques and N. P. Balsara, *Macromolecules* **2005**, *38*, 3567-3570.

[17] S. J. Holder, R. C. Hiorns, N. Sommerdijk, S. J. Williams, R. G. Jones and R. J. M. Nolte, *Chemical Communications* **1998**, 1445-1446.

[18] L. Tian, P. Nguyen and P. T. Hammond, *Chemical Communications* **2006**, 3489-3491.

[19] D. Nolan, R. Darcy and B. J. Ravoo, *Langmuir* **2003**, *19*, 4469-4472.

[20] K.-J. Gao, G. Li, X. Lu, Y. G. Wu, B.-Q. Xu and J.-H. Fuhrhop, *Chemical Communications* **2008**, 1449-1451.

[21] K. Kita-Tokarczyk, J. Grumelard, T. Haefele and W. Meier, *Polymer* **2005**, *46*, 3540-3563.

[22] H. W. Shen and A. Eisenberg, *Macromolecules* **2000**, *33*, 2561-2572.

[23] K. Yu, C. Bartels and A. Eisenberg, *Langmuir* **1999**, *15*, 7157-7167.

[24] C. K. Wong, A. J. Laos, A. H. Soeriyadi, J. Wiedenmann, P. M. G. Curmi, J. J. Gooding, C. P. Marquis, M. H. Stenzel and P. Thordarson, *Angewandte Chemie-International Edition* **2015**, *54*, 5317-5322.

[25] A. A. Reinecke and H. G. Dobereiner, *Langmuir* **2003**, *19*, 605-608.

[26] C. D. J. Parmenter, R. Chen, D. L. Cheung and S. A. F. Bon, *Soft Matter* **2013**, *9*, 6890-6896.

[27] A. T. Nikova, V. D. Gordon, G. Cristobal, M. R. Talingting, D. C. Bell, C. Evans, M. Joanicot, J. A. Zasadzinski and D. A. Weitz, *Macromolecules* **2004**, *37*, 2215-2218.

[28] M. M. Santore, D. E. Discher, Y. Y. Won, F. S. Bates and D. A. Hammer, *Langmuir* **2002**, *18*, 7299-7308.

[29] L. F. Zhang and A. Eisenberg, *Macromolecules* **1996**, *29*, 8805-8815.

[30] L. F. Zhang, K. Yu and A. Eisenberg, *Science* **1996**, *272*, 1777-1779.

[31] H. Bermudez, A. K. Brannan, D. A. Hammer, F. S. Bates and D. E. Discher, *Macromolecules* **2002**, *35*, 8203-8208.

[32] H. Bermudez, D. A. Hammer and D. E. Discher, *Langmuir* **2004**, *20*, 540-543.

[33] P. Bandyopadhyay and P. K. Bharadwaj, *Langmuir* **1998**, *14*, 7537-7538.

[34] Y. Tanaka, M. Miyachi and Y. Kobuke, *Angewandte Chemie-International Edition* **1999**, *38*, 504-506.

[35] O. Terreau, C. Bartels and A. Eisenberg, *Langmuir* **2004**, *20*, 637-645.

[36] F. T. Liu and A. Eisenberg, *Journal of the American Chemical Society* **2003**, *125*, 15059-15064.

[37] J. C. M. Lee, H. Bermudez, B. M. Discher, M. A. Sheehan, Y. Y. Won, F. S. Bates and D. E. Discher, *Biotechnology and Bioengineering* **2001**, *73*, 135-145.

[38] R. Rodriguez-Garcia, M. Mell, I. Lopez-Montero, J. Netzel, T. Hellweg and F. Monroy, *Soft Matter* **2011**, *7*, 1532-1542.

[39] J. P. Reeves and R. M. Dowben, *Journal of Cellular Physiology* **1969**, *73*, 49-60.

[40] M. I. Angelova and D. S. Dimitrov, *Faraday Discussions* **1986**, *81*, 303-311.

[41] K. Akashi, H. Miyata, H. Itoh and K. Kinosita, *Biophysical Journal* **1996**, *71*, 3242-3250.

[42] J. R. Howse, R. A. L. Jones, G. Battaglia, R. E. Ducker, G. J. Leggett and A. J. Ryan, *Nature Materials* **2009**, *8*, 507-511.

[43] P. Bucher, A. Fischer, P. L. Luisi, T. Oberholzer and P. Walde, *Langmuir* **1998**, *14*, 2712-2721.

[44] V. Kralj-Iglic, G. Gomiscek, J. Majhenc, V. Arrigler and S. Svetina, *Colloids and Surfaces a-Physicochemical and Engineering Aspects* **2001**, *181*, 315-318.

[45] M. Mally, J. Majhenc, S. Svetina and B. Zeks, *Biophysical Journal* **2002**, *83*, 944-953.

[46] S. Pautot, B. J. Frisken and D. A. Weitz, *Langmuir* **2003**, *19*, 2870-2879.

[47] B. Alberts, A. Johnson, J. Lewis, D. Morgan, M. Raff, K. Roberts and P. Walter, *Molecular Biology of the Cell, Sixth Edition*, **2015**, p. 1-1342.

[48] M. M. C. David L. Nelson, *Lehninger Principles of Biochemistry 5th Edition*, W. H. Freeman; 5th edition **2008**, p. 1-1294.

[49] S. J. Singer and G. L. Nicolson, *Science* **1972**, *175*, 720-751.

[50] P. Mueller, D. O. Rudin, H. T. Tien and W. C. Wescott, *Nature* **1962**, *194*, 979-980.

[51] A. Beerlink, P. J. Wilbrandt, E. Ziegler, D. Carbone, T. H. Metzger and T. Salditt, *Langmuir* **2008**, *24*, 4952-4958.

[52] N. Malmstadt, L.-J. Jeon and J. J. Schmidt, *Advanced Materials* **2008**, *20*, 84-89.

[53] L. K. Tamm and H. M. McConnell, *Biophysical Journal* **1985**, *47*, 105-113.

[54] E. Sackmann, *Science* **1996**, *271*, 43-48.

[55] O. Purrucker, H. Hillebrandt, K. Adlkofer and M. Tanaka, *Electrochimica Acta* **2001**, *47*, 791-798.

[56] J. Y. Wong, J. Majewski, M. Seitz, C. K. Park, J. N. Israelachvili and G. S. Smith, *Biophysical Journal* **1999**, *77*, 1445-1457.

[57] G. B. Luo, T. T. Liu, X. S. Zhao, Y. Y. Huang, C. H. Huang and W. X. Cao, *Langmuir* **2001**, *17*, 4074-4080.

[58] M. Merzlyakov, E. Li, I. Gitsov and K. Hristova, *Langmuir* **2006**, *22*, 10145-10151.

[59] S. F. Fenz and K. Sengupta, *Integrative Biology* **2012**, *4*, 982-995.

[60] B. Gruber and B. Koenig, *Chemistry-a European Journal* **2013**, *19*, 438-448.

[61] M. Marguet, C. Bonduelle and S. Lecommandoux, *Chemical Society Reviews* **2013**, *42*, 512-529.

[62] R. R. Sawant and V. P. Torchilin, *Soft Matter* **2010**, *6*, 4026-4044.

[63] U. Borchert, U. Lipprandt, M. Bilang, A. Kimpfler, A. Rank, R. Peschka-Suss, R. Schubert, P. Lindner and S. Forster, *Langmuir* **2006**, *22*, 5843-5847.

[64] R. Dimova, U. Seifert, B. Pouligny, S. Forster and H. G. Dobereiner, *European Physical Journal E* **2002**, *7*, 241-250.

[65] B. M. Discher, Y. Y. Won, D. S. Ege, J. C. M. Lee, F. S. Bates, D. E. Discher and D. A. Hammer, *Science* **1999**, *284*, 1143-1146.

[66] E. Cabane, X. Zhang, K. Langowska, C. G. Palivan and W. Meier, *Biointerphases* **2012**, *7*.

[67] X. Armengol and J. Estelrich, *Journal of Microencapsulation* **1995**, *12*, 525-535.

[68] S. Egli, H. Schlaad, N. Bruns and W. Meier, *Polymers* **2011**, *3*, 252-280.

[69] L. R. Montes, A. Alonso, F. M. Goni and L. A. Bagatolli, *Biophysical Journal* **2007**, *93*, 3548-3554.

[70] P. Walde and S. Ichikawa, *Biomolecular Engineering* **2001**, *18*, 143-177.

[71] M. Chemin, P.-M. Brun, S. Lecommandoux, O. Sandre and J.-F. Le Meins, *Soft Matter* **2012**, *8*, 2867-2874.

[72] J. F. Le Meins, C. Schatz, S. Lecommandoux and O. Sandre, *Materials Today* **2013**, *16*, 397-402.

[73] M. Schulz, D. Glatte, A. Meister, P. Scholtysek, A. Kerth, A. Blume, K. Bacia and W. H. Binder, *Soft Matter* **2011**, *7*, 8100-8110.

[74] U.-J. Choe, V. Z. Sun, J.-K. Y. Tan and D. T. Kamei, *Peptide-Based Materials* **2012**, *310*, 117-134.

[75] A. Mecke, C. Dittrich and W. Meier, *Soft Matter* **2006**, *2*, 751-759.

[76] H. Schlaad in *Solution properties of polypeptide-based copolymers*, *Vol. 202* Eds.: H. A. Klok and H. Schlaad), **2006**, 53-73.

[77] S. Egli, M. G. Nussbaumer, V. Balasubramanian, M. Chami, N. Bruns, C. Palivan and W. Meier, *Journal of the American Chemical Society* **2011**, *133*, 4476-4483.

[78] B. Li, A. L. Martin and E. R. Gillies, *Chemical Communications* **2007**, 5217-5219.

[79] S. F. M. van Dongen, M. Nallani, S. Schoffelen, J. J. L. M. Cornelissen, R. J. M. Nolte and J. C. M. van Hest, *Macromolecular Rapid Communications* **2008**, *29*, 321-325.

[80] M. T. Paternostre, M. Roux and J. L. Rigaud, *Biochemistry* **1988**, *27*, 2668-2677.

[81] J. L. Rigaud, M. T. Paternostre and A. Bluzat, *Biochemistry* **1988**, *27*, 2677-2688.

[82] N. Kahya, E. I. Pecheur, W. P. de Boeij, D. A. Wiersma and D. Hoekstra, *Biophysical Journal* **2001**, *81*, 1464-1474.

[83] M. K. Doeven, J. H. A. Folgering, V. Krasnikov, E. R. Geertsma, G. van den Bogaart and B. Poolman, *Biophysical Journal* **2005**, *88*, 1134-1142.

[84] M. M. C. David L. Nelson, *Lehninger Principles of Biochemistry 5th Edition*, W. H. Freeman; 5th edition **2008**,

[85] M. R. Villarreal in *Vol.* Wikipedia, https://en.wikipedia.org/wiki/Endocytosis,

[86] K. Takei and V. Haucke, *Trends Cell Biol* **2001**, *11*, 385-391.

[87] T. F. Roth and K. R. Porter, *J Cell Biol* **1964**, *20*, 313-332.

[88] B. M. Pearse, *Proc Natl Acad Sci U S A* **1976**, *73*, 1255-1259.

[89] H. T. McMahon and E. Boucrot, *Nat Rev Mol Cell Biol* **2011**, *12*, 517-533.

[90] J. Hirst and M. S. Robinson, *Biochim Biophys Acta* **1998**, *1404*, 173-193.

[91] C. Le Roy and J. L. Wrana, *Nat Rev Mol Cell Biol* **2005**, *6*, 112-126.

[92] R. G. Parton and K. Simons, *Nat Rev Mol Cell Biol* **2007**, *8*, 185-194.

[93] G. E. Palade, *Journal of Applied Physics* **1953**, *24:1424*.

[94] E. Yamada, *J Biophys Biochem Cytol* **1955**, *1*, 445-458.

[95] R. R. Bruns and G. E. Palade, *J Cell Biol* **1968**, *37*, 244-276.

[96] D. K. Sharma, J. C. Brown, A. Choudhury, T. E. Peterson, E. Holicky, D. L. Marks, R. Simari, R. G. Parton and R. E. Pagano, *Mol Biol Cell* **2004**, *15*, 3114-3122.

[97] W. I. Lencer, T. R. Hirst and R. K. Holmes, *Biochim Biophys Acta* **1999**, *1450*, 177-190.

[98] B. B. Finlay, S. Ruschkowski and S. Dedhar, *J Cell Sci* **1991**, *99 (Pt 2)*, 283-296.

[99] L. Pelkmans, D. Puntener and A. Helenius, *Science* **2002**, *296*, 535-539.

[100] J. S. Shin and S. N. Abraham, *Microbes Infect* **2001**, *3*, 755-761.

[101] J. Rejman, V. Oberle, I. S. Zuhorn and D. Hoekstra, *Biochem J* **2004**, *377*, 159-169.

[102] A. Yamada, T. Yamanaka, T. Hamada, M. Hase, K. Yoshikawa and D. Baigl, *Langmuir* **2006**, *22*, 9824-9828.

[103] T. Shimanouchi, H. Umakoshi and R. Kuboi, *Langmuir* **2009**, *25*, 4835-4840.

[104] E. Lorenceau, A. S. Utada, D. R. Link, G. Cristobal, M. Joanicot and D. A. Weitz, *Langmuir* **2005**, *21*, 9183-9186.

[105] T. J. Politano, V. E. Froude, B. Jing and Y. Zhu, *Colloids and Surfaces B-Biointerfaces* **2010**, *79*, 75-82.

[106] D. J. Estes and M. Mayer, *Colloids and Surfaces B-Biointerfaces* **2005**, *42*, 115-123.

[107] N. Rodriguez, F. Pincet and S. Cribier, *Colloids and Surfaces B-Biointerfaces* **2005**, *42*, 125-130.

[108] M. Marguet, O. Sandre and S. Lecommandoux, *Langmuir* **2012**, *28*, 2035-2043.

[109] V. Noireaux, Y. T. Maeda and A. Libchaber, *Proceedings of the National Academy of Sciences of the United States of America* **2011**, *108*, 3473-3480.

[110] J. W. Szostak, D. P. Bartel and P. L. Luisi, *Nature* **2001**, *409*, 387-390.

[111] K. Jaskiewicz, A. Larsen, D. Schaeffel, K. Koynov, I. Lieberwirth, G. Fytas, K. Landfester and A. Kroeger, *Acs Nano* **2012**, *6*, 7254-7262.

[112] A. Meinel, B. Traenkle, W. Roemer and A. Rohrbach, *Soft Matter* **2014**, *10*, 3667-3678.

[113] K. A. Smith, D. Jasnow and A. C. Balazs, *Journal of Chemical Physics* **2007**, *127*.

[114] A. Varki, *Essentials of glycobiology, 2nd edition*, Cold Spring Harbor Laboratory Press {a}, 10 Skyline Drive, Plainview, New York 11803, USA, **2009**, p. 1-784.

[115] Y. Gou, J. Geng, S.-J. Richards, J. Burns, C. R. Becer and D. M. Haddleton, *Journal of Polymer Science Part a-Polymer Chemistry* **2013**, *51*, 2588-2597.

[116] S. R. S. Ting, G. Chen and M. H. Stenzel, *Polymer Chemistry* **2010**, *1*, 1392-1412.

[117] M. Ambrosi, N. R. Cameron, B. G. Davis and S. Stolnik, *Organic & Biomolecular Chemistry* **2005**, *3*, 1476-1480.

[118] H. Lis and N. Sharon, *Chemical Reviews* **1998**, *98*, 637-674.

[119] N. Sharon and H. Lis, *Science* **1989**, *246*, 227-234.

[120] N. Sharon and H. Lis, *Glycobiology* **2004**, *14*, 53R-62R.

[121] D. C. Kilpatrick, *Biochimica Et Biophysica Acta-General Subjects* **2002**, *1572*, 187-197.

[122] A. Carlsen, N. Glaser, J. F. Le Meins and S. Lecommandoux, *Langmuir* **2011**, *27*, 4884-4890.

[123] H. C. Shum, J.-W. Kim and D. A. Weitz, *Journal of the American Chemical Society* **2008**, *130*, 9543-9549.

[124] R. Salva, J. F. Le Meins, O. Sandre, A. Brulet, M. Schmutz, P. Guenoun and S. Lecommandoux, *Acs Nano* **2013**, *7*, 9298-9311.

[125] J. F. Le Meins, C. Schatz, S. Lecommandoux and O. Sandre, *Materials Today* **2014**, *17*, 92-93.

[126] J. R. Silvius, *Lipid - Protein Interactions* **1982**, *2*, 239-281.

8. Appendix

8.1. Supplementary information for $P(NGEA)_n$ - b - $(BA)_m$ synthesis and characterisation

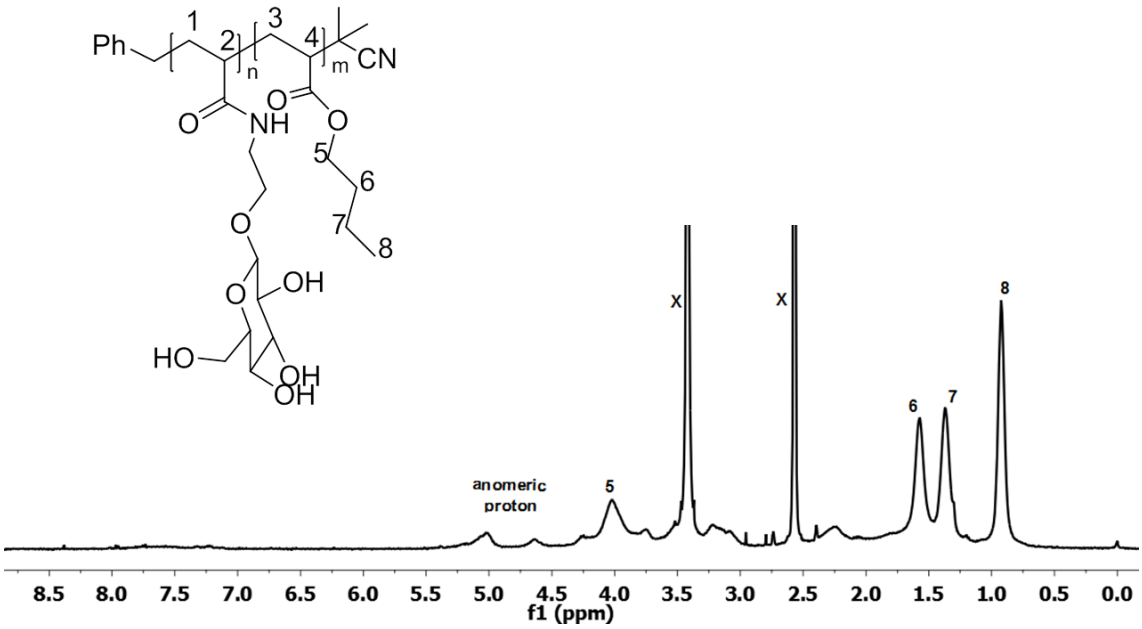

Figure 8-1. ^1H - NMR spectrum of the amphiphilic glycopolymer in DMSO - d_6.

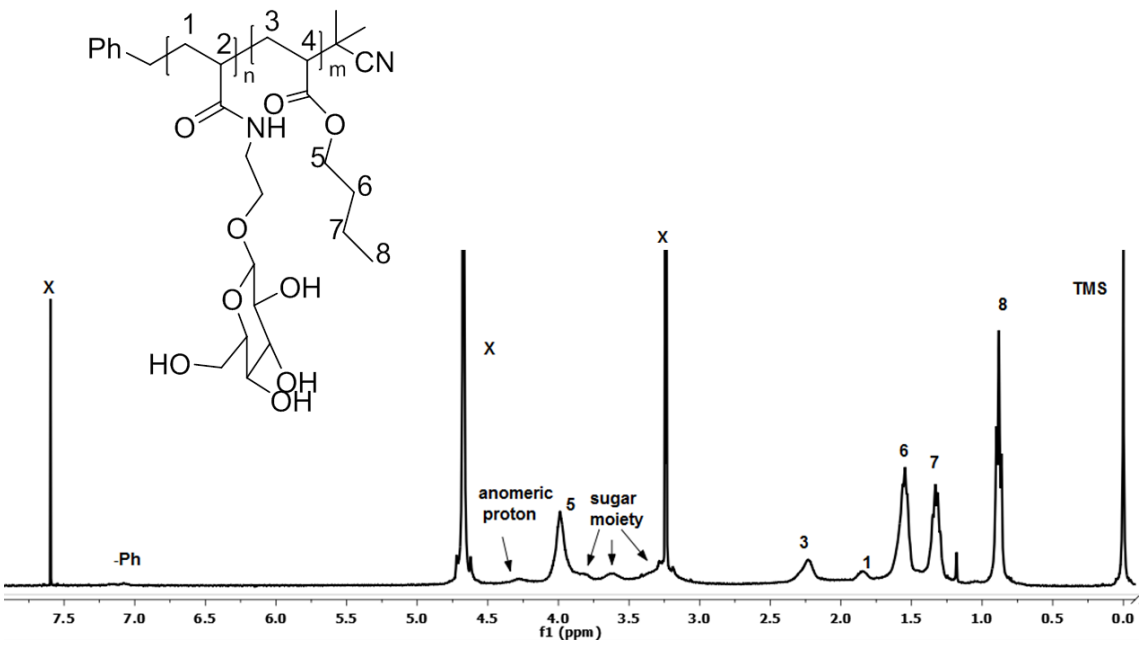

Figure 8-2. ^{1}H - NMR spectrum of the amphiphilic glycopolymer in a mixture of $CDCl_3$ and CD_3OD.

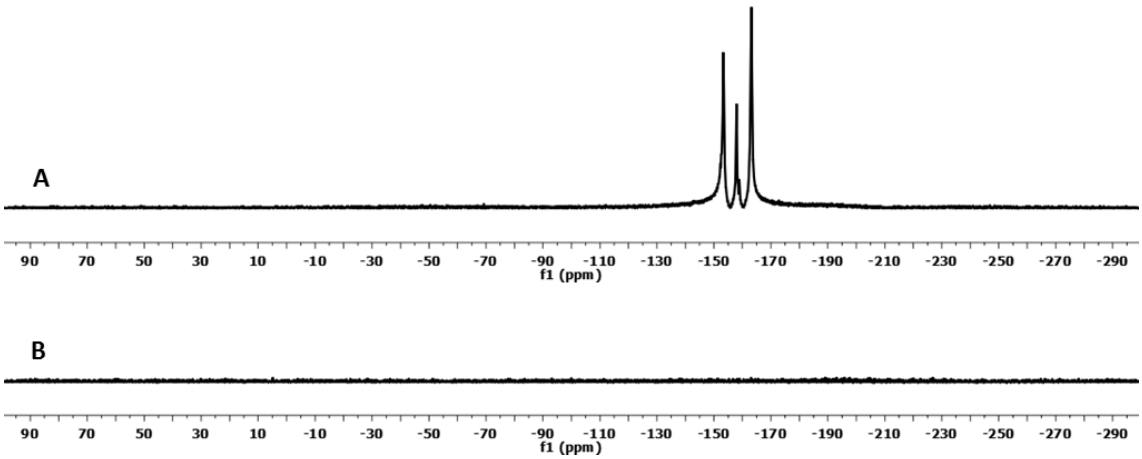

Figure 8-3. Comparison ^{19}F - NMR spectra of P(PFPA) - b - P(BA): A) before treatment with aminoethyl - β - D - glucose and B) after treatment with aminoethyl - β - D - glucose.

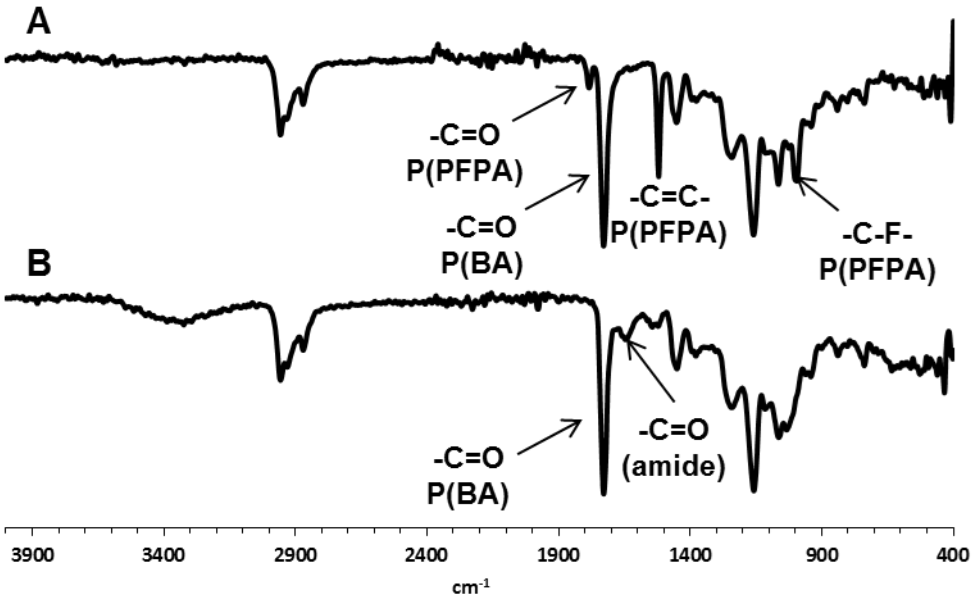

Figure 8-4. Comparison ATR - FTIR spectra of P(PFPA) - b - P(BA): A) before treatment with aminoethyl - β - D - glucose and B) after treatment with aminoethyl - β - D - glucose.

Table 8-1. Properties of glycopolymers utilised in study.

Glycopolymer	n_{theo}	m_{theo}	M_n theor (g/mol)	M_n ^{1}H - NMR (g/mol)	M_n GPC (g/mol)	Đ	n_{obt}	m_{obt}
J1	5	10	2,824	3,659	2,900	1.30	8	10
K1	5	50	7,954	7,248	7,100	1.29	8	38
H1	10	65	12,240	13,000	NA	NA	13	77
E1	10	70	11,600	8,700	7,900	1.32	14	40
A1	10	80	12,880	9,000	17,000	1.10	16	38
M1	10	100	15,729	9,769	9,100	1.26	6	62
H2	10	165	22,620	29,000	NA	NA	13	200

8.2. Supplementary information for PS beads functionalisation with Con A and particle characterisation

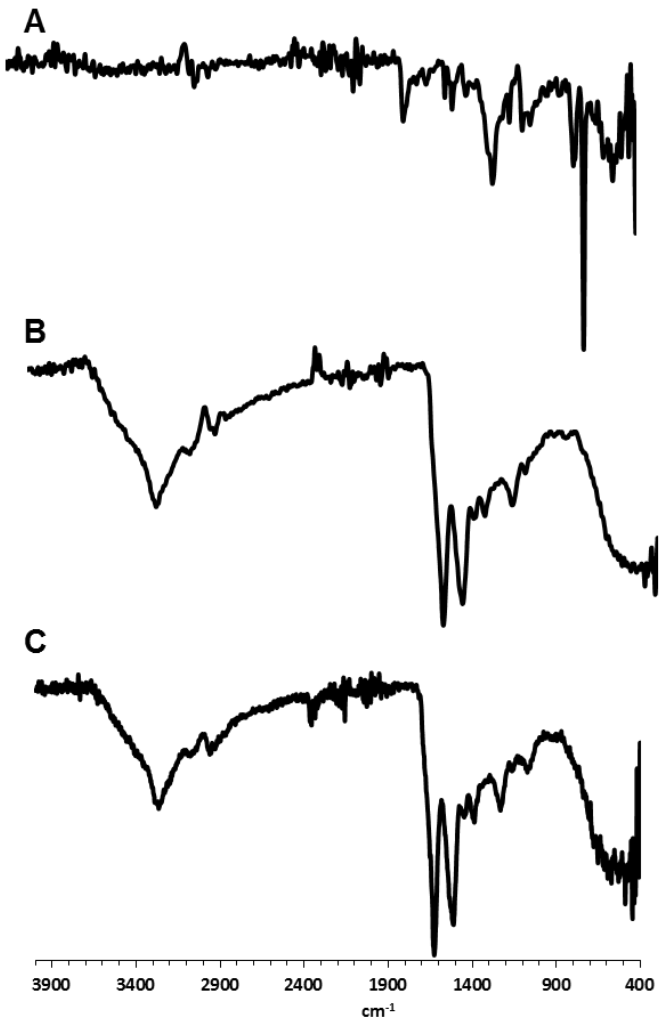

Figure 8-5. Comparison ATR - FTIR spectra: A) carboxylate - modified PS beads, B) lectin Con A and C) lectin Con A functionalized PS beads.

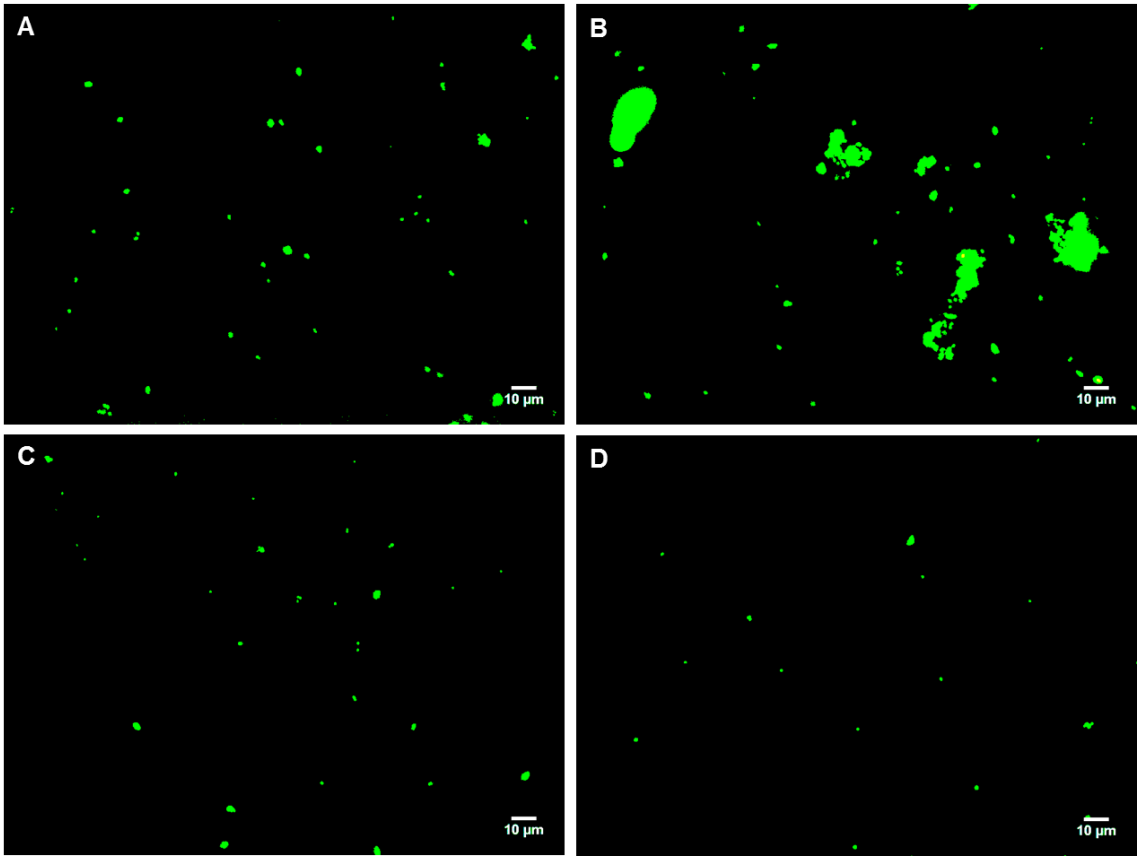

Figure 8-6. Fluorescence micrographs of lectin Con A functionalized PS beads suspensions in HEPES buffer with different additives: A) without additives; B) after addition of a multivalent water - soluble glucose - containing glycopolymer; C) after addition of a multivalent water-soluble fucose - containing glycopolymer; D) control experiment: suspension of carboxylate - modified PS beads in HEPES buffer in the presence of a multivalent water - soluble glucose - containing glycopolymer.